catalysts

MDPI

Review

Recent Progress in Pd-Catalyzed Tandem Processes

Linda Z. Nikoshvili * and Valentina G. Matveeva *

Department of Biotechnology, Chemistry and Standardization, Tver State Technical University, A. Nikitina Street, 22, 170026 Tver, Russia

* Correspondence: nlinda@science.tver.ru (L.Z.N.); matveeva@science.tver.ru (V.G.M.); Tel.: +7-904-005-7791 (L.Z.N.); +7-905-601-0144 (V.G.M.)

Abstract: In recent years, Pd-containing catalytic systems for tandem processes have gained special attention due to their enhanced catalytic properties and their possibility of performing several reactions without the necessity of separating the intermediates. In this review, recent progress in Pd-catalyzed tandem processes is considered. Three types of catalytic systems are described: homogeneous catalysts (including immobilized Pd complexes); heterogeneous catalysts supported on oxides, MOFs, COFs, etc., with particular attention to the supports containing acid/base sites; and metal-enzyme catalysts for chemoenzymatic tandem processes applied in fine organic synthesis and biotechnology. For homogeneous Pd-catalyzed reactions, different tandem reactions were considered, i.e., cross-coupling, cyclization, carbonylation, isomerization, alkylation, arylation, etc.

Keywords: tandem processes; one-pot processes; palladium; bifunctional catalysts; bimetallic catalysts; chemoenzymatic catalysis

1. Introduction

Multiple catalytic processes in one reactor are of high importance due to the time–space economy and global tendency towards greener sustainable processes [1]. However, at present, there are many misinterpretations in the terminology used. As was mentioned by Camp et al. [2], such processes have different names: single-pot catalysis, one-pot catalysis, dominocatalysis, dual catalysis, tandem-catalysis, and multifaceted catalysis. Many papers use the term "tandem" for different processes proceeding one after another. Fogg and dos Santos [3] defined the one-pot catalytic processes that are not tandem catalysis as bicatalytic reactions, in which the second catalyst is added after the first one, which completes the reaction. When all the catalytic species are present in the reactor together, it can be defined as either domino or tandem catalysis. If all the reagents and catalysts are simultaneously present in the reactor, and the functionality formed in the previous step undergoes subsequent transformation, such a process can be classified as domino catalysis. It is important to emphasize that in many cases, domino catalysis is equated to the tandem catalysis, while Fogg and dos Santos [3] indentified of the domino/cascade catalysis as the multiple transformations proceeding via a single catalytic mechanism (Figure 1).

In the instance of tandem catalysis, the substrate is sequentially transformed through a number of mechanistically distinct mechanisms. Moreover, tandem catalysis can be divided in orthogonal, assisted, and auto-tandem catalysis [3]. The difference between auto-tandem and assisted tandem processes is that in the latter case, an additional compound is added in the reactor, switching the second mechanistically distinct reaction. As was mentioned by different authors [4–6], auto-tandem catalysis is an effective method for generating complex molecules from basic starting materials since it can support several mechanistically distinct reactions in a single reactor. When sequential C–C bond-forming processes take place in the reactions, the adoption of the auto-tandem catalysis technique has a very significant effect [6]. In contrast to auto-tandem catalysis, a linear synthetic method would not

check for updates

Citation: Nikoshvili, L.Z.; Matveeva, V.G. Recent Progress in Pd-Catalyzed Tandem Processes. *Catalysts* **2023**, *13*, 1213. https://doi.org/10.3390/catal13081213

Academic Editor: Francis Verpoort

Received: 3 July 2023
Revised: 1 August 2023
Accepted: 10 August 2023
Published: 15 August 2023

be able to produce unstable or sensitive organic intermediates in situ. Although auto-tandem processes have many benefits, it might be challenging to control them. Moreover, interference from side reactions might make them more difficult, particularly when the optimal conditions for certain catalytic cycles differ from one another [4].

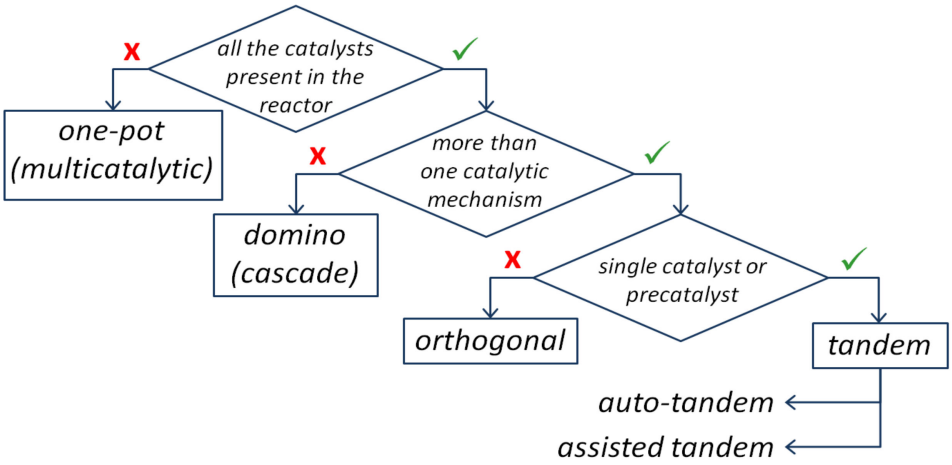

Figure 1. Distinguish between one-pot, domino, and tandem processes (based on [3]).

Tandem catalysis is a powerful tool for the production of a wide range of organic compounds by means of a variety of synthetic transformations, among which are arylation, alkylation, cyclization, cycloaddition, carbonylation, cross-coupling, amination, isomerisation, and other processes. Different metals such as Co [7], Cu [8], Ag [9,10], Au [11], Ni [12], Ru [13], Pt [14,15], and Pd [16] in the composition of both homogeneous [17,18] and heterogeneous [19] systems can catalyze tandem reactions.

Moreover, bimetallic catalytic systems (Cu-Zn [20], Cu-Ni [21], Pd-Cu [22,23], Au-Pd [24,25], Ir-Pd [25], Pd-Ru [26,27], Pd-Rh [28], Ag-Pd [29], Pd-Ni [30], Au-Cu [31], Cu-Ag [10,32], Cu-Bi [10], etc.) can be also used.

Among the transition metals applied for tandem processes, palladium is one of the most widely used. Thus, this review is devoted to the recent advances (for the last five years) in tandem reactions catalyzed by Pd complexes and nanoparticles (NPs), including those catalyzed by bimetallic systems and metal-enzyme catalysts.

2. Pd-Catalyzed Homogeneous Tandem Catalysis

At present, homogeneous Pd-catalyzed processes, including the tandem ones, are the most widespread in fine organic synthesis for the production of active pharmaceutical ingredients (APIs) and polymers.

2.1. Coupling Tandem Processes

Palladium is known as a catalyst for the cross-coupling processes [33,34]. Both sequential and iterative Pd-catalyzed reactions can be carried out in tandem cross-coupling reactions, and the order of C–C bond forms can be regulated by either the attenuated leaving groups of the multireactive substrate or certain catalyst/ligand combinations [35–38]. Both the nucleophilic and electrophilic sites may be coupled in a specific manner. Additionally, in addition to halogen and metal leaving groups, the C–H bond can be used as an appealing leaving group [35].

In the catalytic cycle of cross-coupling reactions, palladium constantly changes its oxidation state from Pd(0) to Pd(II) and vice versa, hence the process can be catalyzed by any form of the metal [39,40]. Lamb et al. [41] employed Pd(II) to catalyze in the one-pot process the dehydrogenation of 2,2-disubstituted cyclopentane-1,3-diones and the oxidative Heck coupling (Figure 2). It was postulated that Pd(II) was an active form, which underwent partial decomposition during the reaction if the ligand loading was unsufficient.

However, it was difficult to create the ideal one-pot conditions since the optimal conditions for the dehydrogenation stage were inappropriate for the oxidative Heck process.

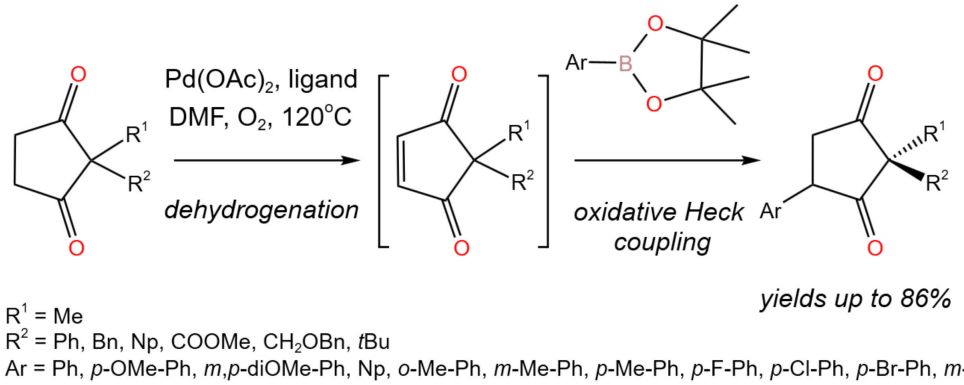

Figure 2. Scheme of the dehydrogenation of 2,2-disubstituted cyclopentane-1,3-diones and the oxidative Heck coupling in a one-pot process [41].

By the example of Np-substituted cyclopentane-1,3-dione, it was shown that due to the presence of unligated Pd, which was likely formed during the aerobic dehydrogenation stage, the established one-pot reaction allowed for the achievement of a reasonable yield of 60% at moderate enantioselectivity at 74:26 e.r. In order to study the telescoped reaction, the reaction mixture was filtered to remove any unligated Pd before the cross-coupling partner was added. Such treatment enabled the e.r. to be comparable to the separate oxidative Heck step (88:12 vs. 90:10 e.r.) with agood 70% yield [41].

The improved synthesis of indolines via tandem decarboxylative amination/Heck/annulation reaction was carried out by Wang et al. [42] (Figure 3).

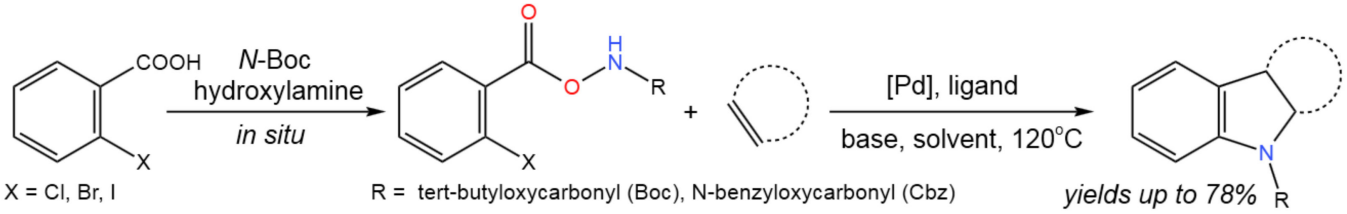

Figure 3. Scheme of the synthesis of indolines via tandem decarboxylative amination/Heck/annulation reaction [42].

Different palladium compounds ($Pd(OAc)_2$, $Pd(TFA)_2$,$Pd_2(dba)_3$, $PdCl_2$) and ligands ((t-Bu)$_3$P·BF_4, Ph3P, etc.) were used. $PdCl_2$ and (t-Bu)$_3$P·BF_4 revealed the best performance. Among the bases (Cs_2CO_3, K_2CO_3, t-BuOK, DBU, and Et_3N), Cs_2CO_3 was optimum. Moreover, different solvents were used (benzene, toluene, xylene, MeCN, $CHCl_3$, and DMF), and benzene was the most preferable one. Toluene was the second in efficiency allowing up to 70% yield of target product. In general, depending on the halogen, protecting group, substituent, and nature of the second substrate, as well as on the reaction conditions, up to 78% yield of the target product was achieved [42]. The reaction mechanism was proposed to proceed via formation of the intermediate of an intramolecular decarboxylation process. The cyclization product was then synthesized by reacting this intermediate with norbornadiene using a tandem Heck-type reaction and nitrogen nucleophilic route. The reaction followed a similar tandem Heck/intramolecular Tsuji–Trost pathway when the 1,3-diene substrate was used [42].

Song et al. [43] developed the synthesis of 2-(1-phenylvinyl)-indoles via the novel Pd(0)-catalyzed intermolecular coupling reaction of 2-*gem*-dibromovinylanilines and *N*-tosylhydrazones (Figure 4). Reaction conditions were optimized, ($PdCl_2(PPh_3)_2$ was chosen as a catalyst, and *t*BuOLi was chosen as a base (the other bases were DMAP, *t*BuOK,

TEA, $CsCO_3$, and CsF)). Using 2-*gem*-dibromovinylanilines as a substrate, the scope of *N*-tosylhydrazones was studied. The reaction products were obtained in moderate to good yields (from 42% up to 94%), depending on the substituents: electrondonating (*p*-OMe and -OCH_2O-) or electronwithdrawing (NO_2 and CN). The substitutions on 2-*gem*-dibromovinylaniline were also studied (-CO_2Me, Br, F, Ns, Ph, 4-F-Ph, 4-Cl-Ph, 4-OMe-Ph, 4-*t*Bu-Ph, 4-Me-Ph, *N*-Ac, *N*-Ms), giving good yields (>80% in most of cases).

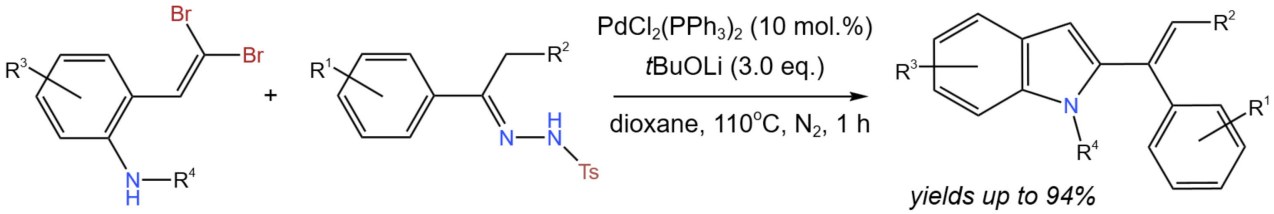

R^1 = H, 3-OMe, 4-OMe, 3,4-(OCH_2O), 4-NO_2, 4-CN, 4-F, 4-Cl, 4-Br, 3-Br
R^2 = H, Me, Et, Ph
R^3 = H, 6-CO_2Me, 5-Br, 6-F, 5-Ph, 5-(*p*-F-Ph), 5-(*p*-Cl-Ph), 5-(*p*-OMe-Ph), 5-(*p*-*t*Bu-Ph), 5-(*p*-Me-Ph) (position is indicated in the indole residue)
R^4 = Ts, Ac, Ms, Ns

Figure 4. Scheme of the tandem reaction of 2-*gem*-dibromovinylanilines and *N*-tosylhydrazones for the synthesis of 2-(1-phenylvinyl)-indoles [43].

The reaction mechanism was also proposed, which included two catalytic cycles, one of which was started from Pd(0) and included oxidative addition, deprotonation, and reductive elimination, resulting in theformation of 2-bromo-1-tosyl-1*H*-indole. The latter entered the second cycle that also started from an oxidative addition to Pd(0) with the formation of the Pd(II)complex. Subsequently, alkylpalladium species were formed with carbene intermediate generated from the diazo compound. Finally, β-H elimination allowed for the synthesis of the desired product and the regeneration of Pd(0) [43].

In situ-produced vinyl fluorosulfate intermediates were coupled with electron-deficient olefin partners (Figure 5) by Revathi et al. [44] to create a protocol for the one-pot conversion of alcohols to 1,3-dienes. The use of DMSO as a solvent was mandatory, due to the involvement in the reaction mechanism. Broad substrate scopes of alcohols were examined for the SO_2F_2-mediated dehydrative cross-coupling. Different starting compounds containing both electron-donating groups (alkyl, aryl, trifluoromethoxy, methoxy, ether, thioether) and electron-withdrawing groups (nitro, trifluoromethyl) including halogens were investigated. Corresponding products were synthesized with the yields varying from 40% up to 99%. Moreover, the substrate scope of electron-deficient olefin coupling partners was studied. The best results were obtained with acrylamide, which provided the corresponding product at a 82% yield, and ethyl vinyl ketone, which produced the corresponding 1,3-diene at a 88% yield [44].

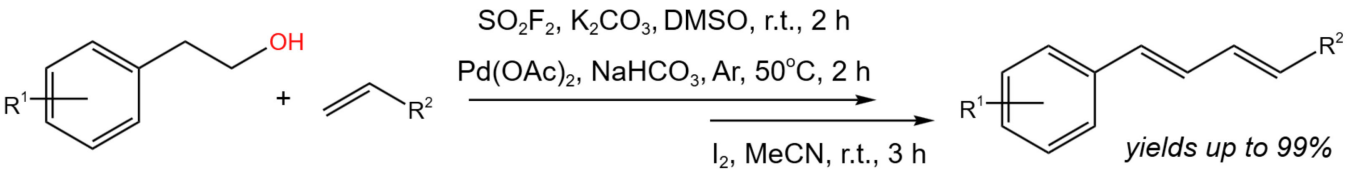

R^1 = H, 4-Ph, 2-Me, 3-Me, 4-Me, 2,5-diMe, 4-OMe, 3,5-diOMe, 3,4,5-triOMe, 4-*t*Bu, 4-CF_3, 3-OCF_3, 4-OCF_3, 2-OBn, 3-OBn, 4-SMe, 4-NO_2, 4-F, 3-Cl, 4-Cl, 3,4-diCl, 2-Br, 3-Br, 4-Br, 4-I, 2,3-benzo, 3,4-benzo

R^2 = COOMe, COOEt, COOPh, $COOCH_2Ph$, COEt, $CONH_2$

Figure 5. Scheme of dehydrative cross-coupling for the conversion of alcohols to 1,3-dienes [44].

The C–C/C–N bond formation in the reaction between *N*-methyl benzamide and arylboronic acid was catalyzed by the dinuclear palladium(II) complex, resulting in the direct synthesis of phenanthridinone (Figure 6) [45]. A broad range of phenanthridinones was synthesized in good to excellent yields (from 79% up to 96%) using 1 mol.% of the catalyst

and a variety of substrates, which also included condensed aromatics and heterocycles (in the case of arylboronic acid).

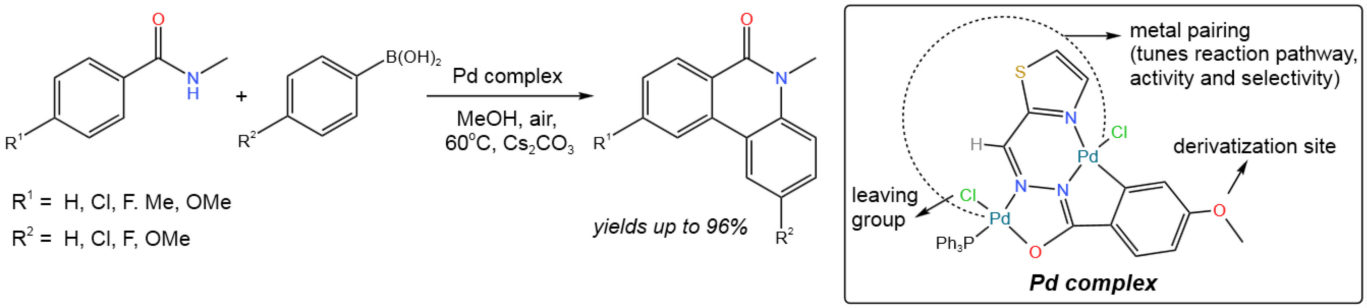

Figure 6. Scheme of the synthesis of phenanthridinones [45].

It was proposed that the reaction proceeds via *ortho*-arylation [45]. First, *N*-methyl arylamide was coordinated with the catalyst along with the *ortho*-C–H bond activation. Then, the transmetalation reaction occurred with participation of an arylboronic acid, leading to the formation of an *ortho*-arylated intermediate, which subsequently resulted in the seven-membered palladacycle. In this process, one of the two Pd(II) nuclei was transformed to Pd(0). Finally, the reductive elimination led to the desired product, while Pd(0) was oxidized by air.

The Pd pincer complex supported by 2,6-bis(pyrrolyl)pyridine ligands was shown [46] to be an efficient catalytic system for one-pot tandem Heck alkynylation (copper-free Sonogashira coupling)/cyclization reaction) (Figure 7). It was shown that a wide range of benzofuran derivatives can be obtained at 90 °C using 0.1 mol.% of catalyst loading for 10 h with high yields (up to 96%).

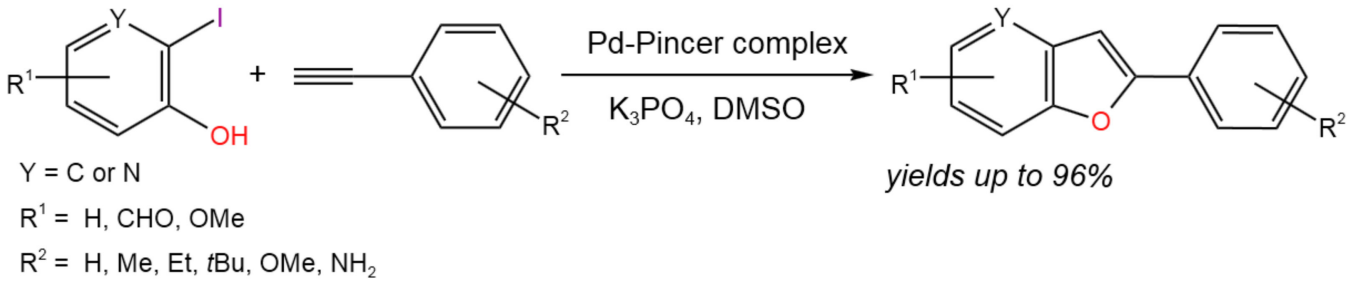

Figure 7. Scheme of the synthesis of benzofuran derivatives via the Heck alkynylation/cyclization reaction [46].

The reaction mechanism included two cycles (Heck alkynylation cycle and intramolecular cyclization cycle) associated with the product of Heck alkynylation, which underwent the cyclization process. It is noteworthy that the first cycle was likely initiated by Pd(II)/Pd(IV) transformations instead of the most common Pd(0)/Pd(II) chemistry [46].

In a similar way, microwave-assisted, domino [Pd]-catalyzed Heck cyclization followed by intermolecular Sonogashira coupling was carried out by Karu and Gedu [47] for the synthesis of substituted dihydrobenzofurans with yields of up to 99% (Figure 8). The reaction was proposed to proceed via a single catalytic cycle including classical Pd(0)/Pd(II) transformations. Initiated by Pd(0), the cyclization took place first, followed by Sonogashira coupling.

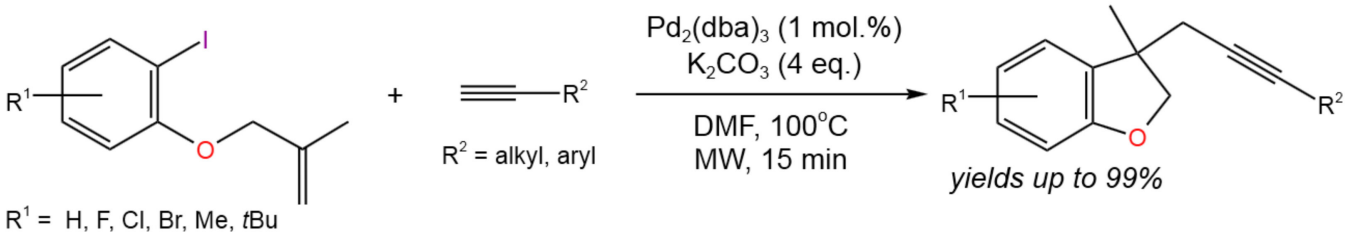

Figure 8. Scheme of the synthesis of substituted dihydrobenzofurans via Heck cyclization followed by Sonogashira coupling [47].

Such a kind of substituted heterocycles, containing a triple carbon–carbon bond, can be a subject of further transformations. For example, Ho et al. [48] developed the one-pot process for the dearomatising spirocyclization/cross-coupling of indole/pyrrole derivatives (Figure 9). In the proposed protocol the use of $Pd(PPh_3)_4$or *trans*-PdBr(*N*-succinimide)$(PPh_3)_2$ allowed up to 97% yields of target products. Palladium complexes were proposed to play a dual role: (i) π-acid to activating the alkyne towards dearomatising spirocyclization, and (ii) cross-coupling catalysts.

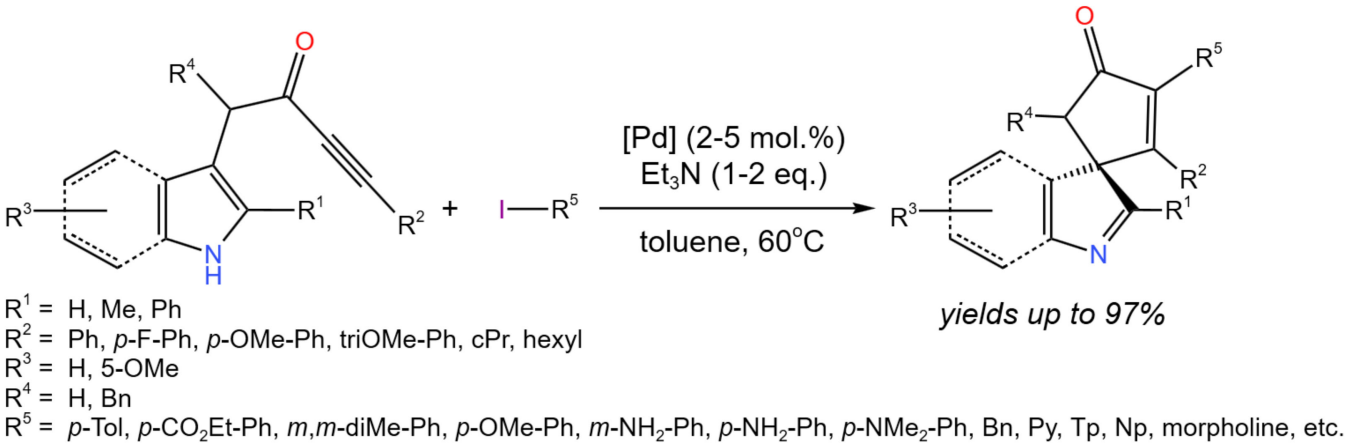

Figure 9. One-pot dearomatising spirocyclisation/cross-coupling [48].

Moreover, a variety of the spirocyclic pyrroline-based compounds, which are important scaffolds in drug development, could be produced with the yields up to 80% via Pd-catalyzed tandem Narasaka–Heck/C(sp^3 or sp^2)-H activation reaction [49] with γ,δ-unsaturated oxime esters as starting materials via the five-membered spiro-palladacycle intermediate.

Functionalized benzofurans, indoles, and phthalanes can be also synthesized by the tandem Ullmann–Goldberg cross-coupling and cyclopalladation-reductive elimination reactions, as well as by the related Pd-catalyzed processes involving hetero-Michael additions and cyclization in a one-pot process [50].

The tandem Heck/Suzuki reaction can be applied for the enantioselective intramolecular cyclization/cross-coupling of olefin-tethered aryl halides with various organoboronic acids [51]. Under the optimized reaction conditions, a number of dihydrobenzofuran derivatives were synthesized (Figure 10) with high yields (up to 99%) and e.r.s (up to 97:3). Moreover, by the same approach, different indolines, chromanes, and indanes were synthesized with yields of up to 99% and high e.r.s, depending on the substituents.

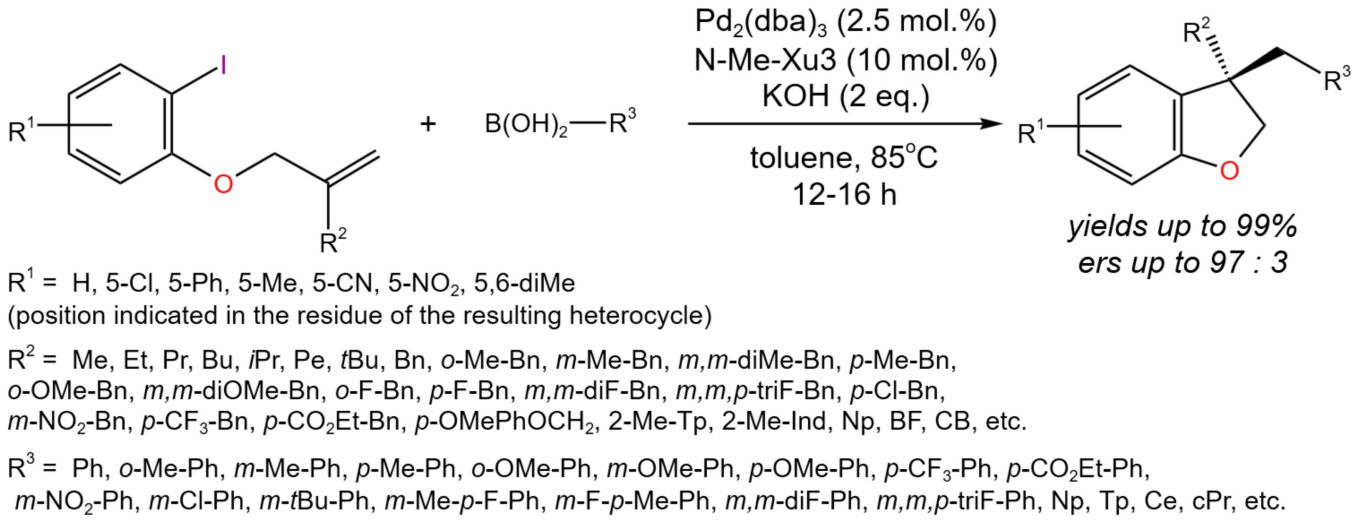

Figure 10. Scheme of the tandem Heck/Suzuki process for the synthesis of chiral compounds by the example of dihydrobenzofurans bearing a quaternary stereocenter [51].

Yokoya et al. [52] suggested fabricating the benzo[*de*]chromene ring followed by its oxidation in order to produce benzo[*de*]chromene-7,8-dione derivatives, which are known to have significant biological and pharmacological effects (Figure 11). Pd- and Cu-catalyzed Sonogashira coupling and cyclization was applied to produce benzo[*de*]chromene-7,8-dione derivatives with yields of up to 69%. It was found that the coupling process was catalyzed by Cu and Pd complexes, according to the established mechanism, while the further cyclization was catalyzed by CuI alone.

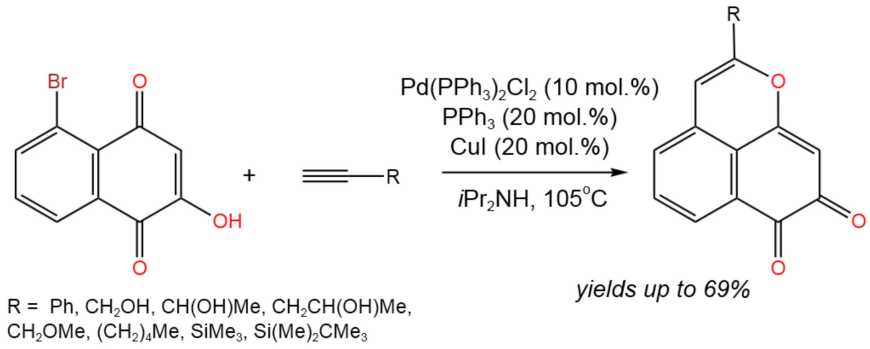

Figure 11. Tandem Sonogashira coupling and intramolecular cyclization with terminal alkynes for the synthesis of benzo[*de*]chromene-7,8-dione derivatives [52].

For the one-pot synthesis of alkenyl-substituted boron dipyrromethene (BODIPY) from Cl-BODIPY and alkyne, the coupling-reduction tandem process (Figure 12) was reported [53]. In comparison to traditional approaches, this synthesis enabled higher yields (up to 80%), a wider range of substrates, and a faster reaction rate by combining the Sonogashira coupling and the reduction process, avoiding the use of a reductant.

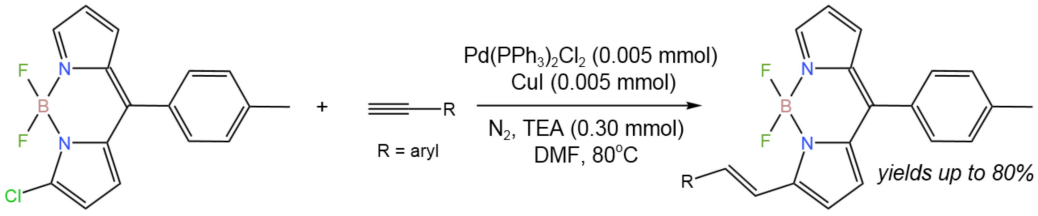

Figure 12. Synthesis of alkenyl-substituted BODIPYs [53].

One of the reactions attributed to the tandem Pd-catalyzed catalytic processes is the synthesis of imidazole derivatives [54–56]. The tandem synthesis of imidazole-fused polyheterocycles (Figure 13) from 2-vinyl imidazoles and aryl halides was reported by Li et al. [54] and involved intermolecular Heck arylation of 2-vinyl imidazoles, followed by an intramolecular aerobic oxidative C–H amination reaction.

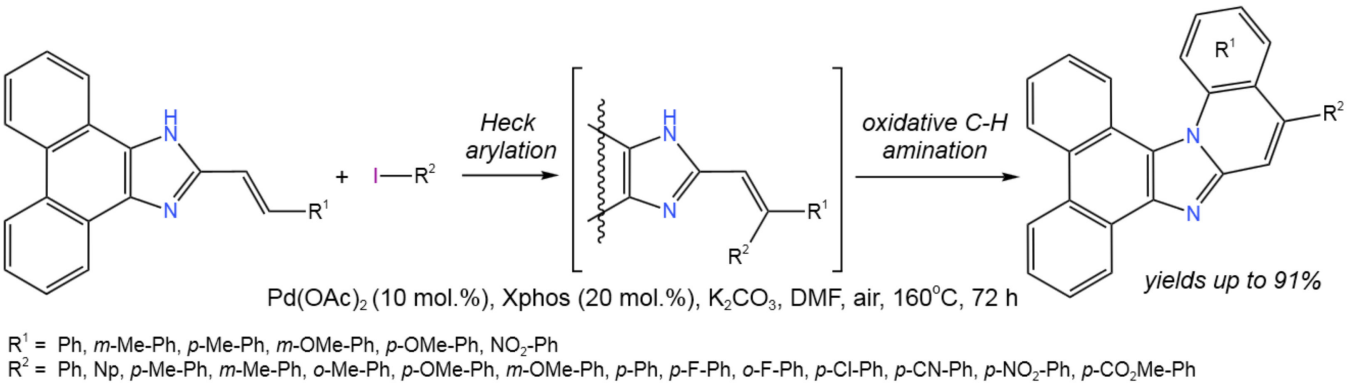

Figure 13. Pd-catalyzed annulation of phenanthroimidazoles with aryl iodides for the synthesis ring-fused phenanthroimidazoles [54].

In this tandem reaction, the Pd(0)↔Pd(II) catalytic cycle was used to simultaneously break two or three C–H bonds, one C–X bond, and one N–H bond. Different catalysts were used ($Pd(OAc)_2$, $PdCl_2$, $Pd(PPh_3)_4$, $Pd_2(dba)_3$), among which the palladium acetate allowed the highest yields of the target products (up to 91%). Potassium carbonate was chosen as an optimum base (other bases were Cs_2CO_3, NaO*t*Bu, NaOH, and Et_3N). DMF was shown to be the most preferable solvent as compared to DMA, DMSO, toluene, and 1,4-dioxane [54].

A tandem reaction involving boronic acids and 2-(bromobenzylsulfenyl)-1-propargyl benzimidazoles catalyzed by Pd was developed [55] (Figure 14). This process involved three different reactions: (i) Suzuki debrominative cross-coupling; (ii) Cu-free desulfenylative coupling at the 2-position of the benzimidazole; and (iii) intermolecular regioselective and stereoselective hydrothiolation of the triple C–C bond of the *N*-propargyl benzimidazole.

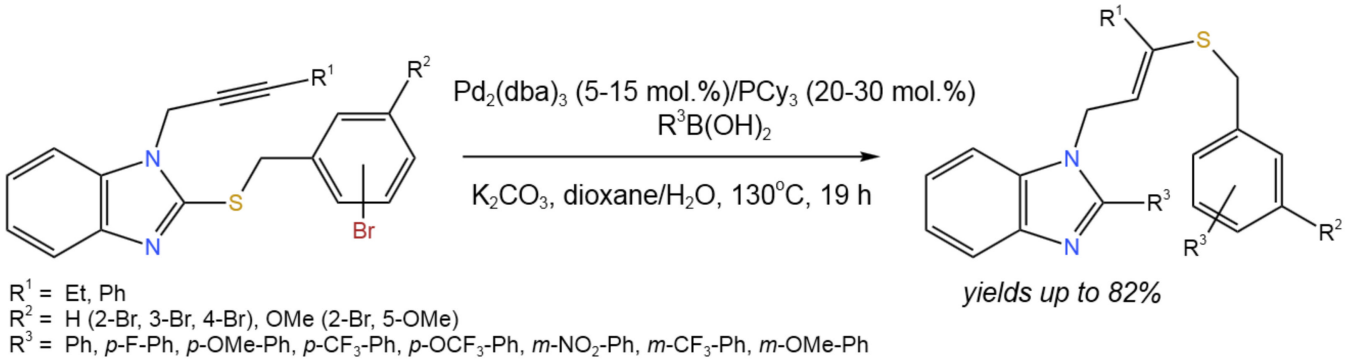

Figure 14. Tandem Pd-catalyzed reaction between boronic acids and 2-(bromobenzylsulfenyl)-1-propargyl benzimidazoles for the synthesis of substituted benzimidazoles bearing a stereodefined alkenyl sulfide [55].

The whole procedure resulted in an alkenyl benzyl sulfide and doubled the amount of boronic acid partner that was incorporated into the final structure. The developed tandem process proceeded with moderate up to high yields (82%), depending on the substituents and ligands. It is noteworthy that the heterocycles other than benzimidazole (i.e., imidazole and indole) were studied, and $Pd(PPh_3)_4$ (15 mol.%) was found to provide higher yields of target products as compared to $Pd_2(dba)_3/PCy_3$ [55].

Luo et al. [56] developed the cross-coupling reaction of isocyanides with α-diazoacetates catalyzed by palladium to form ketenimines, which were subsequently underwent the DABCO-catalyzed aza-Mannich type reaction (Figure 15) under mild reaction conditions (80 °C, CH_3CN—solvent). Different 2-mercaptoimidazoles or 1*H*-benzo[*d*]imidazol-2-oles were transformed to 1,3-bis(β-aminoacrylate)-substituted 2-mercaptoimidazoles and 2-benzimidazolinones with the yields up to 68%.

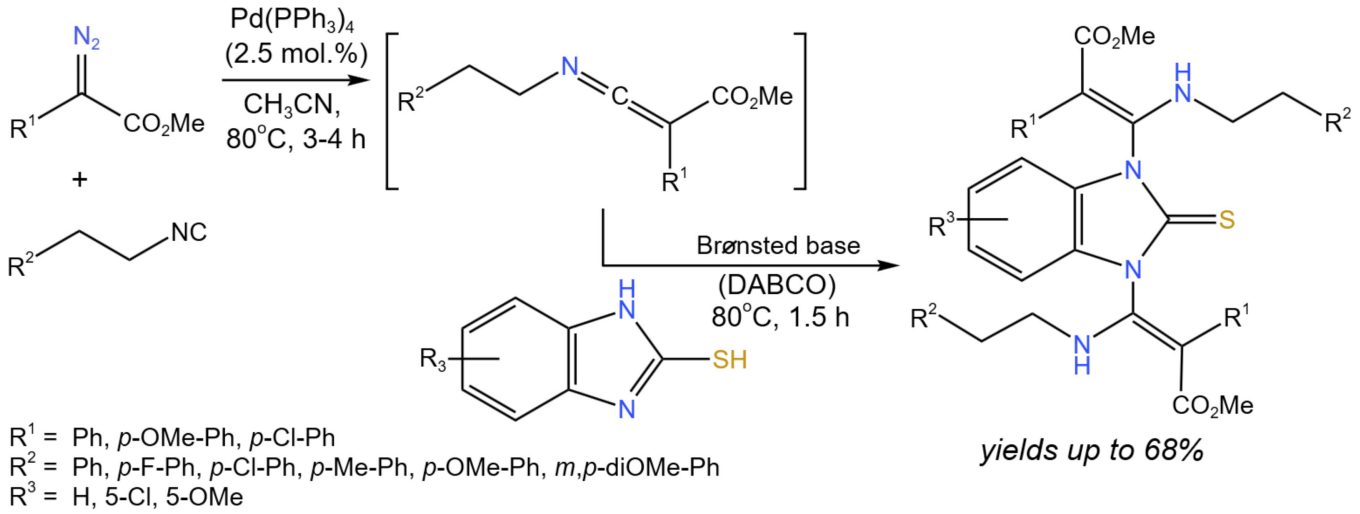

Figure 15. Scheme of the synthesis of 1,3-bis(β-aminoacrylate)-substituted 2-mercaptoimidazole derivatives synthesized in one pot using sequential Pd and Brønsted base catalysis [56].

The proposed reaction mechanism involved two cycles: (i) Pd-catalyzed, and (ii) DABCO-catalyzed. The starting isocyanide compound was coordinated with the palladium catalyst. Then, the diazo compound reacted with the formation of the Pd-carbene intermediate and the release of nitrogen. After that, the resulting intermediate produced ketenimine with regeneration of the catalyst. Ketenimine was trapped by one of the NH groups in DABCO-activated 2-mercaptoimidazole. The intermediate of this step reacted with ketenimine to form the target product [56]. Choi et al. [57] reported the tandem Diels–Alder/cross-coupling (either Stille or Suzuki) process using 2-bromo-1,3-butadienes as substrates, which underwent intermolecular cycloaddition with a variety of activated dienophiles in the presence of Lewis acids (e.g., $BF_3 \cdot OEt_2$, $TiCl_4$, $SnCl_4$). The reaction proceeded with high yields (>70%) and good endo diastereoselectivity with respect to vinyl bromide cycloadducts, which further underwent cross-couplings in the presence of Pd catalysts ($Pd_2(dba)_3$, $Pd(Ph_3P)_4$).

2.2. Isomerization Tandem Processes

Isomerization tandem reactions catalyzed by Pd are possible due to the simultaneous existence of two oxidation states of this metal. Thus, there is double terminology for these reactions: some authors attribute them to orthogonal catalysis [58], othersto tandem catalysis [59]. Arroniz et al. [58] demonstrated the tandem orthogonal process of the conversion of alkynyl epoxides to furans (Figure 14). The developed procedure allowed for high yields (up to 93%) of furan derivatives.

It was found that the reaction proceeded through the formation of allenyl ketone and β,γ-alkynyl ketone as intermediates. The prposed reaction mechanism involved the oxidative addition of Pd(0) into the alkynylepoxide, resulting in the formation of allenylpalladium(II) species, which underwent reductive elimination to enol (shown in brackets in Figure 16). The latter tautomerized to alkynyl ketone and to allenyl ketone. The furanylpalladium complex was formed by the Pd(II)-activated cyclization of allenyl ketone. After the protodepalladation, the target furan's derivatives were produced under mildly

acidic conditions. Moreover, a possible alternative mechanism for the conversion of the alkyne to the furan was suggested [58].

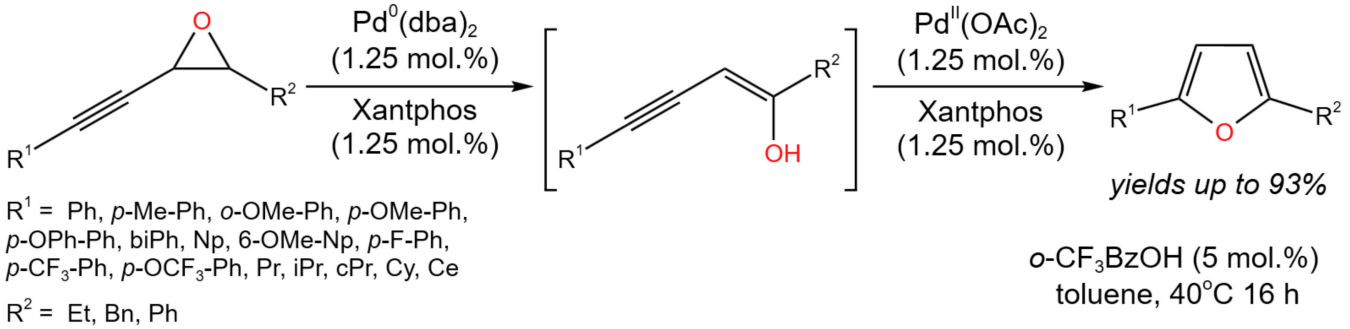

Figure 16. Dual catalytic isomerization of alkynyl epoxides for the synthesis of furans [58].

The synthesis of furans and pyrroles was carried out via the Pd-catalyzed tandem addition/ring-opening/cyclization reaction of 2-(3-aryloxiran-2-yl)acetonitriles with arylboronic acids in aqueous medium (Figure 17) [59].

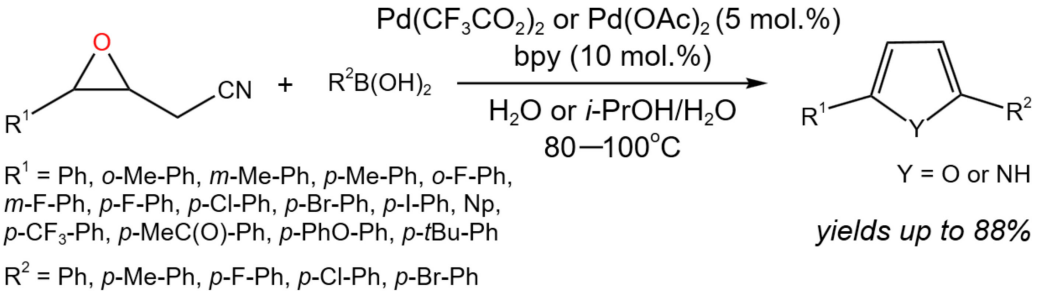

Figure 17. Tandem reaction of epoxyacetonitriles with arylboronic acids for the synthesis of furans and pyrroles [59].

Yu et al. [59] noticed that despite the advances in the Pd-catalyzed ring-opening of epoxides with nonpolar multiple bonds (such as vinyl and alkynyl), the reactions of boronic acids with epoxides with polar groups are less studied due to the lower reactivity.

As a result of the study, an efficient approach for the synthesis of furans and pyrroles with high selectivity was developed, allowing, depending on the catalyst and additives (*p*-toluenesulfonic acid, trifluoromethanesulfonic acid, D-camphorsulfonic acid, methanesulfonic acid, etc.), yields of up to 73% of furan derivatives ($R^1 = R^2 = Ph$) in aqueous medium at 80 °C under air. It is noteworthy that the replacement of air to the oxygen allowed for a noticeable increase in the yield of the target product (up to 86%). In the case of the synthesis of 2,5-diarylpyrroles at 100 °C under nitrogen using a*i*-PrOH/H_2O mixture as a solvent, up to 84% yield was achieved, depending on the substituents. Moreover, it was found that the steric effects of arylboronic acids primarily controlled the chemo-selectivity of the developed tandem process: when 2-(3-aryloxiran-2-yl)acetonitriles were reacting with the less sterically hindering arylboronic acids, the only products were furans due to the hydrolysis of the ketimine intermediate, arising from the carbopalladation of the cyano group, whereas when reacting with the more sterically bulky arylboronic acids, pyrroles were selectively produced [59].

Another one example of isomerization tandem processes is the tandem isomerization/hydrothiolation of allylbenzenes (Figure 18) [60]. In the case of $n = 0$, using $Pd(OAc)_2$ (3 mol.%) as a catalyst in the presence of 3.9 mol.% of the ligand and 12 mol.% of CF_3SO_3H, up to a 78% yield of the target product was able tobe achieved at 40 °C for 15 h, depending on the substituents. When $n = 1$–3 and R = H or 4-OMe, the one-pot process was carried out: (i) isomerization stage in the presence of $PdCl_2(PhCN)_2$ (5 mol.%) in toluene at 60 °C

for 4 h; (ii) hydrothiolation stage in the presence of the ligand (10 mol.%), acid (22 mol.%), and thiol at 50 °C for 22 h, which allowed an up to 43% yield of the target product.

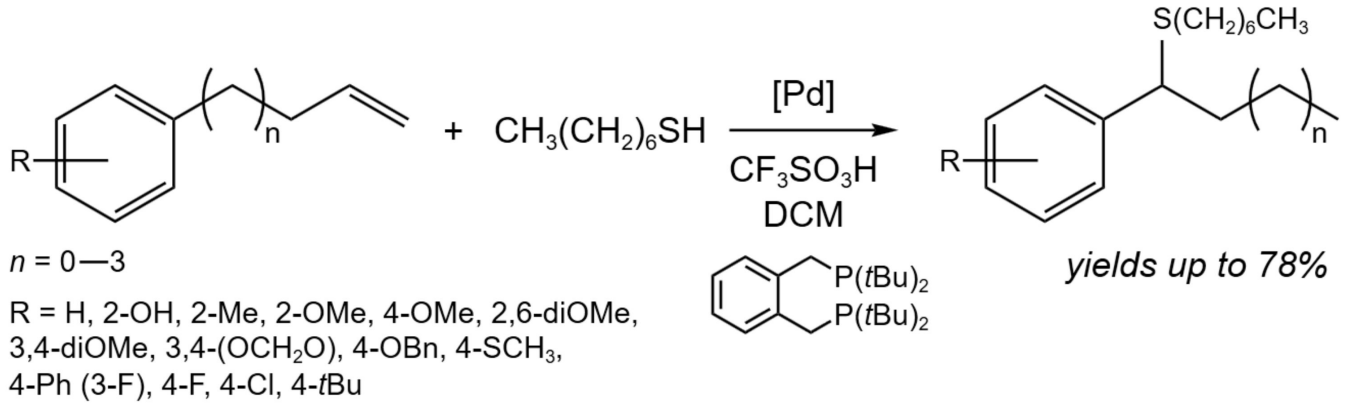

Figure 18. Tandem isomerization/hydrothiolation of allylarenes for the synthesis of benzylic thioethers [60].

It was demonstrated that the highly regioselective catalytic system composed of a Pd(II) precursor, bidentate phosphine ligand, and strong Brønsted acid may convert a wide range of 3-arylpropenes and thiols to branched benzylic thioethers. The reaction was facilitated by an in situ-generated Pd hydride [60].

2.3. Carbonylation Tandem Processes

Over 80% of all the APIs are known to have heterocyclic aromatic rings, with predominating N-containing aromatic heterocycles. Many APIs have the carbolinone ring system as a substructure [61]. Thus, carbonylation reactions are in high demand by the modern chemical industry. These reactions can be carried out in tandem with processes such as cross-coupling, dealkylation, and dehydrogenation.

A tetracyclic isoindoloindole skeleton with three new C–C/C–N bonds that was simultaneously generated, for instance, could be constructed in a one-step process using tandem Pd-catalyzed carbonylation and C–C cross-coupling via C–H activation (Figure 19) [62]. In more detail, the production of *6H*-isoindolo[2,1-*a*]indol-6-ones from commercially accessible substrates involved the carbonylation of aryl dibromides with indoles and the C–H activation of in situ-produced *N*-(2′-bromoaroyl)-indole. C–H activation likely occurred via conventional Pd(0)/Pd(II) transformations. It is noteworthy that glyoxylic acid monohydrate was used as an eco-friendly CO surrogate in the aminocarbonylation stage of the proposed tandem process. As a result, a number of *6H*-isoindolo[2,1-*a*]indol-6-ones were produced with yields of 40–64%.

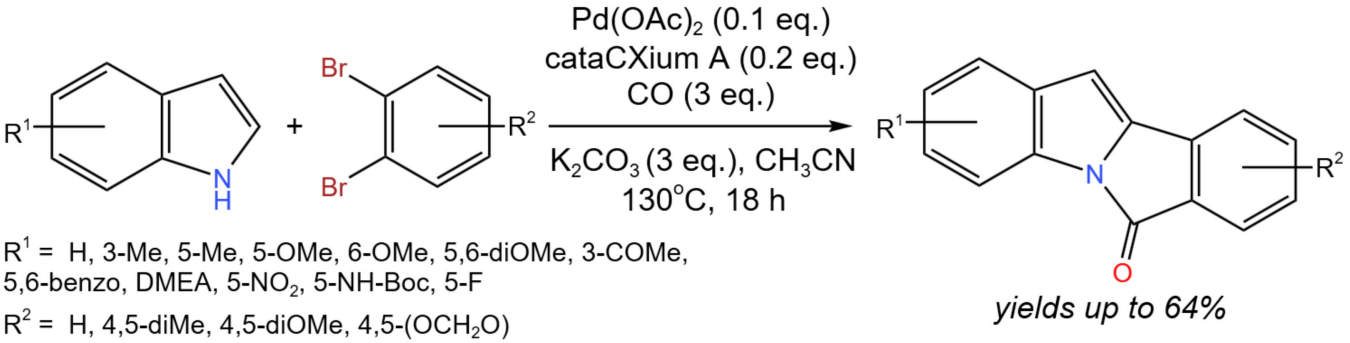

Figure 19. Tandem Pd-catalyzed carbonylation and C-C cross-coupling [62].

Li et al. [63] reported the enantioselective dearomative carbonylation of *N*-arylacyl indoles (Figure 20). The following reaction conditions were varied: Pd source ($Pd_2(dba)_3 \cdot CHCl_3$, $Pd(dba)_2$, $Pd_2(dba)_3$, $Pd(OAc)_2$, $Pd(TFA)_2$), chiral ligands, base additives (Et_3N, DIPEA, DABCO, K_2CO_3), and solvents (MTBE, MeCN, THF, Et_2O, PhOMe, toluene). Under the optimal conditions ($Pd_2(dba)_3$, Feringa ligand (*S*,*S*,*S*)-L1, Et_3N, MTBE) under the atmosphere of CO, the target products were formed yields of up to 89%, up to 97% ee, and dr > 20:1.

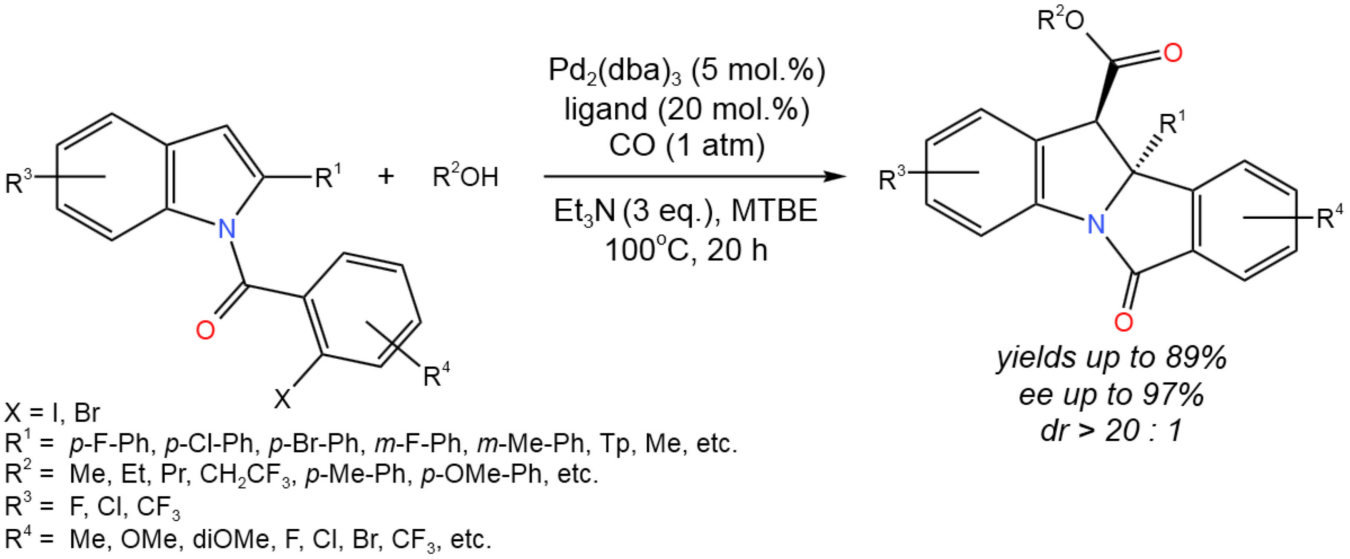

Figure 20. The scheme of thetandem Heck/carbonylation process for the asymmetric dearomatization of *N*-arylacyl indoles [63].

Wang et al. [64] developed the Pd-catalyzed multi-step tandem carbonylation/N-dealkylation/carbonylation reaction with alkyl as the leaving group and tertiary anilines as the nitrogen nucleophile, which allowed for the effective production of isatoic anhydride derivatives (Figure 21). Moderate to good (up to 80%) yields were obtained, depending on the substituents. Moreover, the developed approach was successfully used to synthesize Evodiamine—a biologically active alkaloid—with a 70% yield. The reaction mechanism involved two cycles. In the first cycle, the starting compound interacted with Pd(II) and CO. After the CO insertion and reductive elimination, the intermediate was formed, which then interacted with Cu(II) and O_2 and underwent C-N cleavage. Then, the resulting intermediate entered the second cycle and underwent another one CO insertion with the participation of Pd(II). After the reductive elimination and formation of the target product, the Pd(0) was oxidized by Cu(II) and O_2 to regenerate Pd(II).

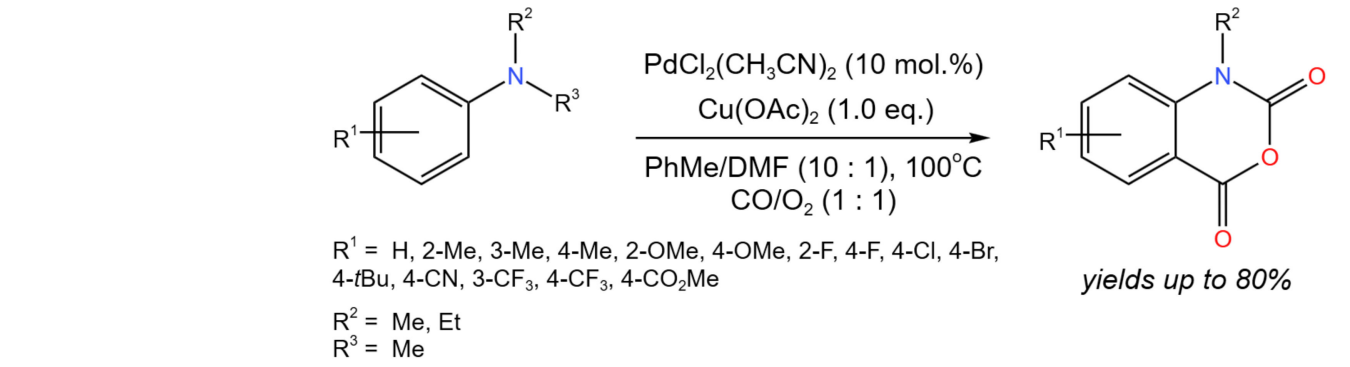

Figure 21. Tandem Pd-catalyzed carbonylation/N-dealkylation/carbonylation reaction of *N*,*N*-dialkyl anilines for the synthesis of isatoic anhydride derivatives [64].

For the synthesis of a variety of carbolinones under mild reaction conditions, Han et al. [61] proposed an effective tandem oxidative C–H aminocarbonylation and a dehydrogenation reaction co-catalyzed by Pd and Cu (Figure 22).

Figure 22. The scheme of the synthesis of β-carbolinones via the Pd/Cu co-catalyzed tandem C–H aminocarbonylation and dehydrogenation [61].

Carbolinones, tetrahydro-β-carbolinones, and tetrahydro-γ-carbolinoneswere selectively obtained with the yields of up to 90% by simply changing the reaction conditions. Strychnocarpine, a natural alkaloid, and its analogs were also produced.

The reaction proceeded through the well-known Pd(0)/Pd(II) transformations. The role of Cu(II) was in the oxidation of Pd(0) to regenerate Pd(II). In this process, Cu(II) was reduced to Cu(I), which was reoxidized with O_2.

A new P,O-hybrid ligand (L1) was developed by Zhao et al. [65] for the Pd-catalyzed bis-hydroaminocarbonylation of alkynes, allowing for the effective production of *N*-aryl substituted succinimides with the isolated yield of 57–90% (Figure 23) in the presence of methanesulfonic acid (MSA) as an additive. The catalyst L1-Pd$(CH_3CN)_2Cl_2$ system was reused for five runs without the precipitation of Pd-black.

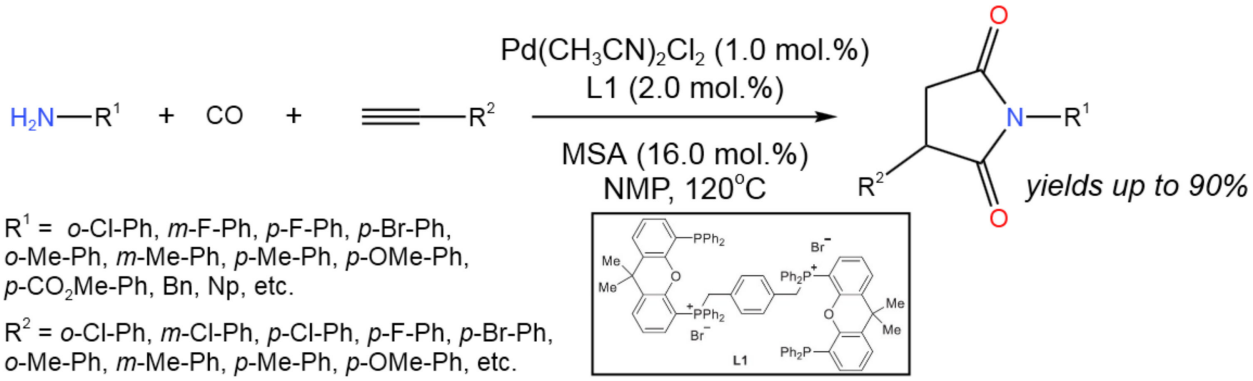

Figure 23. Pd-catalyzed bis-hydroaminocarbonylation of alkynes for the synthesis of *N*-aryl substituted succinimides [65].

One of the widespread reactions for the synthesis of cyclic compounds is the Diels–Alder reaction, which can be also combined with the carbonylation process [66]. Such an approach can provide a variety of functionalized carbocycles with complex architectures. Most of the methods of the synthesis of lactone-containing bridged polycyclic compounds are based on a stepwise protocol, restricting the overall scope and practicality of these transformations.

Therefore, the Pd-catalyzed tandem carbonylative Diels–Alder process was developed by Wang et al. [66] (Figure 24).

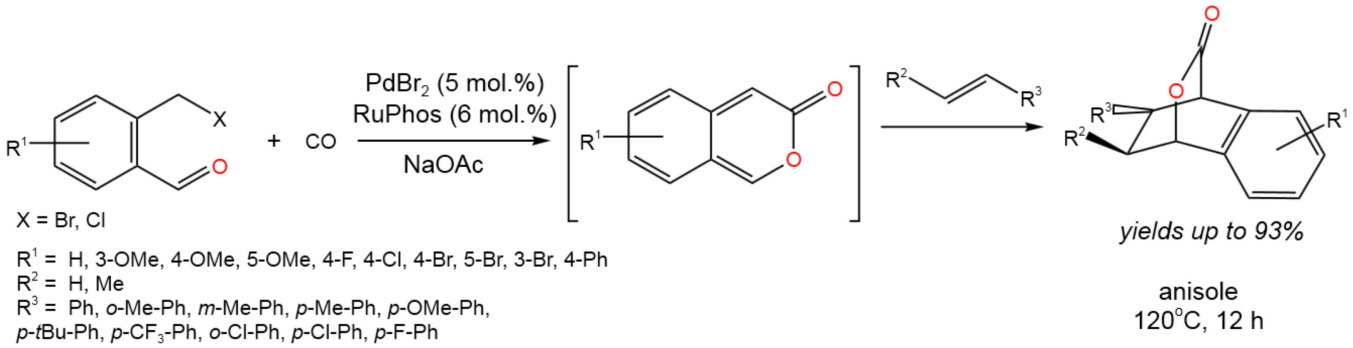

Figure 24. Scheme of the reaction of aldehyde-tethered benzylhalides and alkenes via the Pd-catalyzed tandem carbonylative lactonization and Diels–Alder cycloaddition [66].

It was proposed that the use of the aldehyde functionality as the reactive directing group resulted in good chemo- and stereoselectivity. Moderate to high (93%) yields were achieved, depending of the palladium source, base, and nature of substituents in the initial compounds [66]. The reaction was catalyzed by RuPhos-stabilized Pd(0), which was formed by the reduction of the Pd(II) precursor with CO or the ligand (RuPhos). Then, Pd(0) reacted with the substrate (benzaldehyde compound), producing an intermediate, which further underwent the insertion of CO. The subsequent reductive elimination resulted in the regeneration of Pd(0) and the formation of an intermediate, which underwent deprotonation due to interaction with NaOAc. Finally, the resulting benzopyran-2-one (shown in brackets in Figure 24) underwent [4 + 2]-cycloaddition with an alkene.

2.4. Cyclization Tandem Processes

Cyclization is another type of reaction widely used in fine synthesis [67–76]. Such reactions can proceed with the in situ-generated active species as a part of tandem catalytic transformations. For example, in order to produce EGFR (epidermal growth factor receptor) inhibitors, Ansari et al. [72,73] established a four-component procedure for the synthesis of pyrazolo[1,5-*c*]quinazolines with a small polar substitution of the pyrazole ring (Figure 25). In this tandem process, azomethine imine was generated in situ. Then, acetonitrile, having the electron-withdrawing group (EWG) at α-position (malononitrile, α-cyanocaboxyalate, orβ-ketonitrile), participated in the reaction.

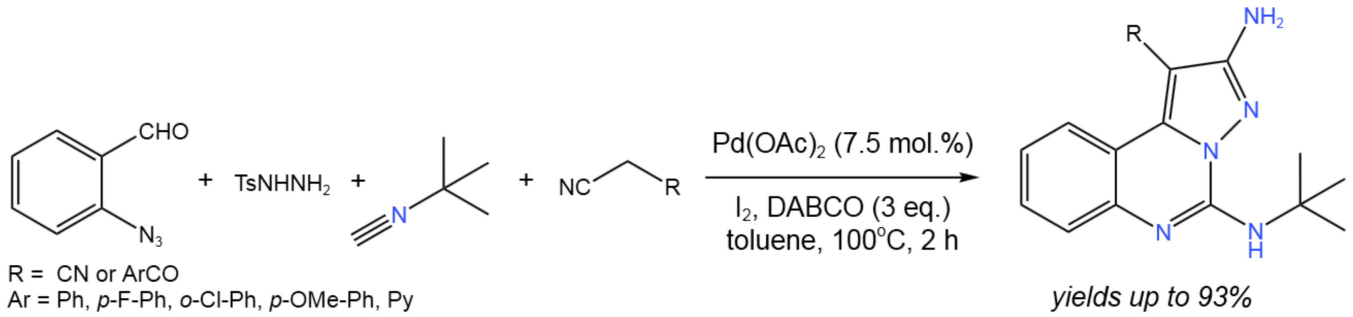

Figure 25. Four-component one-pot synthesis of pyrazolo[1,5-*c*]quinazoline [72].

In order to create 6-fluoroalkyl-phenanthridines in the absence of an oxidant, Bao et al. [77] developed a Pd-catalyzed tandem cyclization of fluorinated imidoyl chlorides using 2-bromophenylboronic acid (Figure 26). The developed procedure allowed for high yields (up to 97%) of target compounds using fluorinated imidoyl chlorides as fluorine-containing synthons. The authors [77] proposed the generally accepted Pd(0)/Pd(II) mechanism with Pd(0) as a starting active form, which interacts with fluorinated imidoyl chloride to form Pd(II). However, it was mentioned that the other pathway Pd(II)/Pd(IV) cannot be excluded.

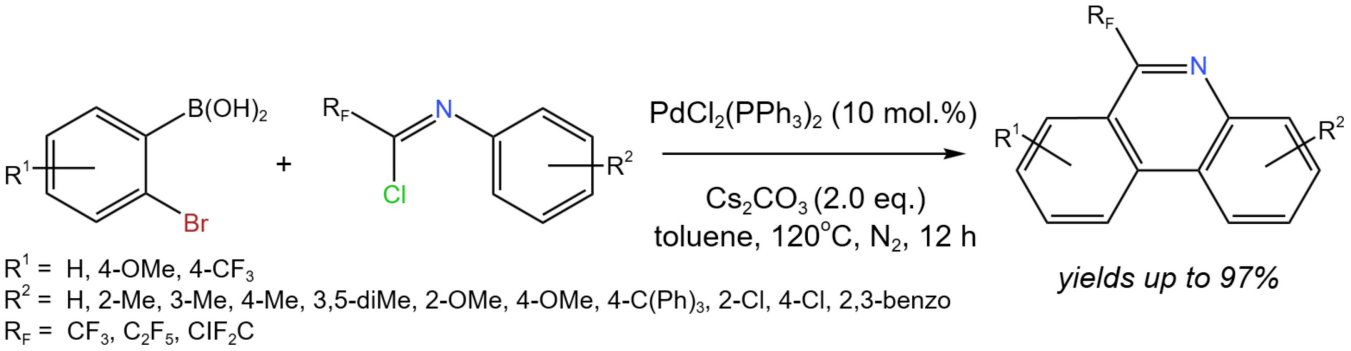

Figure 26. Synthesis of 6-fluoroalkyl-phenanthridines [77].

Another example of cyclization reactions proceeding with the participation of organic cyanides is the Pd-catalyzed tandem reaction of cyanomethyl benzoates with arylboronic acids developed by Dai et al. [78]. According to this approach, the selective synthesis of oxazoles and isocoumarins, through the intermediate imine–Pd complex obtained by carbopalladation of the nitrile, was found to depend strongly on substitution at the 2-position of starting cyano-compounds. Thus, 2,4-diaryloxazoles were selectively produced from cyanomethyl benzoates (3-benzoyl-4-aryl-isocoumarinsfrom 2-benzoyl-substituted cyanomethyl benzoates) with yields of up to 93% (Figure 27). To achieve high yields, different catalysts ($Pd(acac)_2$, $Pd(TFA)_2$, etc.), ligands (2,2′-bipyridine and its derivatives), additives (TfOH, TFA), and reaction conditions, such as solvent nature (THF, dioxane) and atmosphere (air, N_2), were applied.

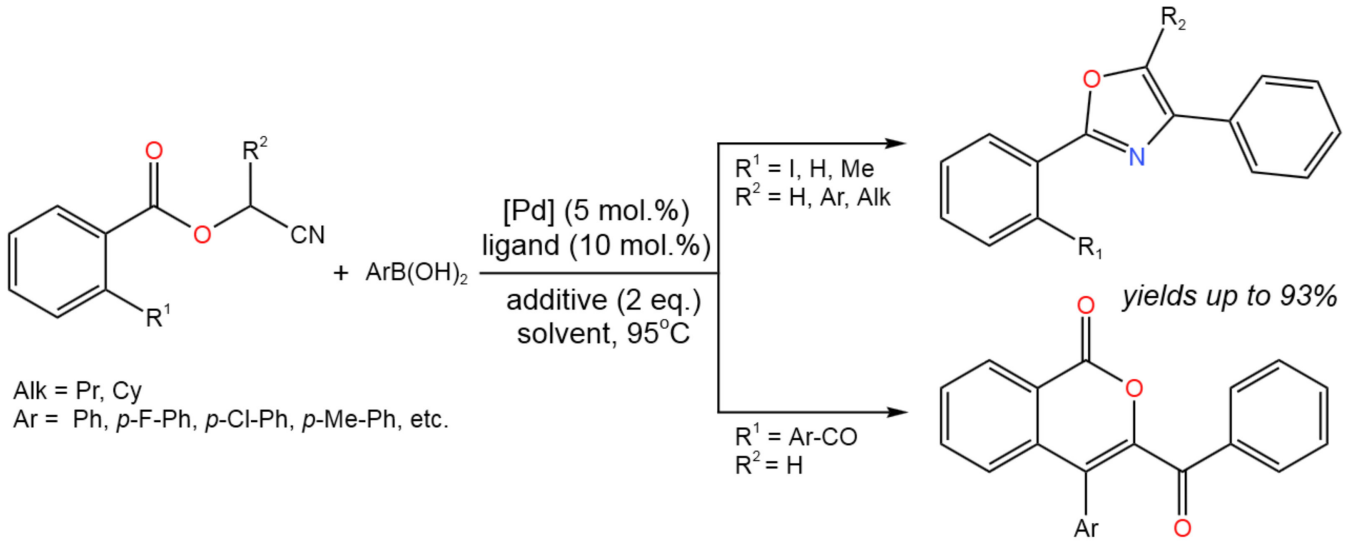

Figure 27. Scheme of the tandem reaction of cyanomethyl benzoates with arylboronic acids for the synthesis of oxazoles and isocoumarins [78].

By using the Pd-catalyzed tandem reaction of 2-aminostyryl nitriles with arylboronic acids, Xu et al. [79] developed a new protocol for the synthesis of 2-arylquinolines (Figure 28). The proposed procedure is an alternative synthetic route as compared to the common condensation reaction of (*E*)-2-aminostyryl ketones. It is noteworthy that the reaction was catalyzed by Pd(II), which interacted with arylbotonic acid, the resulting aryl-palladium complex, then reacted with the nitrile.

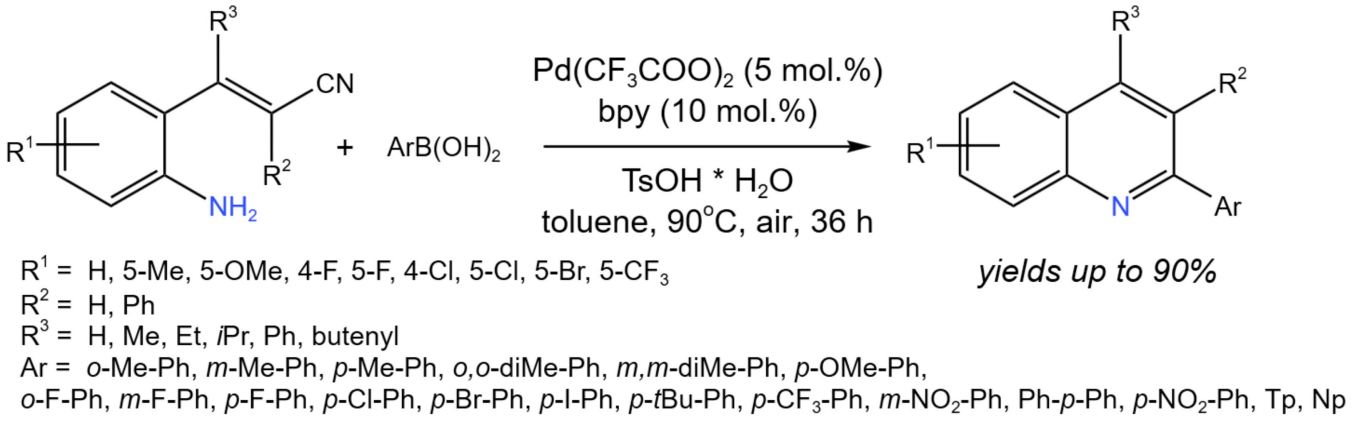

Figure 28. Pd-catalyzed tandem reaction of 2-aminostyryl nitriles with $ArB(OH)_2$ [79].

In a similar manner, Yao etal. [80] implemented the tandem Pd-catalyzed cascade carbopalladation/cyclization/aromatization of arylboronic acids with 5-oxohexanenitrile and its derivatives to synthesize 2-methyl-6-arylpyridines. Different catalysts ($Pd(OAc)_2$, $Pd(CH_3CN_2)Cl_2$, $Pd(CF_3CO_2)_2$, $PdCl_2$, $Pd(PPh_3)_2Cl_2$, $Pd_2(dba)_3$), ligands, and solvents (THF, DMSO, DMF, 1,4-dioxane, toluene, acetone, MeOH, EtOH, nPrOH, *i*PrOH, nBuOH, 1-PeOH, H_2O) were studied. As a result, the optimum conditions were found ($Pd_2(dba)_3$ (5 mol.%), 2,2′-bipyridine ligand (10 mol.%), MeOH), which allowed for up to 94% yields of the target product for 12 h, depending on the substituents in the initial substrate molecules, with CF_3COOH as an additive at 90 °C in air.

Ye et al. [81] established a palladium-catalyzed approach for the tandem reaction of 2-(arylamino)benzonitrile with arylboronic acids in water to produce 9-arylacridine derivatives posessing estrogenic biological activity (Figure 29).

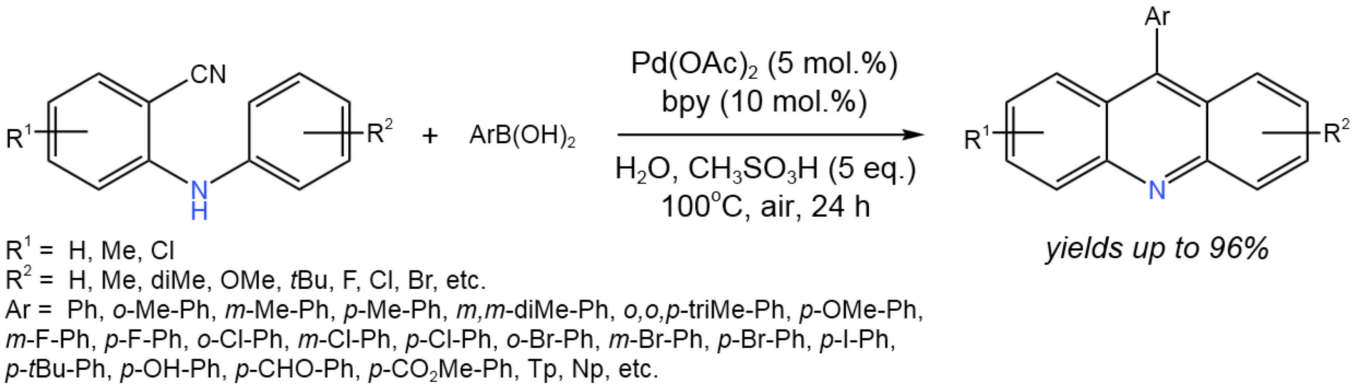

Figure 29. Tandem reaction of 2-(arylamino)benzonitrile with arylboronic acids for the synthesis of 9-arylacridine derivatives [81].

High yields of the desired products (up to 96%) were achieved via the proposed tandem process, involving the nucleophilic addition of aryl Pd species to the nitrile to produce an aryl ketone intermediate, which then underwent an intramolecular Friedel–Crafts acylation and dehydration to produce acridines.

A method for the production of benzoxazinones or quinazolinones was reported by Lang et al. (Figure 30) [82].

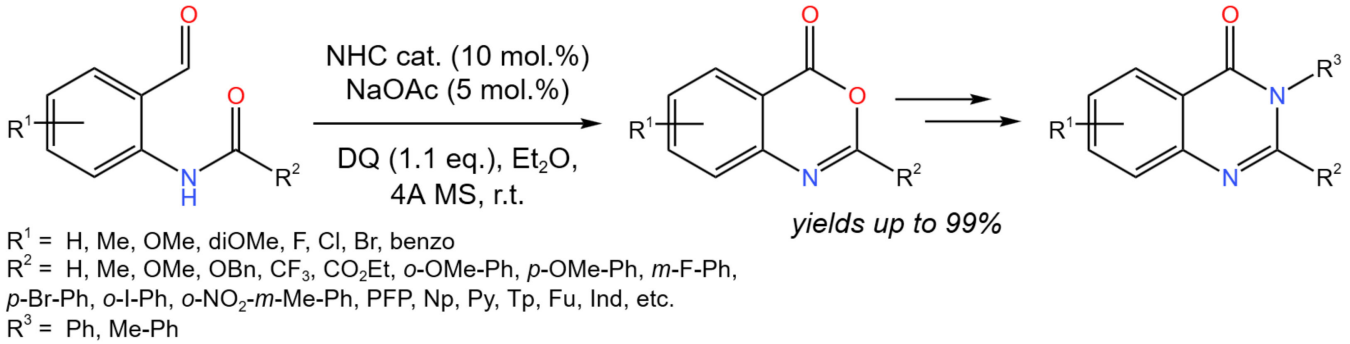

Figure 30. Carbene-catalyzed tandem isomerization/cyclisation for the synthesis of benzoxazinones or quinazolinones [82].

It was mentioned that other protocols are carried out under harsh conditions, restricting the functional group tolerance. According to the proposed strategy, benzoxazinone skeletons were synthesized via utilizing an oxidative carbene-catalyzed tandem isomerization/cyclisation process, which, under mild conditions, allowed for the production of a number of valuable benzoxazinones or quinazolinones from a wide range of substrates.

By using a one-pot intramolecular C–N coupling cyclization reaction, Patel et al. [83] created promising catalytic process to incorporate four-membered ring systems between the benzimidazole and 4-phenyl quinoline cores (Figure 31). This protocol was proposed to be an attractive route for the synthesis of different heterocycles, considering its high efficiency (yields up to 94%), wide substrate scope, and mild reaction conditions [83].

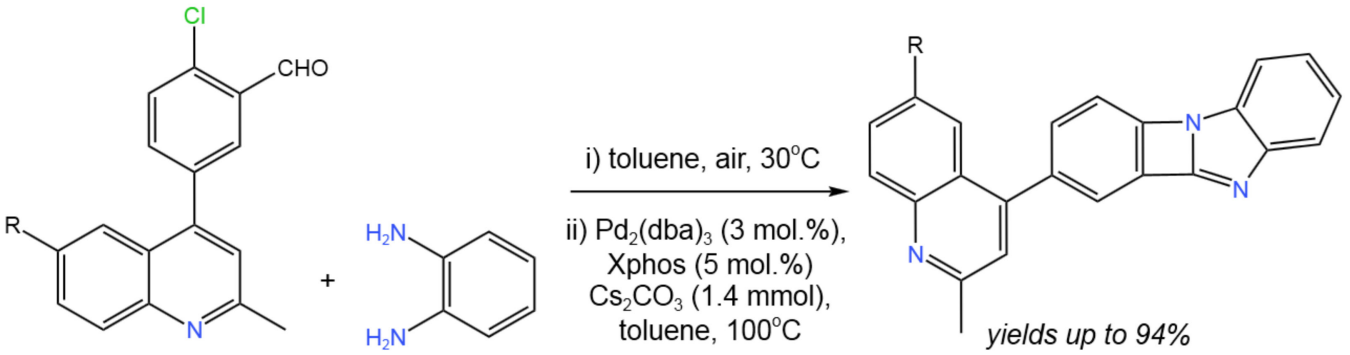

Figure 31. Scheme of the Pd-catalyzed intramolecular C–N coupling cyclization reaction [83].

The reaction likely begun with the condensation of *o*-phenylenediamine with 2-chloro-5-(*N*-substituted-2-methylquinoline-4-yl) benzaldehyde. The resulting intermediate then underwent C–N coupling via conventional Pd(II)/Pd(0) chemistry, starting with the oxidative addition to Pd(0) [83].

Another example of intramolecular cyclization is the work of Jin et al. [84], who developed new method for the synthesis of a cyclopenta-fused acenaphtho[1,2-*b*]indole (ANI) scaffold (Figure 32).

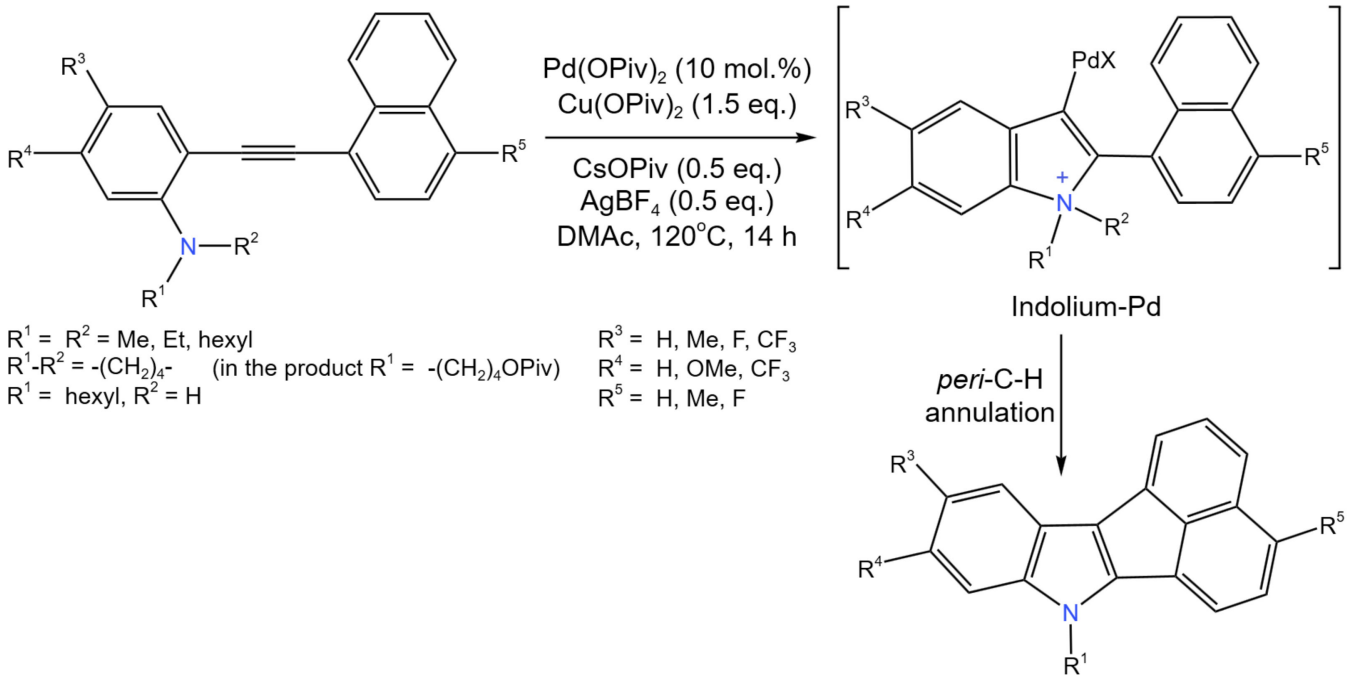

Figure 32. Scheme of Pd-catalyzed intramolecular C–N coupling cyclization reaction [84].

This Pd-catalyzed cascade process involved indolization, *peri*-C–H annulation, and N-dealkylation. Numerous *o*-alkynylanilines containing different substituents and tethered with various polyaromatic hydrocarbons having a *peri*-C–H bond were studied, allowing an up to 79% yield of the target product. It is noteworthy that, in contrast to the secondary aniline, the substrate with a *N*,*N*-dihexyl substituent resulted in an ANI with 100% selectivity [84].

In a similar way, Siciliano et al. [85] carried out the cyclisation of *o*-alkynyl-anilines using a ligand-free $Pd(OAc)_2$ catalyst in 3 wt.% TPGS-750-M/H_2O medium. Since the amino group was unprotected, the 2-substituted indoles were obtained with a yield of up to 76%, depending on the conditions (catalyst loading (2–10 mol.%), temperature (80–100 °C), type of heating (MW or oil bath), additive (AcOH, $C_{11}H_{23}COOH$, DPBA), and reaction duration (from 10 min to 16 h). Moreover, the tandem process Sonogashira/indole cyclisation was implemented according to the Cu-free mechanism, with the Pd(II) as the active species, which allowed for an up to 40% yield of the target product [85]. It is noteworthy that 2-substituted indoles can be also obtained via tandem Sonogashira coupling, followed by reductive cyclization with 1-halo-2-nitrobenzenes and terminal alkynes as starting compounds [69].

The Pd-catalyzed cascade addition/cyclization/aromatization of heteroarenes (e.g., thiophenes, furans, pyrroles, and indoles) with 2-(cyanomethoxy)chalcones was shown to be a promising approach for the synthesis of various benzofuro [2,3-*c*]pyridines (Figure 33) [86]. The following reaction conditions were varied: catalyst ($PdCl_2$, $Pd(CF_3CO_2)_2$, $Pd(acac)_2$, $Pd(OAc)_2$), solvent (DMA, NMA, THF, DMF, toluene), temperature (60–120 °C), oxidant (Ag_2CO_3, $Cu(Oac)_2$, $AgNO_3$, Ag_2O, $AgSbF_6$, $AgCF_3CO_2$), and additive (D-CSA, CF_3CO_2H, CF_3SO_3H, *p*-TsOH, CH_3CO_2H). As a result, the optimum parameters were chosen (catalyst $Pd(OAc)_2$; solvent NMA; additive CH_3CO_2H; temperature $\geq$ 80 °C; and, optionally, $AgCF_3CO_2$), which provided the yields of target products of up to 86%.

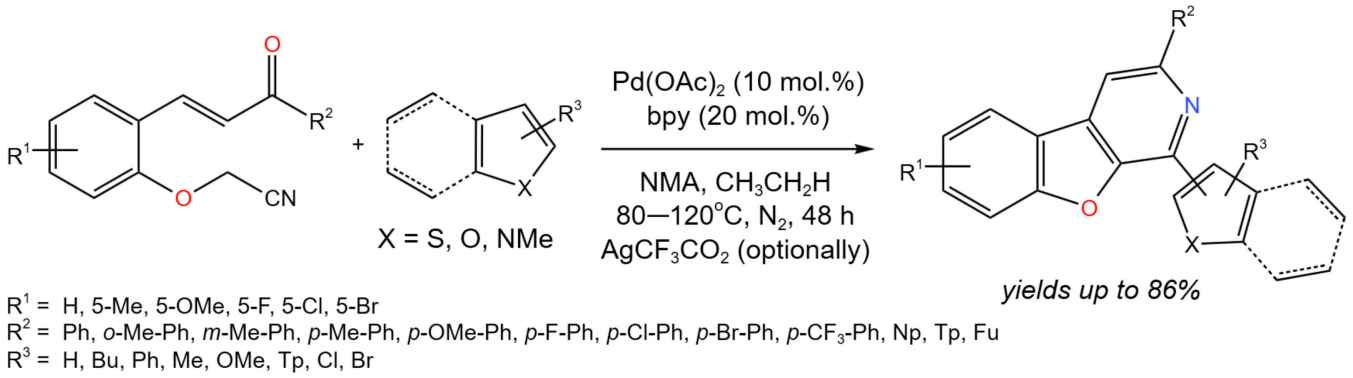

Figure 33. Pd-catalyzed cascade reaction of 2-(cyanomethoxy)chalcones with heteroarenes [86].

A novel procedure for the tandem intramolecular addition of active methylene compounds to internal alkynes, followed by coupling with aryl and heteroaryl bromides, was described by Błocka et al. [87] (Figure 34).

Figure 34. Tandem Pd-catalyzed carbocyclizationcoupling of methylene compounds bearing an internal alkyne group with aryl and heteroaryl bromides [87].

As a catalyst, third-generation (G3) Buchwald palladium precatalysts in combination with diphenyl-2-pyridylphosphine (DPPPY) ligand was used. This method allowed for the obtaining of a variety of vinylidenecyclopentanes with yields of up to 90%, providing high regio- and stereoselectivity and tolerance to the wide range of substituents. Thus, the the *5-exo-dig* intramolecular addition proceeded with high efficiency.

The mechanism involving oxidative addition, cyclization, and reductive elimination was also confirmed by the computational study. The rate- and configuration-determining step was found to be the 5-*exo-dig* intramolecular nucleophilic addition of the enol intermediate to the alkyne activated via coordination with Pd(II) [87].

2.5. Other Tandem Processes

There are many other tandem reactions homogeneously catalyzed by palladium. Below, we provide several examples, among which are alkylation, alkenylation arylation, cycloaddition, and carboannulation.

For example, Hu et al. [88] developed a one-pot approach for the synthesis of a triphenylene core under ligand-free conditionsusing commercially available (hetero)aromatic carboxylic acids and cyclic diaryliodonium salts (Figure 35). The obtained triphenylenes can be used as the electrontransport materials. The proposed reaction mechanism involved an acid-directed *ortho*-C–H arylation/intramolecular decarboxylative annulation sequence mediated by Pd(II)/Pd(IV) transformations.

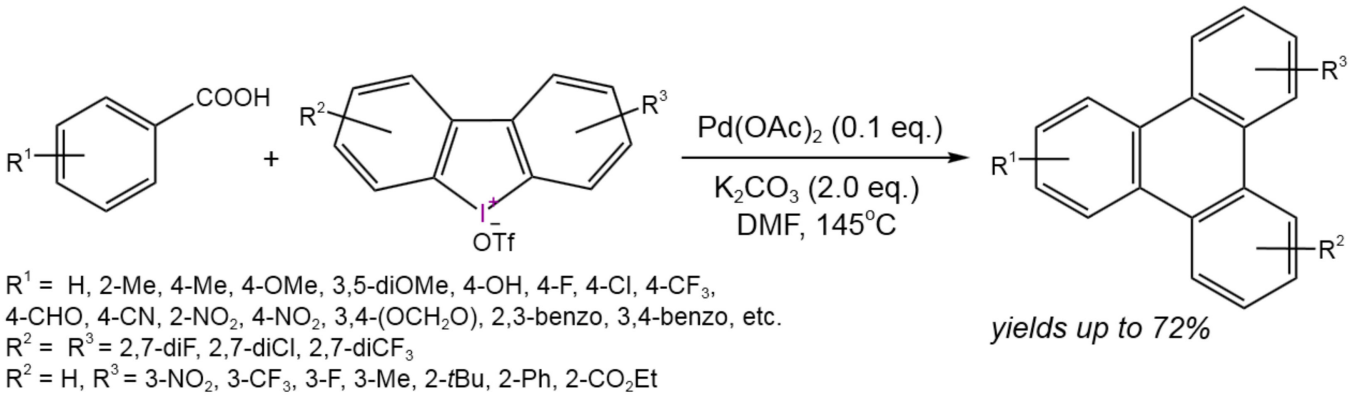

Figure 35. Scheme of tandem C–H arylation/decarboxylative annulation for the synthesis of functionalized triphenylenes [88].

The novel procedure of arylation-cyclization was developed for the synthesis of 3-aryl-2-quinolone (Figure 36) and 4-aryl-2-quinolone derivatives from simple *E*/*Z* geometric isomer precursors using oxygen as a co-oxidant [89].

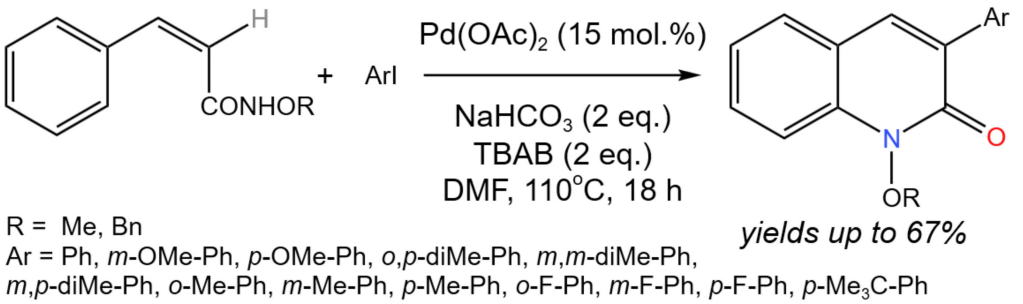

Figure 36. Scheme of tandem arylation-cyclization for the synthesis of 3-aryl-2-quinolones [89].

Ghosh and Chattopadhyay [74] identified the following Pd-catalyzed tandem procedures, which can be applied for the synthesis of 4-aryl-2-quinolones:

(i) intramolecular hydroarylation of yanamides;
(ii) hydroarylation-heterocyclization of 2-aminophenyl propiolate;
(iii) Heck-heterocyclization;
(iv) oxidative Heck-heterocyclization;
(v) arylation of *ortho*-halo-cinnamides, followed by Buchwald-type intramolecular amidation.

In the developed approach, the unusual complementary regioselectivity was found in the tandem C–H-arylation C–H-amidation of isomeric substrates. The origin of selectivity was proposed at the C–H-arylation step [89].

Domańskiet al. [90] described the tandem Pd-catalyzed three-component reaction that allowed for regio- and stereoselective perfluoroalkylative borylation of a variety of terminal and internal alkynes in the presence of perfluoroalkyl iodide and $(Bpin)_2$. Thus, the first example of anti-addition across C–C multiple bonds of groups originating from two separate electrophiles to functionalize alkynes by reductive dicarbofunctionalization was shown. Iodoperfluoroalkylation, borylation, and coupling are the three fundamental processes responsible for this sequential transformation, and mechanistic studies have shown that their rates significantly differ (Figure 37).

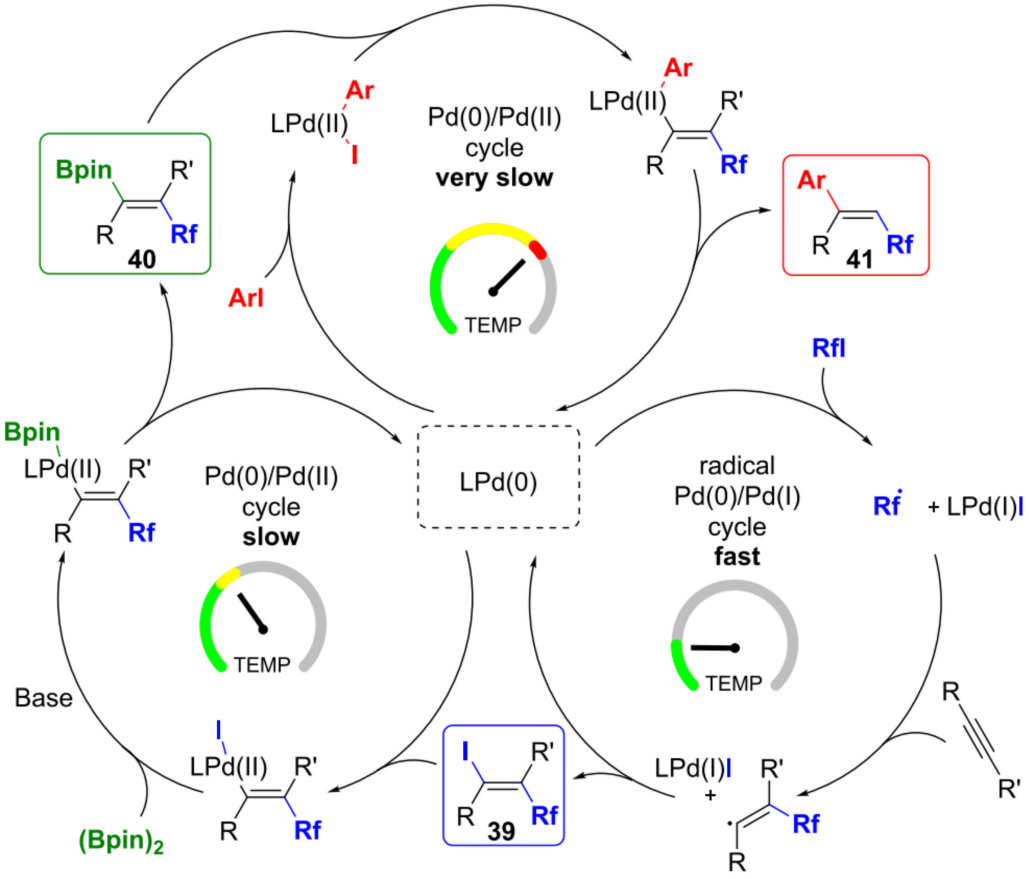

Figure 37. Proposed reaction mechanism of perfluoroalkylative borylation. Reproduced with permission from [90]. Copyright 2019 American Chemical Society.

According to the developed tandem process, from the same reaction mixture and under the same reaction conditions, the fluoroalkyl-substituted vinyl iodides, vinyl boronates, or olefins can be produced by changing the temperature program [90].

The Pd-catalyzed direct tandem C–O/C–H activation method for the C–C bond formation was described by Fernández et al. [91]. To accomplish base-free direct C–H alkenylation, the novel approach combined coordinated metalation–deprotonation of functionalized heterocycles with a C–O oxidative addition at enol pivalates (Figure 38).

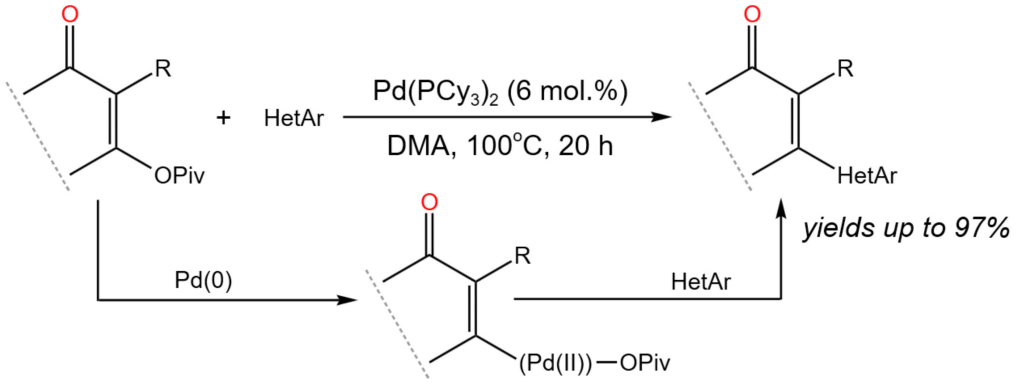

R = H, Ph, Bn, *o*-F-Bn, *m*-Me-Bn, *p*-CN-Bn, *p*-CF_3-Bn

Figure 38. General scheme of Pd-catalyzed tandem C–O/C–H activation [91].

According to mechanistic studies, the C–O oxidative addition to Pd(0) was shown to be reversible, and the product of the Pd(II) C–O oxidative addition directly resulted in C–H activation [91].

Zhang et al. [92] developed a prospective route for the synthesis of poly-substituted quinolines via a three-component tandem reaction. 2-Aminobenzonitriles, arylboronic acids, and ketones were used as the substrates. Pd-catalyzed aryl addition to the cyano group was followed by hydrolysis and Friedländer-type cyclization to produce the quinoline compounds, with the yields of up to 96%. The described above cyclization tandem process developed by Xu et al. [68] resulted in lower yields, while comparing the same structures of target products.

Through the three-component tandem arylation and allylic etherification of 2,3-allenol with aryl iodides and alcohols, an effective approach for the synthesis of arylated allylic ethers was implemented [93]. By this method, functionalized 1-arylvinylated 1,2-diol derivatives were produced with yields of up to 83% and complete selectivities.

Tang et al. [94] reported a Pd-catalyzed tandem reaction of 3-allyloxybenzocyclobutenols that involved proximal C–C bond cleavage, C–O bond cleavage, and allylic alkylation of the C–H bond. Thus, a novel approach to *meta*-*β*-keto phenols bearing an allylic group with 100% atom economy was developed. It is noteworthy that, by adjusting substituents on various positions of benzocyclobutenols, sequential proximal or distal C–C bond cleavage/deallylation could be implemented.

Li et al. [95] developed a tandem process for the selective assembly of tri- or tetrasubstituted vinylsilanes. It was shown that using this method, *ortho*-vinyl bromobenzenes can be formed in situ from 1-bromo-2-iodobenzenes and *N*-tosylhydrazones and disilylated to produce two C–Si bonds and two C–C bonds (Figure 39).

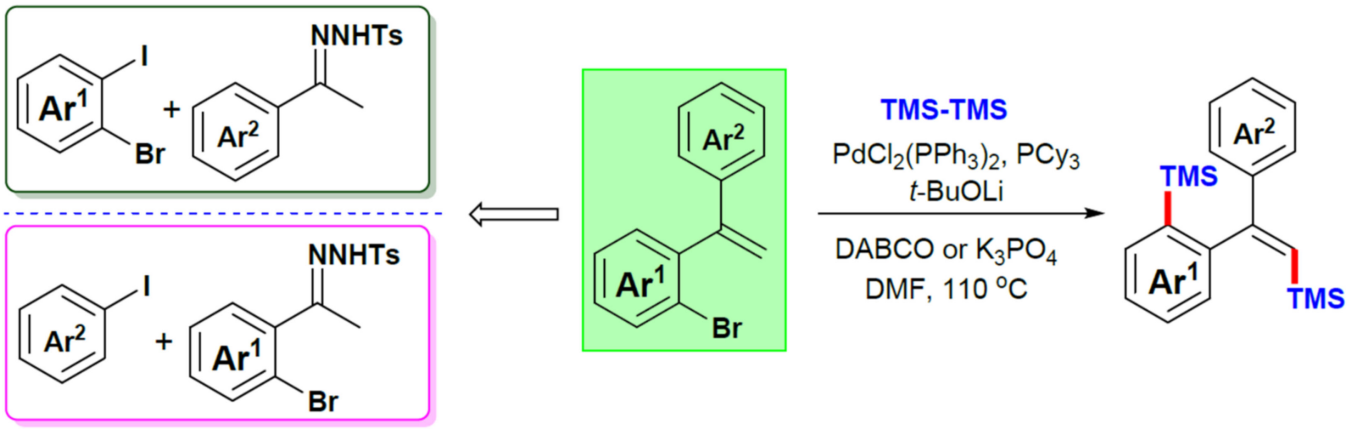

Figure 39. General scheme of the disilylation of C(aryl),C(vinyl)-palladacycles. Reproduced with permission from [95], RCS, 2020.

It was determined that the *ortho*-vinyl bromobenzenes produced from 1-bromo-2-iodobenzenes and *N*-tosylhydrazones are the crucial intermediates needed to manufacture vinylsilanes by disilylating the C(aryl),C(vinyl)-palladacycle, which is formed by a direct vinylic C–H bond activation [95].

By the reaction with aldehydic *N*-tosylhydrazones, the treansformation of 1-aryl- and 2-aryl-1,2-dihydro-3*H*-indazol-3-ones into 1,2-di(hetero)aryl- and 2,3-di(hetero)aryl-2,3-dihydroquinazolin-4(1*H*)-ones was carried out (Figure 40) [96]. The method involved a cascade process that included base-mediated Pd-carbenoid production via the decomposition of *N*-tosylhydrazones, a nucleophilic attack of indazolone on the Pd-carbenoid complex, and intramolecular ring expansion by N–N bond cleavage.

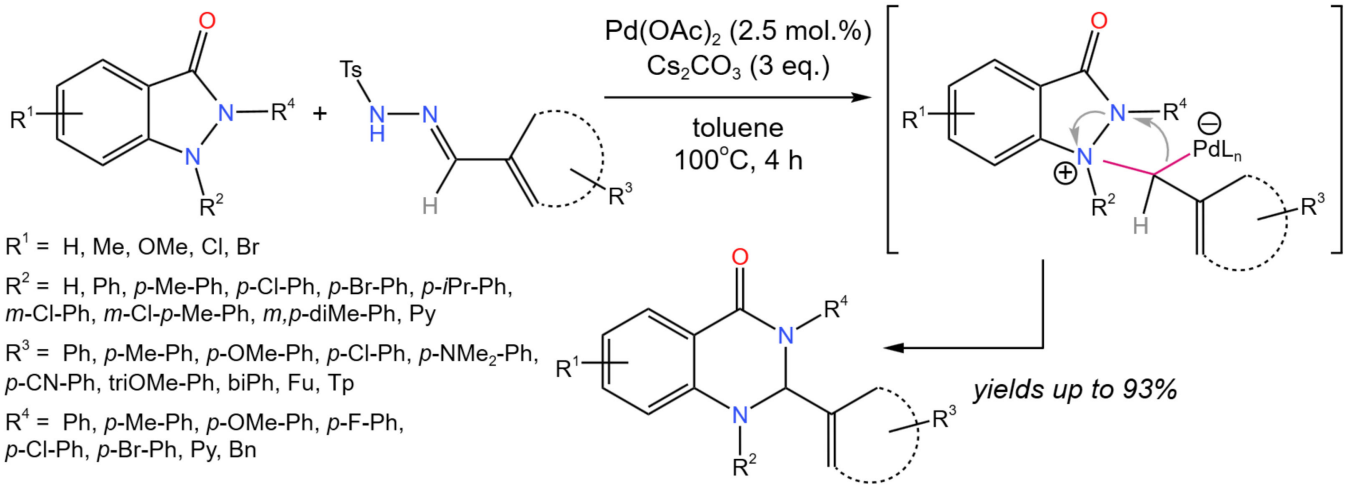

Figure 40. General scheme of Pd-catalyzed tandem C–O/C–H activation for the synthesis of 1,2-di(hetero)aryl- and 2,3-di(hetero)aryl-2,3-dihydroquinazolin-4(1*H*)-ones [96].

An interesting approach to the synthesis of [4,5]-spirocycles in a cascade Pd-catalyzed reaction was reported by Azizollahi et al. [97]. It was found that, when varying the type of ligand, the reaction pathway can be switched from carbopalladation to β-C-elimination: monodentate phosphine ligand (IMes·HCl, PCy_3) affords [4,5]-spirocycles, while bidentate phosphines (Xantphos, DPPF, DPE-Phos) results in the formation of heteroaromatics (Figure 41).

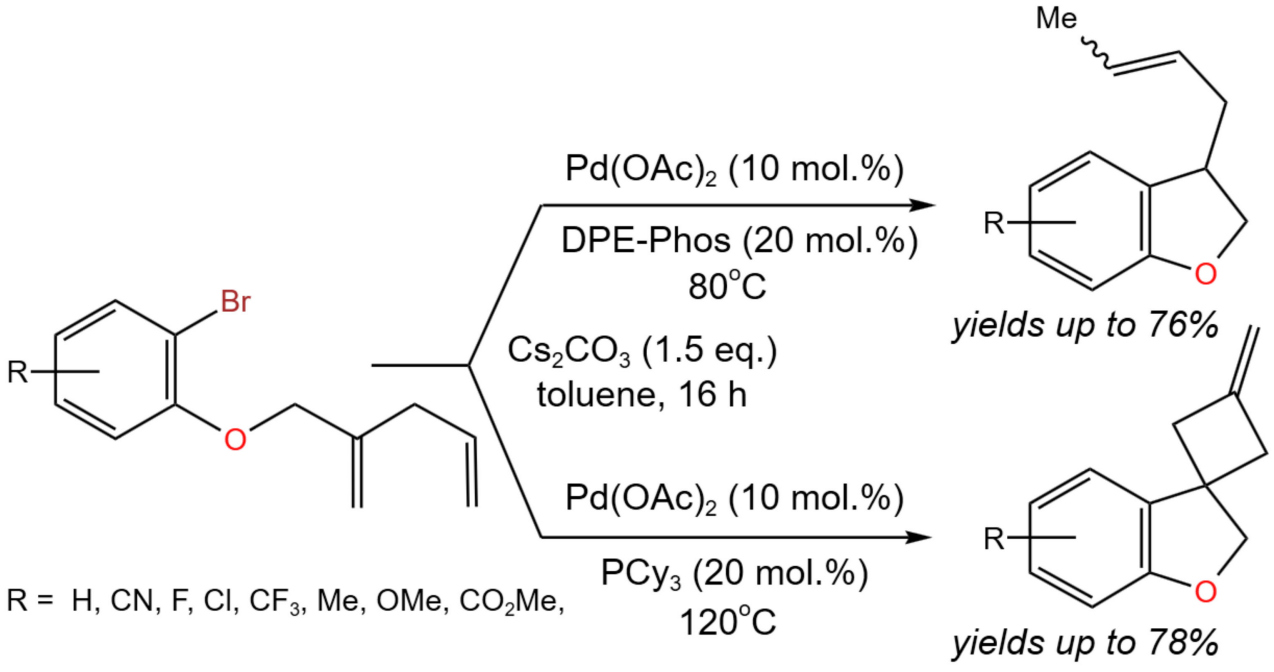

Figure 41. Ligand-controlled cascade synthesis of [4,5]-spirocycles from skipped dienes [97].

Another example of switchable cascade reactions was the oxidation of *N*-allyl-2-aminophenols [98] in the presence of hypervalent iodines and Pd catalyst ($Pd(OAc)_2$). In the absence of palladium, the dearomatization of the substrate and intramolecular Diels-Alder reaction occurred with the formation of tricyclic systems (yields of up to 72%), while the Pd-catalyzed process resulted in the methylacyloxylated dihydro-1,4-benzoxazines (yields of up to 86%).

Activated tetrasubstituted alkenes made from phthalides or butyrolactone were combined with vinylethylene carbonates in an unprecedented [5 + 2] cycloaddition/ring-contraction tandem process by Xiong et al. [99] under Pd(0) catalysis (Figure 42). The proposed approach was practical and mechanistically novel. In contrast to the traditional spirolactonization method, benzo-[5,5]-spiroketal lactones and [5,5]-spiroketal lactones bearing two vicinal tetrasubstituted centers can be obtained by this tandem [5 + 2] cycloaddition/ring-contraction mechanism with moderate to high yields.

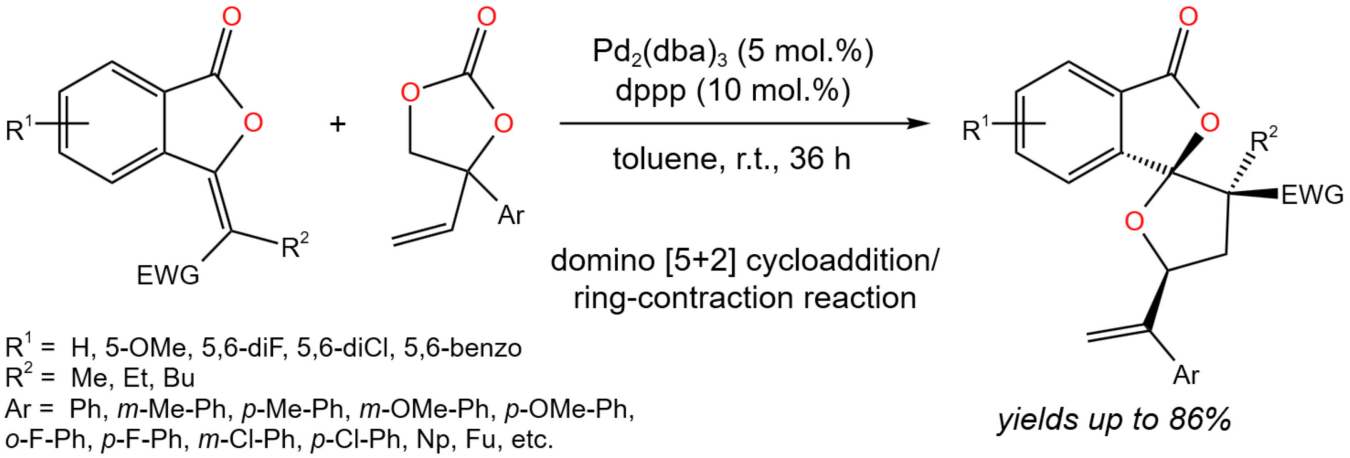

Figure 42. Pd-catalyzed [5 + 2] cycloaddition/ring-contraction tandem process [99].

It was proposed that the reaction was started from the formation of a zwitterionic π-allyl palladium intermediate via the interaction of vinylethylene carbonate with Pd(0), accompanied by the decarboxylation. Then, the intermediate reacted with activated phthalide or butyrolactone through [5 + 2] cycloaddition. Thus, a complex of Pd(0) and a spiro-oxepene phthalide was formed, which further facilitated the ring-opening reaction, resulting in a new zwitterionic π-allyl palladium intermediate. Finally, the branched allylic etherification occurred with the formation of a target product [99].

The first example of a transition-metal-catalyzed multicomponent carboannulation reaction of [60]fullerene was reported by Liu et al. [100]. In a Pd-catalyzed three-component tandem coupling–carboannulation process, [60]fullerene, 2-(2,3-allenyl)-malonates, and (hetero)aryl iodides were converted into a variety of polysubstituted [60]fullerene-fused cyclopentanes with a wide range of substrates and excellent functional group compatibility (Figure 43).

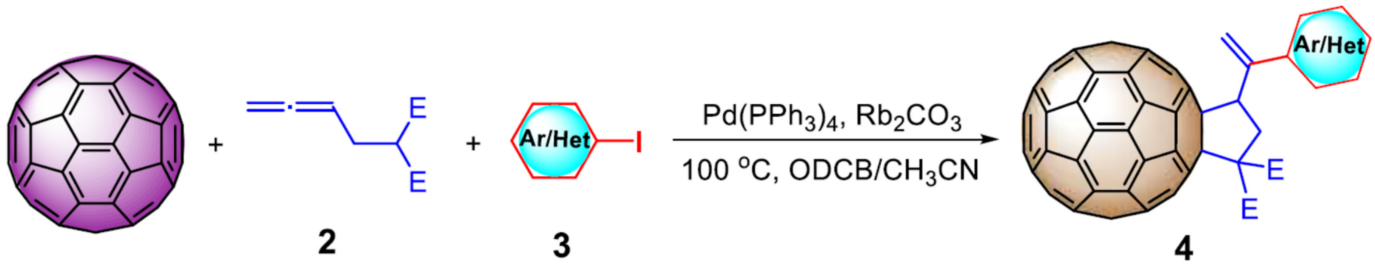

Figure 43. Scheme of Pd-catalyzed tandem coupling–carboannulation for the regioselective synthesis of polysubstituted C_{60}-fused cyclopentanes. Reproduced with permission from [100]. Copyright 2020 American Chemical Society.

Different reaction conditions were explored: catalysts ($Pd(PPh_3)_4$, $Pd(dba)_2$, $Pd_2(dba)_3 \cdot\cdot CHCl_3$), bases ($Li_2CO_3$, Cs_2CO_3, K_2CO_3, K_3PO_4, Rb_2CO_3, DMAP, and DABCO), and co-solvents (CH_3CN, THF, 1,4-dioxane, DMF, and DMSO). Thus, the optimal conditions were found ($Pd(PPh_3)_4$, Rb_2CO_3, 100 °C, solvent 1,2-dichlorobenzene (ODCB), cosolvent CH_3CN), which allowed for an up to 62% yield of the reaction product [100].

Zhang et al. [101] developed the Pd-catalyzed tandem synthesis of 2-trifluoromethylthio-(seleno)-substituted benzofurans, benzothiophenes, and indoles (Figure 44) in acceptable to good yields (up to 93%). The reaction likely proceeded via the intramolecular cross-coupling followed by trifluoromethylthiolation.

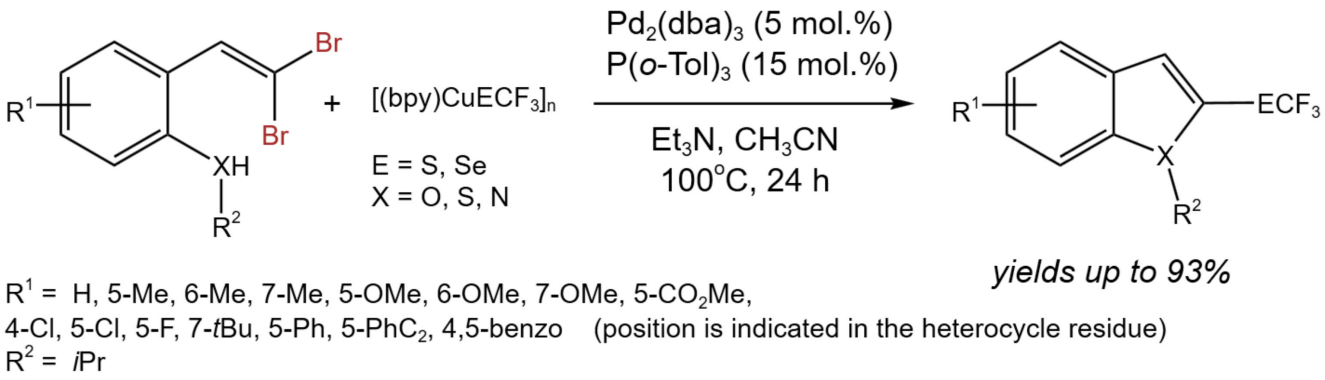

Figure 44. Pd-catalyzedtandem synthesis of 2-trifluoromethylthio-(seleno)-substituted benzofurans, benzothiophenes, and indoles [101].

Yang et al. [102] reported the asymmetric tandem C–C bond activation/Cacchi reaction between cyclobutanones and *o*-ethynylanilines (Figure 45). The chiral σ-alkylpalladium intermediates were formed via the enantioselective C(sp^3)–C(sp^2) bond activation of cyclobutanones and then promoted the cyclization of *o*-ethynylanilines, leading to one-carbon-tethered chiral indanone-substituted indoles. An all-carbon quaternary stereocenter was simultaneously formed, along with the two C–C bonds and one C–N bond. Under the optimum conditions (catalyst: $[Pd(allyl)Cl]_2$ (0.05 eq.), TADDOL-derived phosphoramidite: L1 (0.1 eq.), base: K_2CO_3 (2.5 eq.), solvent: 1,4-dioxane, temperature: 90 °C), the indanone-substituted indoles with both central and axial stereogenic elements were synthesized with good yields (up to 85%) and excellent enantioselectivity (up to 99:1 e.r.).

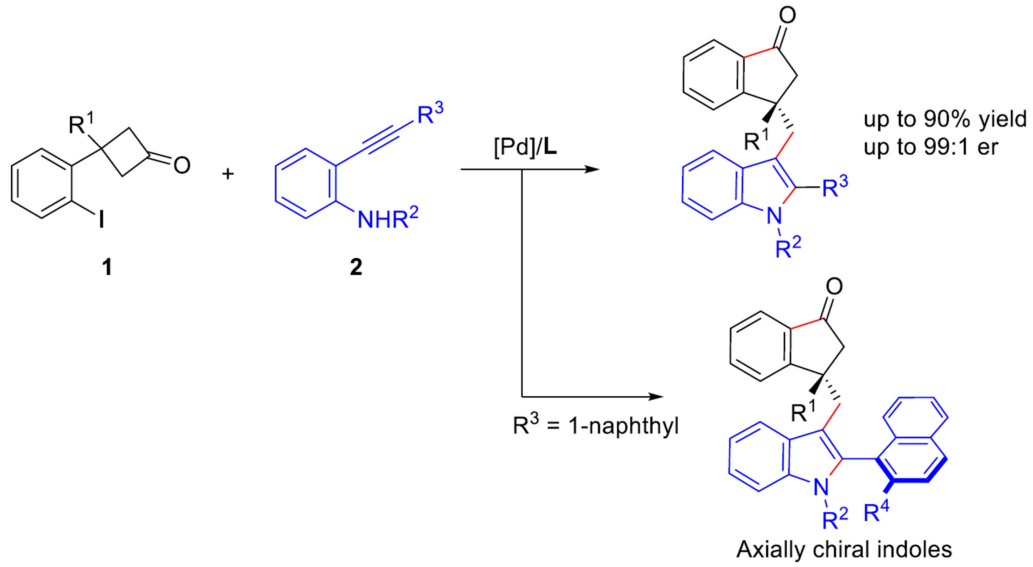

Figure 45. Pd-catalyzed enantioselective tandem ring-opening/Cacchi reaction. Reproduced with permission from [102]. Copyright 2021 American Chemical Society.

The borrowing hydrogen (BH) reaction (hydrogen autotransfer) is another example of Pd-catalyzed tandem processes that can be mentioned [103] as a powerful strategy that combines transfer hydrogenation (avoiding the direct use of molecular hydrogen) with one or more intermediate reactions to synthesize more complex molecules without the need for time-consuming separation or isolation processes. The strategy of the BH process relies on three steps, namely, (i) dehydrogenation, (ii) intermediate reaction, and (iii) hydrogenation, among which the intermediate reaction works in tandem with the metal-catalyzed hydrogenation/dehydrogenation step.

3. Heterogenized PdComplexes in Tandem Processes

Homogeneous Pd complexes can be anchored to the different organic or inorganic supports. Such heterogenized complexes can be also used in tandem catalytic processes.

As for the examples of heterogenized Pdcomplexes reported for the last five years in terms ofapplication in tandem reactions, the works of Fan et al. [104] and Esfandiary et al. [105] can be mentioned. In both cases, Pd catalyzed the chosen tandem process homogeneously, while the support facilitated the separation and reuse of the catalysts.

Fan et al. [104] synthesized a polyethyleneimine (PEI)-capped microcrystalline cellulose(MCC)-supported polyamidoamine (PAMAM) dendrimer (MCC-$PAMAM_{G2.5}$-PEI) for the loading of Pd^{2+} and Cu^{2+} ions. In this catalytic system, $PAMAM_{G2.5}$ served as the carrier to immobilize Pd^{2+} ions, and PEI provided the coordinating sites to selectively chelate Cu^{2+} species. The Pd/Cu@MCC-$PAMAM_{G2.5}$-PEI was tested in a Sonogashiracyclization tandem reaction (Figure 46), revealing excellent catalytic activity, recyclability, and robustness. The synergetic effect between Pd and Cu was observed.

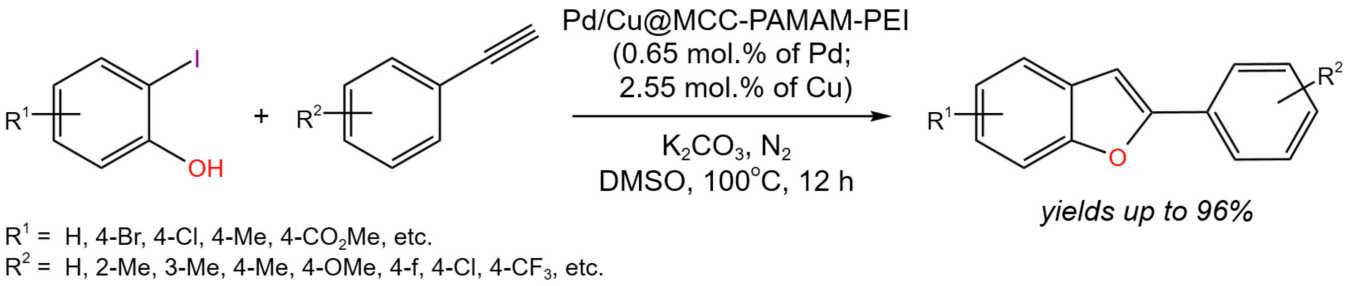

Figure 46. Scheme of Pd/Cu@MCC-$PAMAM_{G2.5}$-PEI-catalyzed Sonogashira cyclization tandem reaction [104].

A novel magnetic γ-Fe_2O_3@Cu-LDH@Cysteine-Pd dual nanocatalyst system was designed by Esfandiary et al. [105]. The surface of magnetic NPs was modified by the substitution of Cu(II) metal cations with layered double hydroxide (LDH) cations. Then, the Pd(II) complex was immobilized on the interface defect structure of LDH (Figure 47).

Using the synthesized catalyst, the A^3 coupling followed by C–N coupling and intramolecular cyclization was carried out for the synthesis of quinolines (yields of up to 94%) from 2-bromobenzaldehyde as a low-cost simple starting material (Figure 48). The suggested nanocatalyst easily activated terminal alkynes in the absence of base using recyclable choline azide as a green solvent and reagent. The catalyst could be reused up to four times without significant loss of activity [105].

Meng et al. [106] created a bifunctional catalytic system based on a water-soluble thermoresponsive polymer (poly(ethane-*co*-*N*-isopropylacrylamide) and hollow-shell-structured mesoporous silica as a support for Ru-(MesRuArDPEN) and Pdcomplexes ($Pd_2(dba)_3$ + PMe_3). This catalytic system (polymer@Pd@Ru) was applied in the cascade Suzuki cross-coupling/asymmetric transfer hydrogenation reactions of various iodoacetophenones and aryl boronic acids, allowing high yields and ee (up to 97%). By regulating the polymer layers on the outer silica shell, two catalysts selectively controlled the catalytic behavior for the implementation of switchable enantioselective cascades.

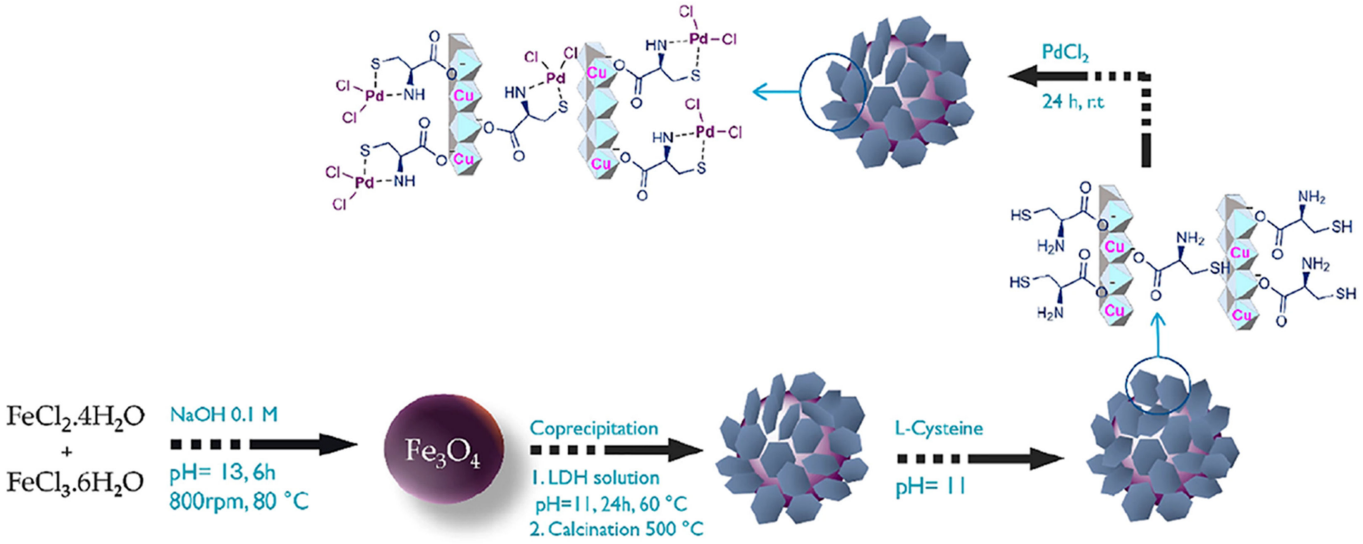

Figure 47. Schematic procedure of the synthesis of γ-Fe_2O_3@Cu-LDH@Cysteine-Pd. Reproduced with permission from [105], Elsevier, 2020.

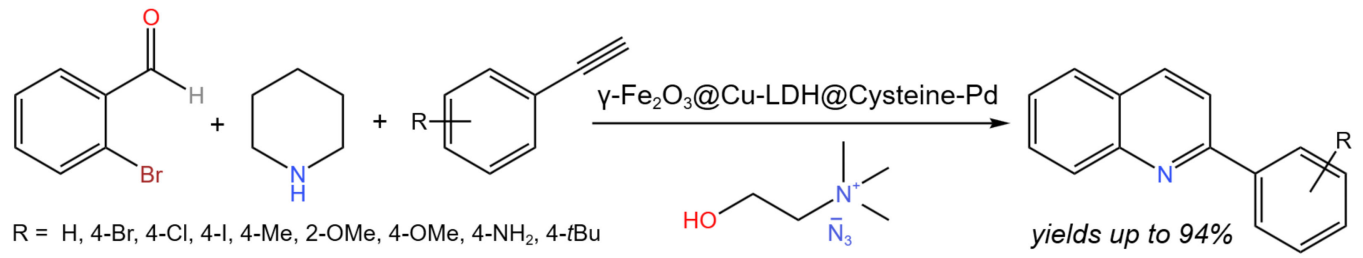

Figure 48. Scheme of the synthesis of 2-substituted quinolines in the presence of γ-Fe_2O_3@Cu-LDH@Cysteine-Pd [105].

Rajabi et al. [107] developed a new environmentally friendly universal protocol for the one-pot conversion of aliphatic, aromatic, and unsaturated aldehydes into esters under ambient conditions in the presence of oxygen using a palladium nanocatalyst supported on mesoporous organosilica (SBA-15). Palladium bearing a functionalized cytosine (Cyt) on the surface of mesoporous silica (Pd-Cyt@SBA-15) allowed for a selective large-scale conversion of a broad range of short-chain alcohols with aldehydes, including aromatic and aliphatic aldehydes to the corresponding ester products with yields of up to 98% and TON (98,000). The catalyst Pd-Cyt@SBA-15 revealed high stability and reusability over ten reaction runs.

4. Heterogeneous Pd-Catalyzed Tandem Processes

Aiming at the implementation of tandem catalysis, multiple reactions can be carried out in one pot by using bifunctional heterogeneous systems for the simultaneous activation of substrates and reagents in various Lewis/Brønsted acid, acid/base, metal/base, metal/acid, or metal/metal-catalyzed processes. The bifunctional catalyst can be designed in such a way that the two different catalytic functions (e.g., acidic and basic site) act in a collaborative way in the transition state, or each one catalyzes a different reaction in a multistep process [19].

Besides the common approaches to the desing of the multifunctional catalyst, Cho et al. [15] defined the following additional directions in the desing of tandem processes:

(i) size and shape selectivity, with active sites only accessible to substrates and intermediates with specific sizes and shapes;
(ii) surface and solvent engineering that exploits differences in the hydrophobicity, hydrophilicity, and other properties of the catalizate's components;

(iii) metal site engineering through controlled size, exposed facets, composition, and their spatial distribution;
(iv) reactor and process engineering (i.e., chemical looping, reactive separations, andmultiple sequential catalyst beds in flow reactors) [15].

For example, Sheetal et al. [108] developed the direct one-pot carbonylation of iodobenzene and NaN_3 as a N-atom source under Pd@PS catalyzed conditions utilizing $(CO_2H)_2$ as an environmentally benign CO surrogate in a DMF solvent system. The proposed approach was based on the use of two vials with different solvents: (i) an outer vial with $(CO_2H)_2$ and DMF, and (ii) an inner vial containing iodobenzene and NaN_3, along with a catalyst in xylene solvent conditions (Figure 49).

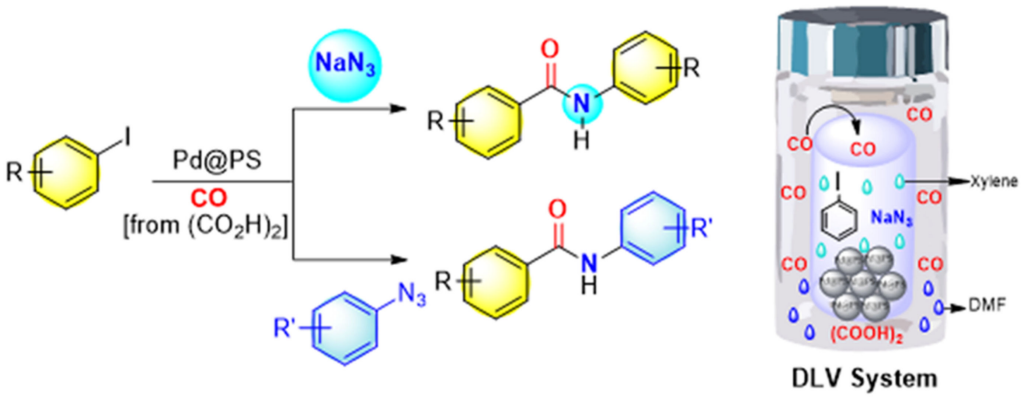

Figure 49. Tandem approach to the synthesis of *N*-aryl benzamides through the bifunctional transformation of aryl iodides in a double-layer vial (DLV) system. Reproduced with permission from [108], Elsevier, 2021.

Thus, the use of aryl iodides as bifunctional reactants under base, ligand, and additive-free conditions allowed for the carrying out of the simultaneous C–C and C–N bond formations to obtain the desired products (*N*-phenyl benzamide derivatives) with good to moderate yields (up to 70%) at 140 °C for 24 h [108].

Heterogeneous catalysts with acid sites in the composition of supports are widely used in catalysis, especially in biomass processing. Zeolites are a common example of such supports since they have high thermal and hydrothermal stabilities, homogeneous porosity, shape-selective properties, and tunable acidities [109]. Amoo et al. [109] in their review mentioned that the design of metal-zeolite composite catalysts is prospective for syngas conversion. For example, alkali surfaces are known to favor the adsorption and subsequent conversion of CO to olefins over Fe-based catalysts due to the preffered formation of Fe–C over a high pH surface. The acid sites of zeolites might alter the intrinsic pH of the Fe-zeolite composite catalyst, and thus the interaction between these two active components located in proximity will benefit in tandem catalysis (such as oligomerization, isomerization, alkylation, and hydrocracking) [109].

Mesoporous silica materials, which have ordered pore size, a high specific surface area, a large pore volume, and the ability to synthesize a wide range of morphologies and shapes, can be utilized as an alternative to zeolites [110–116]. Mesoporous silica, such as MCM-41 and SBA-15, used as supports for metal NPs and widely applied in catalysis, including tandem processes. Recently, propylamine, diethylamine, and pyrrolidine were used by Hernández-Soto et al. [115] to create the single basic sites in organic–inorganic hybrid bifunctional organosiliceous catalysts with pendant amine groups in addition to Pd NPs.In the developed catalysts, heterogenized amine groups and palladium NPs were found to be homogeneously distributed and stabilized in the mesochannels of the MCM-41. The steric effects around the amine groups in mesochannels were proposed to have a strong influence on the catalytic activity. Moreover, longer amines exhibited higher interaction with the silica surface, decreasing the catalytic activity [115].

In the presence of Pd/MCM-41 bearing the propylamine groups, furfural and methyl isobutyl ketone underwent a tandem aldolcondensation/crotonization reaction in a single reactor, followed by hydrogenation (Figure 50). At 100 °C in the presence of toluene, an almost complete conversion of furfural and 82% yield of 1-(furan-2-yl)-5-methylhexan-3-ol was achieved. It was shown that in a dual fixed-bed reactor, the catalyst robustness may be improved, providing 20% furfural conversion for 12 h on stream with the preferential production of 1-(furan-2-yl)- 5-methylhexan-3-one [115]. It is noteworthy that the reaction products can be used as a renewable biosolvent and biofuel precursors.

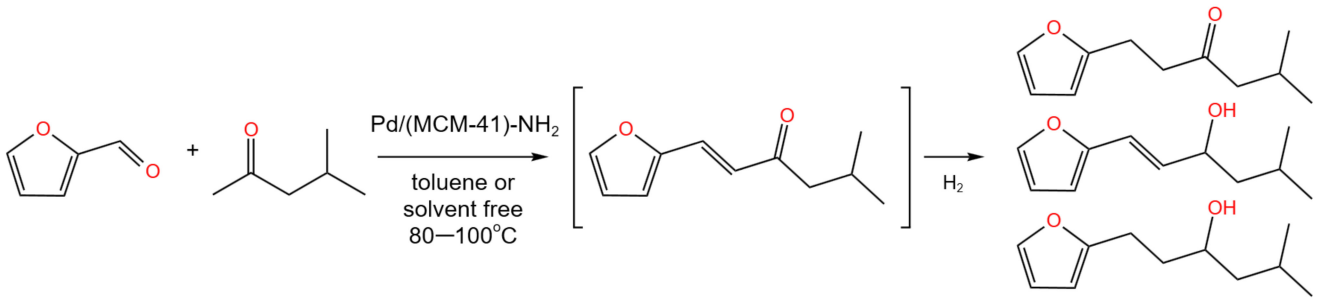

Figure 50. Scheme of tandem aldol condensation/crotonization of furfuraland methyl isobutyl ketone, followed by hydrogenation [115].

Maties et al. [116] synthesized Pd-containing Al-SBA-15 materials for the valorization of trans-ferulic acid into stilbenes via tandem decarboxylation/Mizoroki–Heck coupling (Figure 51). Under mild reaction conditions (100 °C, 3–6 h), quantitative product yields were obtained with over 90% selectivity to target stilbene products. The sizes of Pd NPs were found to be an important factor with a significant impact on the catalytic activity. The catalyst deactivation via sintering of Pd NPs was also observed.

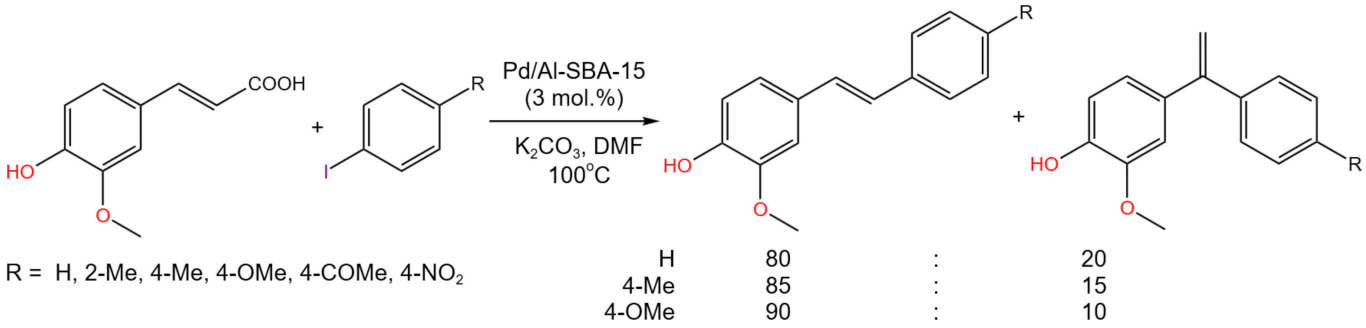

Figure 51. Stilbene synthesis by decarboxylative C–C coupling of trans-ferulic acid and iodoanisole over Pd/Al-SBA-15 catalyst [116].

Tungsten oxide (WO_x) is one of the most wellknown and widely used oxides with surface acid–base properties, being often combined with other oxydes (ZrO_2 [117–119], SiO_2 [120–122], Al_2O_3 [123,124]), and zeolites [121,125]. Chu et al. [126] reported the synthesis of a multifunctional Pd-Cu-WO_x/SiO_2 catalyst for the one-pot conversion of cellulose to ethanol. This catalyst allowed an ethanol yield of 42.5% at 300 °C under 4 MPa H_2 in aqueous medium. It was shown that the cellulose conversion to ethanol followed the following consecutive steps: (i) cellulose hydrolyzed to glucose over acid sites; (ii) glucose then converted to glycolaldehyde over W species; (iii) glycolaldehyde hydrogenated to ethylene glycol over Pd; (iv) ethylene glycol hydrolyzed to ethanol over Cu. It was shown that the three metal components, Pd, Cu, and WO_x, were in appropriate balance, allowing for the achievement of an ethanol formation rate of 0.163 g/(g_{cat}·h).

The versatility of MOFs as highly porous acidic supports for metal NPscan be used for one-pot tandem processes [16,127–129].

MIL-101(Cr) (Figure 52) contining Pd NPs (about 3 nm) at 0.2–1.0 wt.% was used to catalyse one-pot tandem reductive amination of 4′-fluoroacetophenone with benzylamine (Figure 53) under 10 bar of H_2 [16].

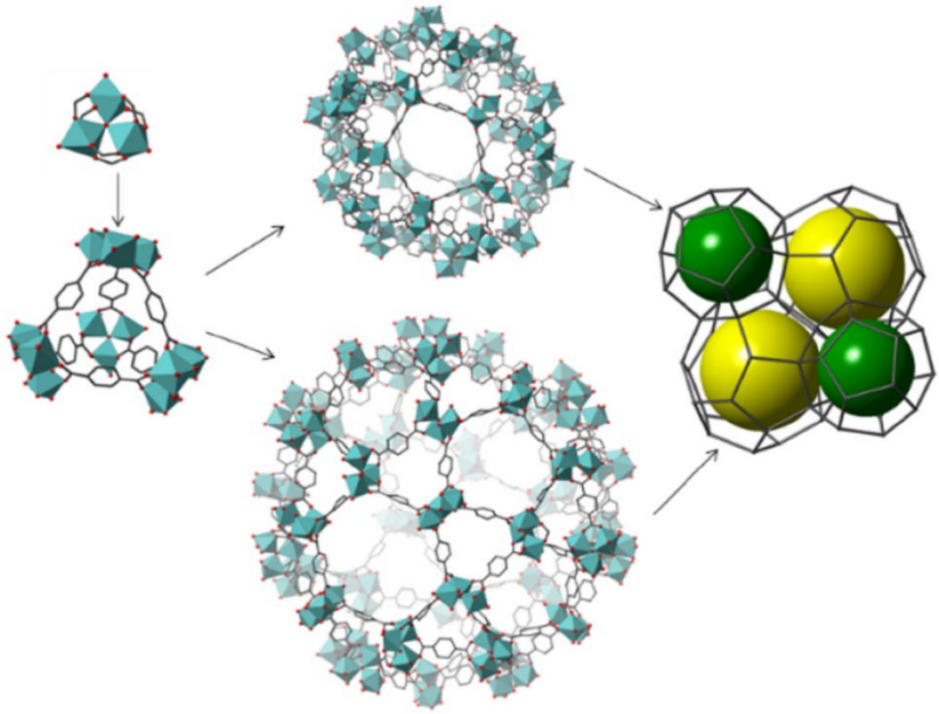

Figure 52. Scheme of MIL-101(Cr), showing the $Cr_3O(O_2C–)_6$ cluster, the super-tetrahedral building units, and the smaller (green spheres) and larger cages (yellow spheres). Reproduced with permission from [16], Springer Nature, 2018.

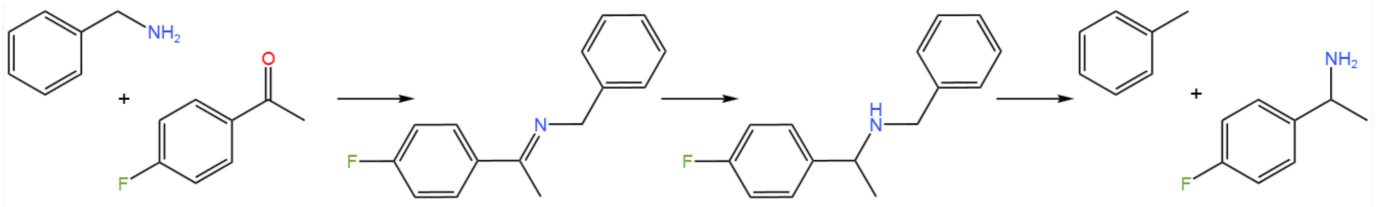

Figure 53. Synthesis of 4′-fluoro-α-methyl-*N*-(phenylmethyl)benzenemethanamine via the reductive amination reaction [16].

The MOF's Lewis acidity and the Pd NPs' capacity for catalytic hydrogenation werecombined in the bifunctional catalyst. The selectivity in the reductive amination reaction was found to be significantly influenced by altering the Pd loading within the MOF to tune the ratio of active sites. Higher metal loadings led to a significant amount of undesired product (4′-fluoro-α-methylbenzenemethanamine). Higher selectivity was achieved by decreasing the total number of Pd sites compared to Lewis acidic sites; the 0.4 wt.% Pd MIL-101 allowed for nearly 90% of the target amine (4′-fluoro-methyl-*N*-(phenylmethyl)benzenemethanamine) after 7 h. Moreover, the synthesized catalysts were reusable and maintained crystallinity and small highly dispersed NPs after reaction.

The bifunctional catalyst Pd@MIL-101-SO_3H was developed by Liu et al. [127] and was applied in the one-pot oxidation–acetalization reaction (Figure 54), the products of which are widely utilized as fuel additives, perfumes, and pharmaceuticals, and in polymer chemistry.

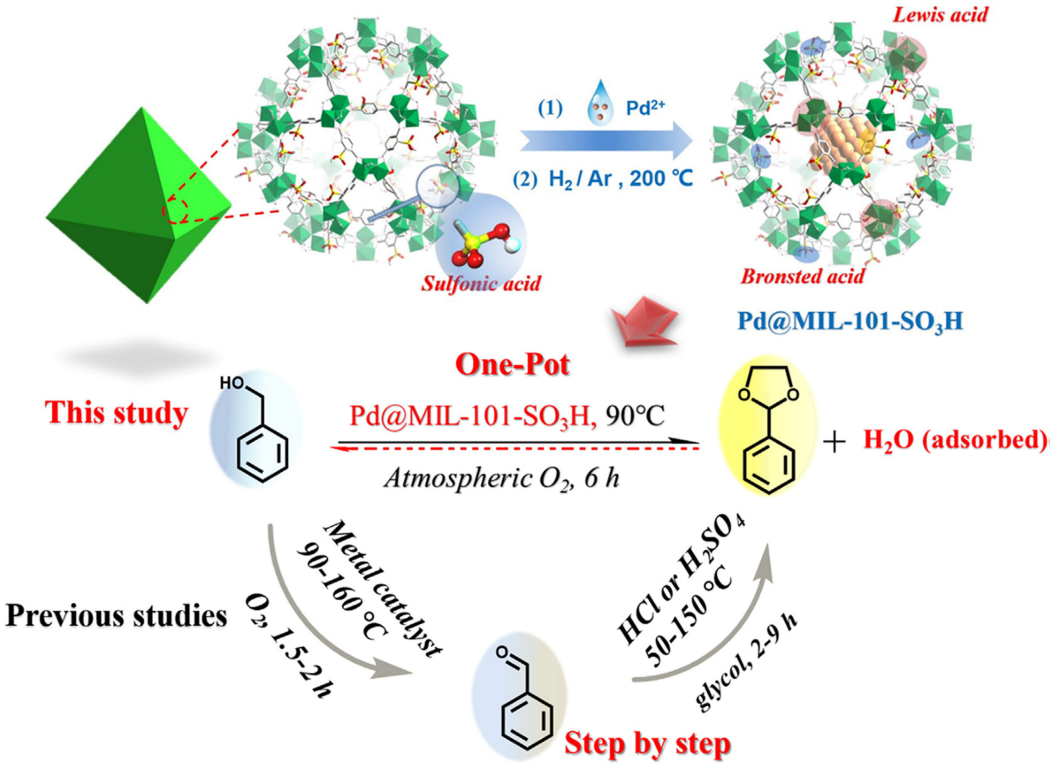

Figure 54. Scheme of the synthesis of Pd NPs immobilized in MIL-101-SO_3H and one-pot transformation of benzaldehyde glycol acetal. Reproduced with permission from [127], Elsevier, 2019.

High yields (>99%) were ascribed to the combined actions of Pd NPs, responsible for oxidation, and Lewis and Brønsted acid sites, responsible for acetalization, which wereencapsulated in sulfonated MIL-101(Cr). The high capacity of MIL-101(Cr) for water adsorption aided the shift in equilibrium by impeding the reversible process.Thus, the nonpolar solvents were demonstrated to be the optimum ones.The reaction mechanism is presented in Figure 55. Moreover, the Pd@MIL-101-SO_3H could be reused for at least eight times without loss of catalytic activity [127].

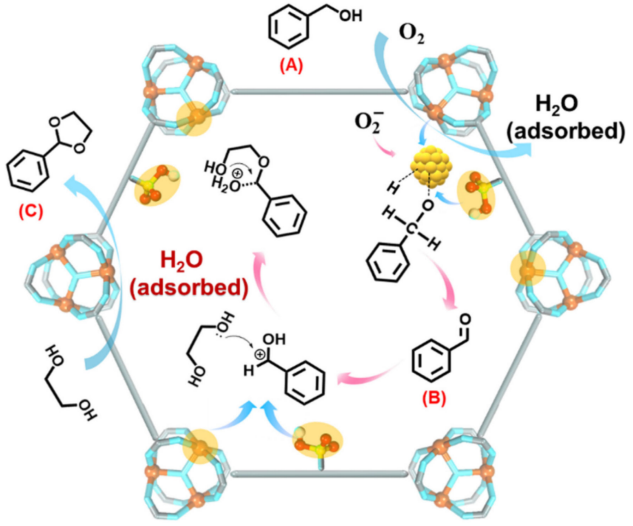

Figure 55. Proposed mechanism of the one-pot oxidation–acetalization. Reproduced with permission from [127], Elsevier, 2019.

Tandem heterogenous catalysis of bimetallic Cu-Pd on an aminofunctionalized Zr-based metal–organic framework (UiO-66(NH_2)) incorporated into sulfonated graphene

oxide (Cu-Pd/UiO-66(NH_2)@SGO) was investigated by Insyani et al. [128] for the one-pot conversion of disaccharides and polysaccharides into 2,5-dimethylfuran (2,5-DMF) (Figure 56).

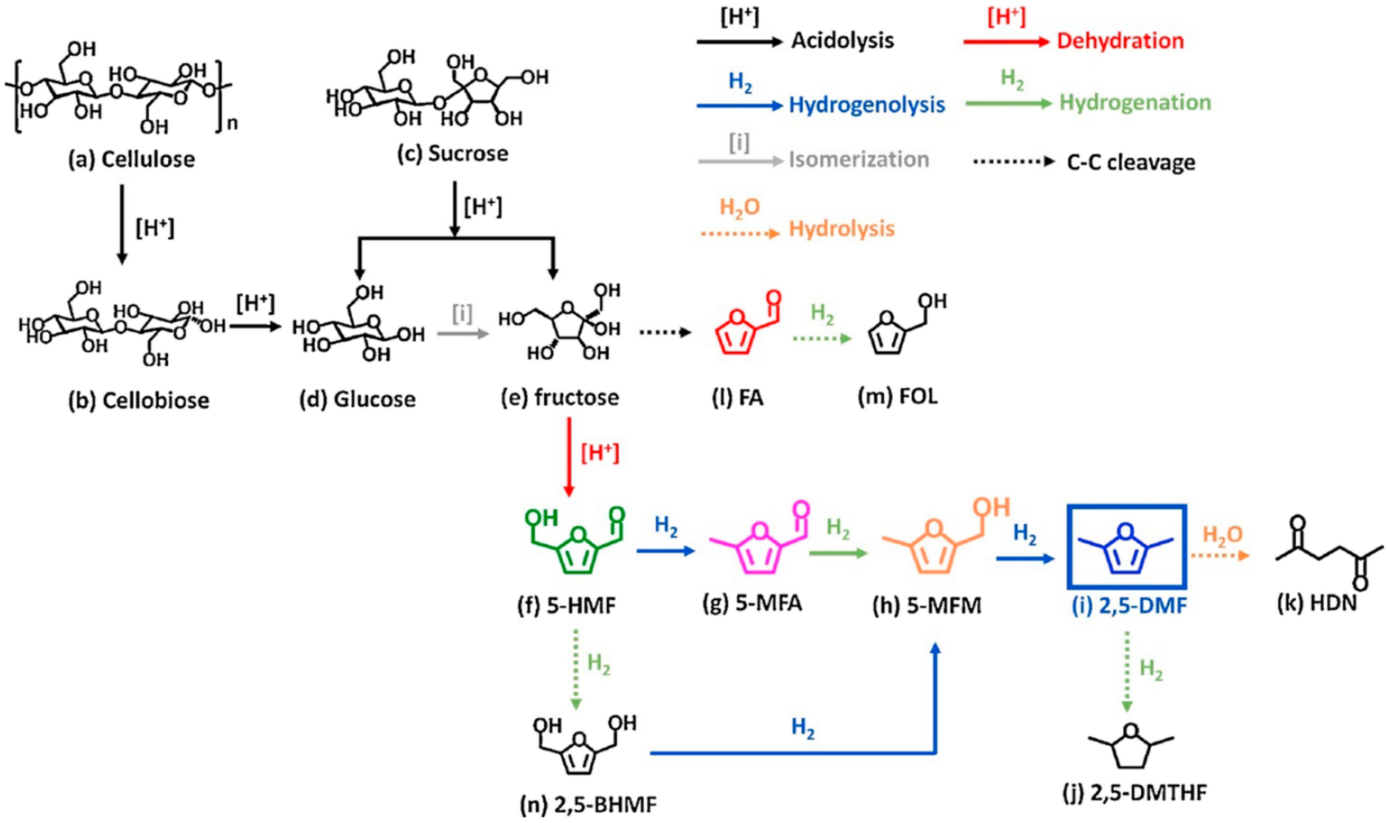

Figure 56. Reaction pathway for di- and polysaccharide conversion into 2,5-DMF: (**a**) cellulose, (**b**) cellobiose, (**c**) sucrose, (**d**) glucose, (**e**) fructose, (**f**) 5-hydroxymethylfurfural (5-HMF), (**g**) 5-methylfurfural (5-MFA), (**h**) 5-methyl-2-furanmethanol (5-MFM), (**i**) 2,5-dimethylfuran (2,5-DMF), (**j**) 2,5-dimethyltetrahydrofuran (2,5-DMTHF), (**k**) 2,5-hexanedione (HDN), (**l**) furfural (FA), (**m**) furfuryl alcohol (FOL), and (**n**) 2,5-bis-hydroxymethylfurfural (2,5-BHMF). Reproduced with permission from [128], Elsevier, 2019.

Sequential glycosidic bond cleavage, isomerization, and dehydration of sucrose led to a high yield (75.8%) of 5-(hydroxymethyl)furfural (5-HMF) by altering the strength and ratio of the Lewis and Brønsted acid sites by varying the ratios of UiO-66(NH_2) to SGO. Bimetallic Cu-Pd, in contrast to monometallic Cu and Pd, favored sequential C–OH hydrogenolysis and C=O hydrogenation of the intermediates, resulting in the production of 2,5-DMF with a high yield of 73.4% during the one-pot conversion of sucrose at 200 °C and 1 MPa H_2 for 3 h. 2,5-DMF was produced during the conversion of starch with a53.6% yield. In the presence of 0.01 M HCl, cellulose was converted into 2,5-DMF with ayield of 29.8% [128].

Another example of tandem catalytic processes is the one-pot three-step deacetalization–Knoevenagel–hydrogenation (D–K–H) reaction (Figure 57), requiring the synergetic catalysis and the closelocation of the acid, base, and metal sites.D–K–H can be successfully carried out using a trifunctional integrated catalyst (Pd@HPW@HP-UiO-66-NH_2): phosphotungstic acid (HPW) immobilized on the hierarchically porous UiO-66-NH_2 acting as a support for Pd NPs [129].

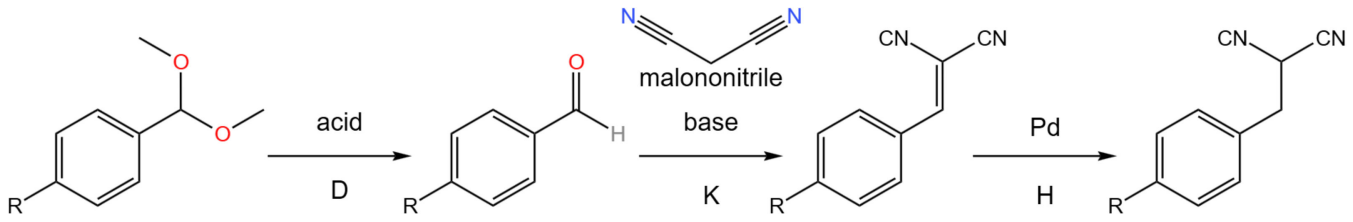

Figure 57. Proposed mechanism of the one-pot oxidation–acetalization [129].

While controlling the ratio of immobilized HPW and amino groups, acidic and basic properties can be easily tuned, and thus the catalytic performance of Pd NPs and its stability can be controlled.The as-prepared catalyst revealed good catalytic activity in the one-pot D–K–H tandem processes, allowing up to 99% substrate conversion and 97% yield of the target product (toluene, 80 °C, 12 + 24 h). Moreover, due to the strong interaction between the MOF (HP-UiO-66-NH_2) and the guest molecules, the catalyst could be reused at least five times without noticeable loss of its activity [129].

By using a straightforward two-step post-synthetic modification, Lee et al. [130] sunthesized an acid–base bifunctional zeolitic imidazolate framework catalyst (ZIF-8-A61-SO_3H) with amine and sulfonic acid groups. First, amine-functionalized ZIF-8 with amine contents of 61% (ZIF-8-A61) was obtained by the ligand exchange of 2-mIM with 3-amino-1,2,4-triazole (Atz). Then, the sulfonic acid functionalization by the ring-opening reaction of 1,3-propanesultone with $–NH_2$ groups in ZIF-8-A61 was carried out. Different amine-functionalized ZIF-8-A materials (15%, 34%, and 61% ofamine content) were prepared by controlling the synthesis time. The catalysts were used for one-pot deacetalization–Knoevenagel (D-K) condensation tandem reaction (the reaction is similar to the one presented in the Figure 51). The ZIF-8-A61-SO_3H catalyst allowed for 100% conversion of the reactant and 98% selectivity of the final Knoevenagel product at mild conditions (0.1 g of catalyst, 1,4-dioxane/H_2O, 80 °C, 4 h) [130]. The developed ZIF-8-A61-SO_3H [130] seemedto possess higher efficiencyin in the D-K process as compared to HPW@HP-UiO-66-NH_2 [129]. Thus, the immobilization of Pd NPs in ZIF-8-A61-SO_3H may result in the further improvement of the D–K–H tandem reaction.

As an another example of a bifunctional catalyst, a double-shelled hollow polymer microsphere wasdeveloped [131]. Pd NPs were found mostly in the outer shell of the catalytic material and stabilized by pyrrolidone groups. The inner shell P(EGDMA-co-AA) contained the acid sites. Theresulting bifunctional catalytic system (void@PAA/PNVP@Pd) was applied for the deacetalization–hydrogenation tandem process (Figure 58), demonstrating the viability of the plan to load distinct catalytic sites onto the walls of double-shelled hollow polymer microspheres.Deacetalization of benzaldehyde dimethyl acetal was followed by hydrogenation with the formation of benzyl alcohol. As a result, the conversion of benzaldehyde dimethyl acetal reached 99% with a 96% yield of the benzyl alcohol [131].

Bifunctionalcatalytic system of Pd/C and water-tolerant Lewis acid (i.e., $Sm(OTf)_3$, $La(OTf)_3$, $Cu(OTf)_2$) were applied for the synthesis of fuel precursors from biomass liquefaction with high efficiency in both water and ethanol [132]. The maximum yield of bio-oil (49.71 wt.%)was achieved for 30 min at supercritical ethanol (300 °C) in the presence of Pd/C and $La(OTf)_3$.

Raza et al. [133] synthesized highly dispersed Pd NPs immobilized over covalent triazine polymer (CTP) functionalized with sulfonic acid groups (CTP-SO_3H/Pd). The sulfonic acid groups were shown to be responsible for the uniform dispersion of palladium NPs over the CTP. The obtained bifunctional catalyst was used in the one-pot hydrogenation–esterification (OHE) reaction and revealed promising catalytic activity with a 94% yield of the target product at 95% conversion (Figure 59).

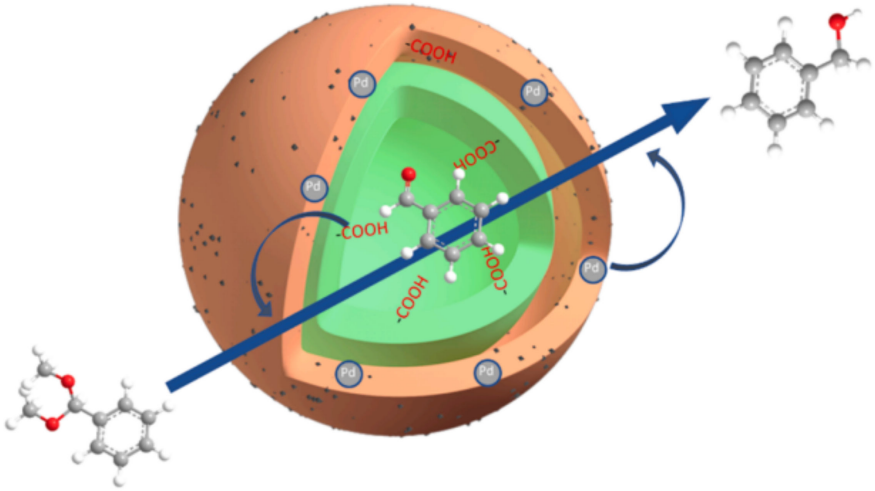

Figure 58. The void@PAA/PNVP@Pd hollow multishell microspheres as a nanoreactor for the tandem reaction. Reproduced with permission from [131], Elsevier, 2023.

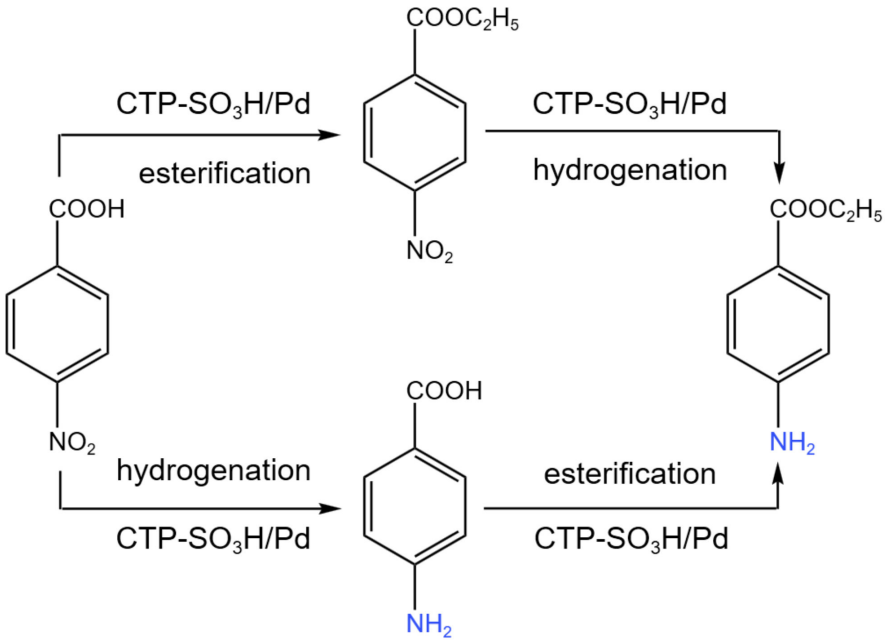

Figure 59. Scheme of the OHE reaction [133].

After the reaction, the catalyst was separated by simple filtration. It was shown that the CTP-SO_3H/Pd catalyst could be reused for at least five times with a slight loss of catalytic activity, indicating its potential usage in OHE reactions. The cooperative effect of functional acidic and metal sites was proposed [133].

Covalent organic frameworks (COFs) are widely used as a support for catalytic applications [134–137], including tandem one-pot processes [138]. The COFs possess a variety of chemical structures, which may be precisely tuned to control the surrounding coordination environment and electronic interaction between metal NPs and supports, in contrast to other materials used for NPs immobilization.The uniform porous structure in COFs allows for numerous metal active sites, which enhances the catalytic activity [139]. A simple hydrothermal synthesis was recently used by Wang et al. [139] to produce COF. Noble metals (Pt, Pd, and Rh) were introduced to the COF matrix for further application in the reductive amination of benzaldehyde.The optimum Pd/COF catalyst revealed a 91% yield of a secondary aminesat 1.2:1 M ratio of aldehyde and ammonia under mild reaction conditions (2 MPa of H_2 and 90 °C, 15 h) [139].

5. Chemoenzymatic Processes

At present, the enzymatic catalysis is considered a powerful tool for synthetic chemists, providing access to a wide range of compounds. Advances in the field of immobilization, molecular biology, and bioinformatics have paved the way for biotransformation in various environments, improving the stability and activity of biocatalysts, opening up new enzymatic pathways. The capacity of enzymes is attracting increasingly more attention, since they can be successfully combined with other types of catalysts, as shown by recent achievements in their joint action with metals [140–142]. This section is devoted to the consideration of the combination of palladium and enzymatic catalysts for chemoenzymatic processes. This combination gives the advantages of conducting tandem processes in a single reactor, which simplifies the complex routes, avoiding the separation of unstable intermediates to obtain final products with a higher yield.

In the recent review by Gonzalez-Granda et al. [140], the combination of enzymes and transition metals in catalysis for asymmetric synthesis was considered. Reactions such as Suzuki cross-coupling [143–145], Wacker–Tsuji oxidation [146–148], and Buchwald–Hartwig cross-coupling [149–151] were discussed.

Metal-enzymatic parallel and sequential transformations were described, involving Pd, Ru, Au, Ir, and Fe, which catalyze numerous organic transformations (C-C coupling, isomerization, hydrogenation, etc.). The combination of catalytically active metals with enzymes in the chemoenzymatic processes allows for the obtaining of chiral products due to the action of stereospecific enzymes, including alcohol oxidases, aldolases, alcohol dehydrogenases, amine dehydrogenases, amino acid dehydrogenases, aminotransaminases, arylmalonate decarboxylase, enreductase, iminoreductase, nitrile hydratase, or phenylalanine monialiases, among others. It was noticed [140] that incompatibilities between chemical and enzymatic steps can be often found, such as cross-prohibitions due to the presence of cofactors, reagents, or intermediates, or the preference for different solvents or temperatures, and thus these protocols must be accomplished sequentially.

A stereoselective one-pot tandem reduction of 3-methyl-2-cyclohexenone to 3-(1*S*,3*S*)-methylcyclohexanol (Figure 60) was carried out by Coccia et al. [152] using Pd and Pt NPs as the metal precatalyst and a NAD^+-dependent thermostable alcohol dehydrogenase isolated from *Thermus* sp. ATN1 (TADH).

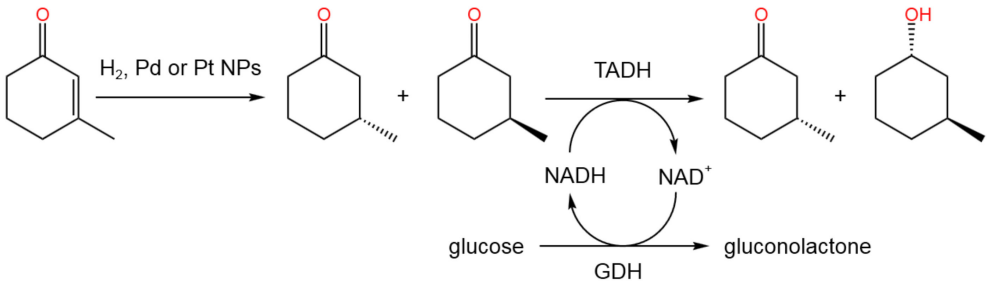

Figure 60. Scheme of the tandem selective reduction of the C=C bond with metal (Pd or Pt) NPs and the asymmetric reduction of the keto group by TADH(GDH—glucose dehydrogenase) [152].

The Pd and Pt NPs possess a high surface-to-volume ratio, simple preparation, and good "solubility" in water. Moreover, the metal NPs can work without significant pH or temperature limitations and can be used in different reactions such as oxidation and reduction. TADH revealed a broad substrate scope including aldehydes, aliphatic ketones, cyclic ketones, and double-ring systems [152].

The assumptions were made on the interactions between the chemo- and the biocatalyst. The sizes of NPs were demonstrated to be a crucial parameter for mutual inhibition: the larger the NPs, the higher the enzyme inhibition, and vice versa: the smaller the NPs, the lower the TADH denaturation. In general, the chemocatalysts possessed high deactivation sensitivity, which was highly dependent on the amount of enzyme utilized, i.e., the inhibition of the biocatalyst could be greatly decreased by reducing the NPs/TADH

ratio. In order to avoid the direct binding of NPs to TADH, the use of large Pd NPs protected with a silica shell is promising: the yield of 3-(1*S*,3*S*)-methylcyclohexanol was increased up to 36% [152].

Combining metal ions or NPs with biocatalysts in a single system is a promising strategy for implementation in the one-pot chemoenzymatic cascade reactions [153], especially for asymmetric syntheses. For example, Li et al. [154] developed a one-pot chemoenzymatic cascade reaction to asymmetric synthesize (*R*)-1-(4-biphenyl) ethanol (Figure 61) while using a highly active and selective enzyme–metal–single-atom catalyst. In the facilitation of the production of chiral biaryl alcohols, the Pd single-atom-anchored lipase (Pd1/CALB-P) may effectively drive one-pot cascade reactions in aqueous solution at 30 °C. The production rate was 30 times higher than that catalyzed by the commercial Pd/C and CALBP.

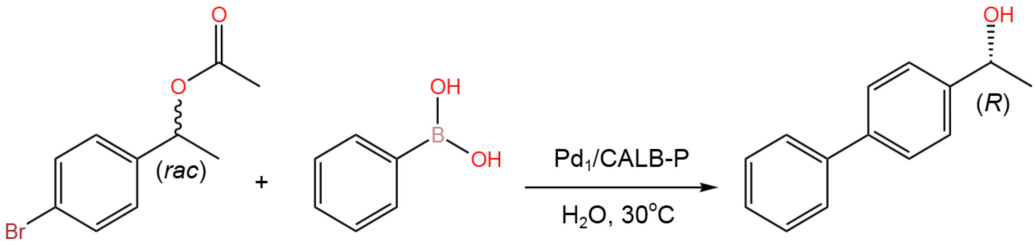

Figure 61. Synthesis of (*R*)-1-(4-biphenyl)ethanol by a one-pot chemoenzymatic reaction [154].

In an other recent work of Li et al. [155], a bimetallic PdCu/CALB CLEAs hybrid catalyst was synthesized by the in situ reduction of PdCu nanoclusters immobilized on cross-linked lipase aggregates (CALB CLEAs).

Cross-linked enzyme aggregates (CLEAs) were prepared from *Candida antarctic* lipase B (CALB) by their precipitation and subsequent cross-linking with the glutaraldehyde. The bimetallic PdCu nanoclusters were formed in situ on CALB CLEAs (Figure 62) by the reduction of Pd^{2+} and Cu^{2+} ions in an aqueous solution containing 20% (v/v) methanol, which served as an additional reducing agent. The obtained PdCu nanoclusters were highly dispersed (sizes of 1.5 ± 0.2 nm). The strong synergistic effect between Pd and Cu in PdCu/CALB CLEAs allowed for high activities in the Sonogashira cross-coupling reaction and one-pot chemoenzymatic reaction, resulting in the synthesis of (*R*)-*N*-[1-(4-(phenylethynyl)phenyl)ethyl]acetamide (Figure 63) [155].

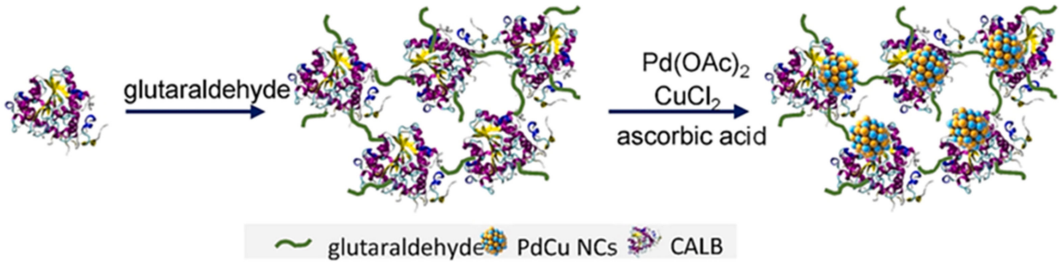

Figure 62. Schematic illustration of the strategy used to synthesize PdCu/CALB CLEAs via in situ reduction. Reproduced with permission from [155], Elsevier, 2021.

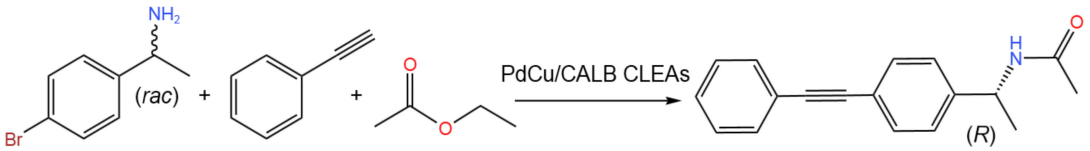

Figure 63. Synthesis of (*R*)-*N*-[1-(4-(phenylethynyl)phenyl)ethyl]acetamide by one-pot chemoenzymatic reaction [155].

In this reaction (Figure 63), CALB catalyzed the acylation of (*R*)-enantiomer of the amine, while PdCu nanoclusters were responsible for the Sonogashira cross-coupling and the racemization of (*S*)-enantiomer of the amine. It was proposed that Cu-alkynyl and Pd-aryl particles were formed simultaneously by surface coordination. The coordinated Pd and Cu particles were then subjected to the transmetalation stage, which facilitated the cross-coupling reaction. Catalytic activity increased with the increase in the content of PdO [155]. It is noteworthy that the higher activity of PdO as compared to metallic palladium was described earlier for the reaction of Suzuki cross-coupling by Collins et al. [156].

Deiana et al. [157] developed the bioinspired multicatalytic system based on an artificial plant cell wall (APCW) containing the lipase and Pd NPs for the transformation of racemic amine into the corresponding enantiomerically pure amide with a yield of up to 99% (Figure 64), which involves a synergistic interaction between the racemization reaction catalyzed by Pd(0) and the enantioselective amidation catalyzed by CALB.

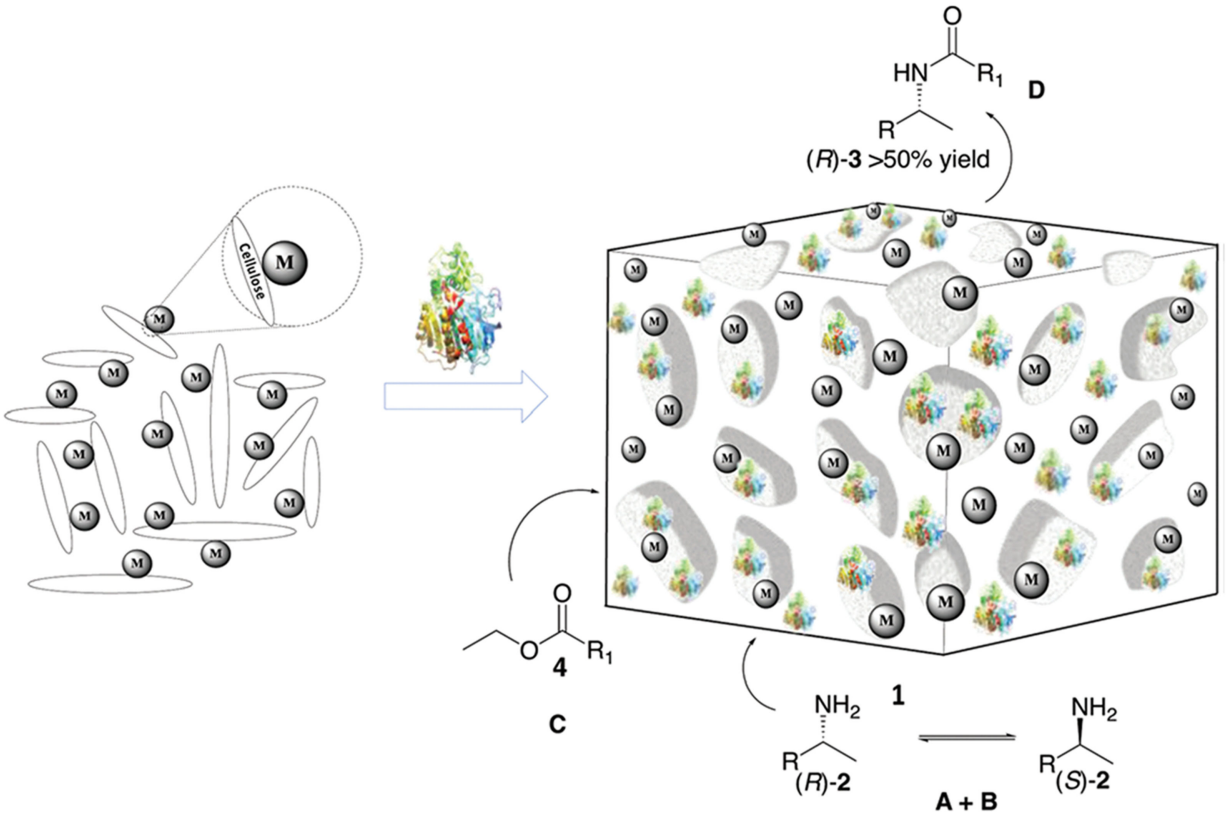

Figure 64. Simplified scheme of self-assembly of components to create an APCW, which simultaneously catalyzes racemization and amidation of racemic amines. M = metal. Reproduced with permission from [157], RSC, 2021.

The main component of the developed multicatalytic system is MCC or nanofibrillated cellulose, the surface of which is modified with aminopropylsilane, which allows for the retention of Pd NPs. The best approach for the self-assembly of the resulting hybrid catalyst was a non-covalent modification of CALB with surfactant polyethylene glycol hexadecyl ether (Brij) in a phosphate buffer. TEM data confirmed the formation of Pd NPs with a narrow size distribution (from 1.6 nm up to 2.8 nm). The hybrid heterogeneous multicatalytic system APCW9 was more efficient and chemoselective as compared to the mixture of Pd NPs on MCC and CALB on MCC [157].

By the example of different aryl and heteroaryl scaffolds, Craven et al. [158] showed that flavin adenine dinucleotide (FAD)-dependent halogenases (Fl-Hal) can be used in combination with Pd-catalyzed cyanation to affect the C–H functionalization cascades that deliver nitriles in a highly regioselective manner. As a non-toxic cyanation reagent,

$K_4[Fe(CN)_6]$ was used. It was shown that this approach can be extended by including nitrile hydratase (NHase) or nitrilase (NITR) to create integrated cascades of three catalysts for the regioselective installation of amide and carboxylic acid groups (Figure 65).

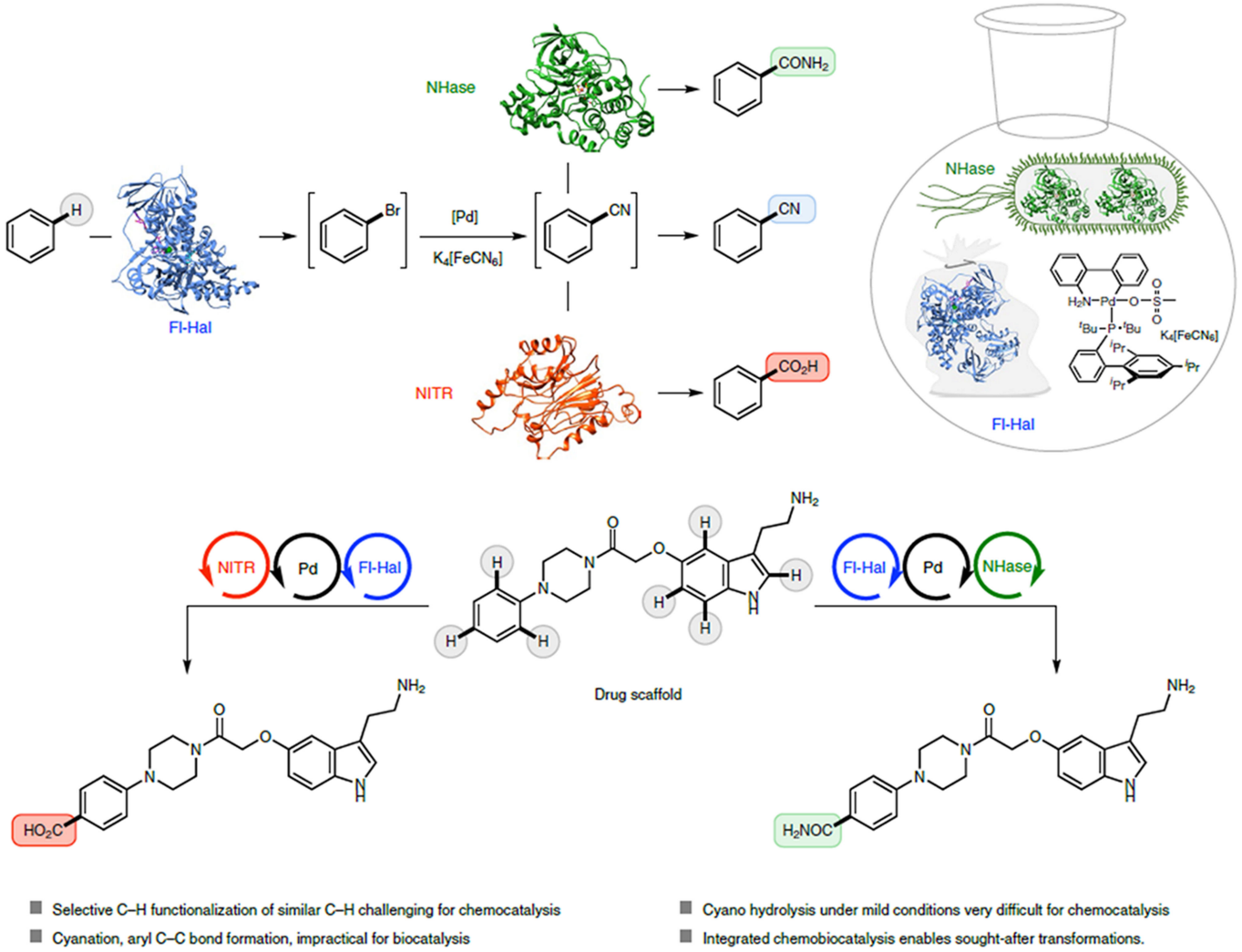

Figure 65. Overview of site-selective C–H functionalization cascades. Reproduced with permission from [158], Springer Nature, 2021.

It was emphasized [158] that the recent advances in the discovery, engineering, and synthesis of Fl-Hal biocatalysts can significantly broaden the application of this strategy. New Fl-Hals with improved catalytic characteristics, modified substrate specificities, and altered regioselectivity are continuously emerging from genome mining and directed-evolution programs. The inclusion of the Fl-Hals will boost the potential of the proposed programmable integrated cascades, enabling the integration of rich functionality into a variety of candidate scaffolds and facilitating the manufacturing of target molecules.

PdCu hydrogel nanozymes with a hierarchically porous structure were synthesized by Huang et al. [159] to immobilize horseradish peroxidase (HRP) (PdCu@HRP). The 3D porous nanowire networks of resulting hydrogels with high porosity served as biocompatible supports for immobilizing HRP. The affinity of Cu and Pd to proteins simplified the procedures of the enzyme immobilization without the addition of other cross-linking agents. The immobilization of HRP on PdCu hydrogels enhanced the thermal and chemical stabilities of HRP, realizing the reuse of the enzyme. Moreover, PdCu@HRP exhibited synergistically enhanced HRP activity as compared to native HRP and PdCu hydrogel nanozymes. The improved catalytic activity was likely due to specific interactions between

PdCu hydrogel nanozymes and enzymes as well as the enrichment of substrates around enzymes by electrostatic adsorption of hydrogels. Using catalytic cascade reactions, colorimetric biosensing of the carcinoembryonic antigen (CEA) was carried out while applying the PdCu@HRP and the glucose oxidase encapsulated in ZIF-8.The obtained biosensor allowed for the quantitative probing of the CEA concentration in a wide range from 5 to 1000 pg/mL with a LOD of 1.4 pg/mL and nearly 6.1-fold increase in the detection sensitivity as compared to the conventional HRP-based enzyme-linked immunosorbent assay [159].

It is important to highlight the work of Ming et al. [160], who developed a novel tandem Pd-Ru/Uricase@RBC nanoreactor, including Pd-Ru nanosheets, uricase, and red blood cell (RBC) membrane for hyperuricemia treatment (Figure 66). A new highly active 2D nanozyme Pd-Ru was covalently bounded with the uricase and immobilized on the surface of RBCs. It is noteworthy that the RBC membrane coating is a new biomimetic technique that gives nanomaterials a natural surface, and it can significantly increase the time that they circulate in the bloodstream [160].

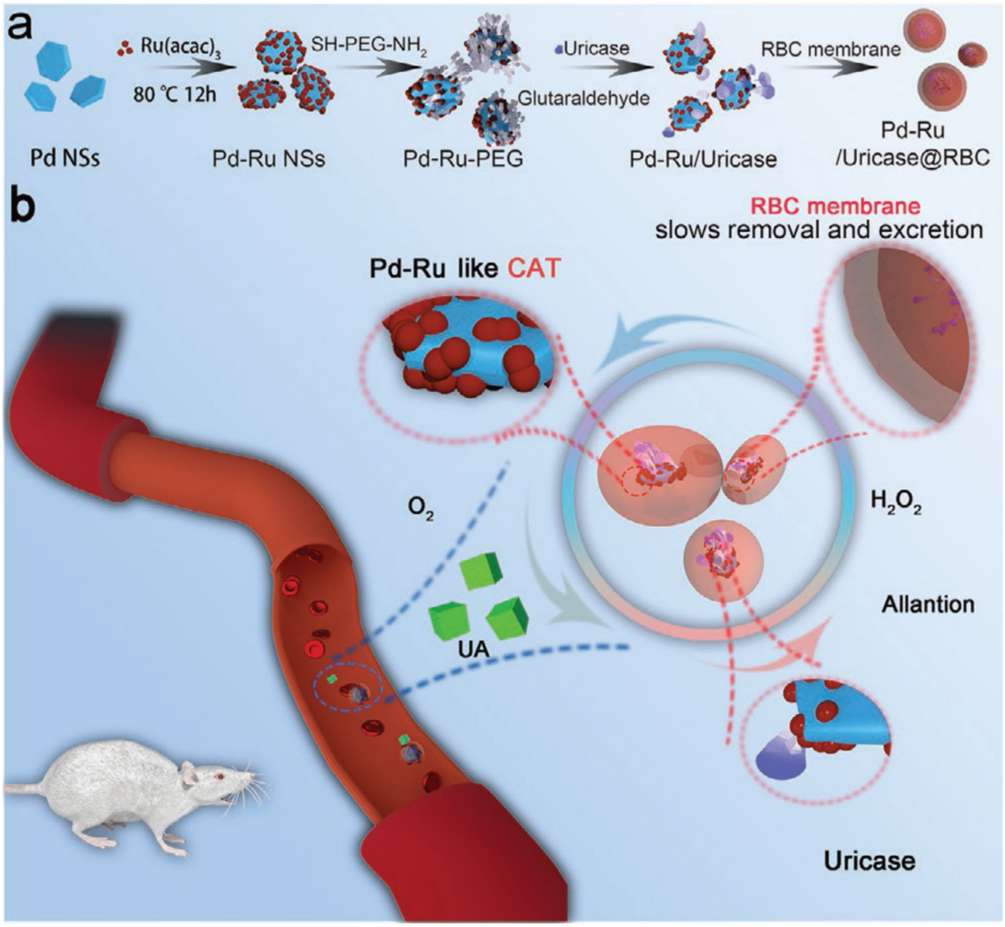

Figure 66. Schematic illustration of the construction procedure of Pd-Ru/Uricase@RBC (**a**) and its treatment of hyperuricemia (**b**). Reproduced with permission from [160], John Wiley and Sons, 2021.

The prepared Pd-Ru/Uricase@RBC demonstrated high catalase-like activity (Pd-Ru nanosheets decomposed H_2O_2 to rapidly generate O_2) and stability against various extreme pH values, temperatures, and forms of proteolytic degradation during biological transport. Moreover, the Pd-Ru nanozyme and uricase being in close proximity to each other allowed for the achievement of the efficient cascade reactions: degradation of the uric acid by uricase to allantoin and H_2O_2, as well as the removal of H_2O_2 by Pd-Ru nanosheets. The generated O_2 even facilitated the catalytic degradation of the uric acid [160]. Thus, the

cascade reactions based on the nanozymes were shown to be an effective strategy for the treatment of diseases due to its high efficiency and low level of side effects.

Zhang et al. [161] developed bifunctional biocatalysts based on mesoporous silica NPs (MSN), the surface hydrophobicity of which was created via alkylation. Pd NPs and the enzyme CALB were separately loaded into compartmentalized locations (Figure 67).

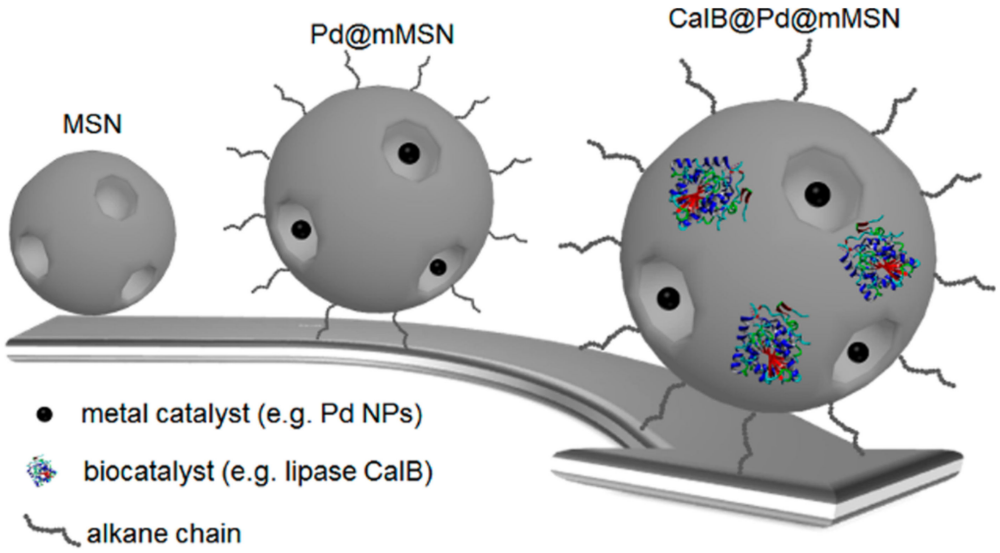

Figure 67. Schematic illustration of the construction of CalB@Pd@mMSN. Reproduced with permission from [161], Copyright 2018 American Chemical Society.

Pd(0) NPs were loaded into the MSN by the in situ reduction of Pd acetatewith $NaBH_4$. Then, the surface of Pd@MSN was modified with long-chain alkanes (obtaining Pd@mMSN). Subsequently, CALB was immobilized via hydrophobic interactions (bifunctional biocatalyst was denoted as CalB@Pd@mMSN) [161].

The CalB@Pd@mMSN was tested in a one-pot cascade reaction, in which Pd NPs first reduced the benzaldehyde, and then the immobilized CalB converted the benzyl alcohol into benzyl hexanoate (Figure 68). The developed catalyst was highly active and reusable: after four times of reuse, the reaction yield (4 h) remained higher than 80%.

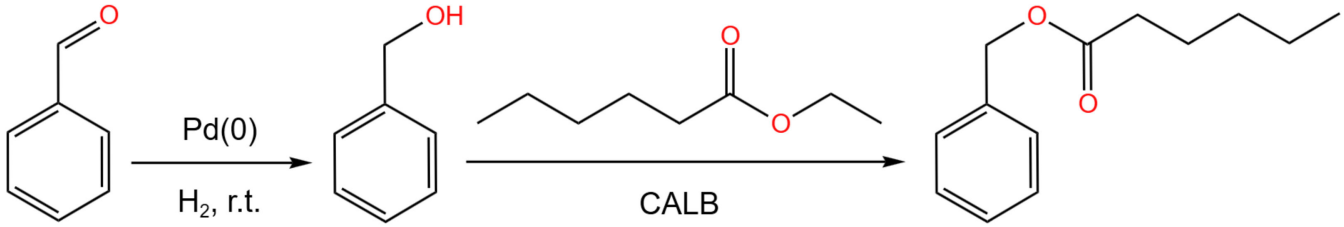

Figure 68. Scheme of the one-pot cascade reaction of benzaldehyde with ethyl hexanoate [161].

The developed bifunctional biocatalyst provides a universal platform with a large surface area for the transfer of catalysts to various organic solvents. Thus, it can be developed as a tool for adding other chemical and biocatalysts (such as glucose oxidase and other proteins) to the reaction medium of interest [161].

As was shown in the review by Metzger et al. [162], the combination of inorganic supports and catalysts into tandem systems is an actively developing area of tandem catalysis, since the durability of the systems allows for their application in industrial processes. Compartmentalization was shown to be a method for overcoming the difficulties associated with mixing several incompatible catalysts into a one-pot system. Compartmentalization can decrease side reactions, inhomogeneity, and catalyst deactivation that are often experienced when incompatible catalysts are in close proximity. Thus, the application of MSNs and MOFs as supports in tandem chemoenzymatic processes is promising.

Chemoenzymatic tandem reactions for the synthesis of pharmacologically active compounds in continuous flow was developed by Lackner et al. [163]. While using two sequential packed bed reactors hosting encapsulated phenolic acid decarboxylase from *B. subtilis* (*Bs*PAD) facilitating enzymatic decarboxylation as well as a heterogeneous Pd catalyst for Heck coupling, stilbene derivativeswere synthesized (Figure 69).

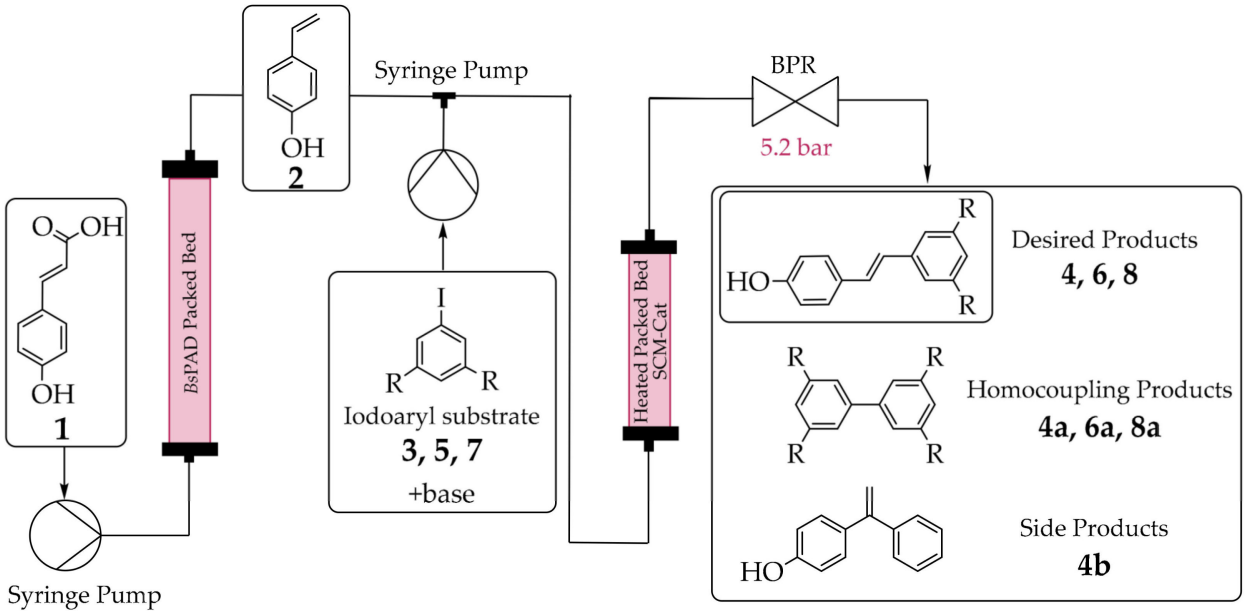

Residue [1]	Product	Iodoaryl substrate	Homoproduct
R = H	4-hydroxystilbene **4**	**3**	**4a**
R = OH	resveratrol **6**	**5**	**6a**
R = OMe	pterostilbene **8**	**7**	**8a**

[1] All compounds in the same row have the same residue

Figure 69. Scheme of the chemoenzymatic cascade for the synthesis of stilbenes in continuous flow [163].

Varying the reaction conditions of the cross-coupling step (pH, carbonate concentration, temperature) allowed for the obtaining of the 4-hydroxystilbene and other products (resveratrol and pterostilbene) with yields of 32–54%. By changing the substrate being subjected to enzymatic decarboxylation and using more complex iodoaryl coupling partners, this chemoenzymatic cascade is likely to be further expanded to the production of other valuable stilbenes [163].

6. Conclusions

Tandem processes is a hot area of catlytic reasearch aimed at performing the traditional stepwise reactions in one-pot mode. Palladium, as one of the most abundant metalcatalysts, is oftenly used in tandem processes.

In many homogeneouslycatalyzed reactions, the tandem processes can be implemented due to the known ability of palladium to constantly change its oxydation state during the reaction course. This ability of Pd to catalyze the reactions while being in different oxidation states generated from a single precatalyst is effectively used in those tandem processes, which include, for example, the C–C coupling (Heck, Suzuki, Sonogashira, etc.), isomerization, cyclization, and carbonylation, as some of the reactions in tandem. Thus, some authors refer such processes to the orthogonal catalysis, considering Pd(II) and Pd(0) as two different catalysts. Since in homogeneouslycatalyzed tandem processes, the catalysts are rather ordinar (Pd salts or complexes), the current trends are towards the development

of new routes to the one-pot tandem syntheses of certain structures, which would allow for higher efficiency at milder reaction conditions.

In heterogeneous catalysis for tandem processes, two or more active sites are required with their rational desing to act independently or synergistically. Many of such processes are not truly tandem and rather can be attributed to orthogonal catalysis, especially those related to the biomass processing in the presence of supported Pd-containg catalytic systems bearing acid sites (Figure 70). For the last years, materials such as zeolites, oxides (especially mesoporous), MOFs, and COFs gained attention as supports for the development of heterogeneous Pd-containing materials for tandem processes.

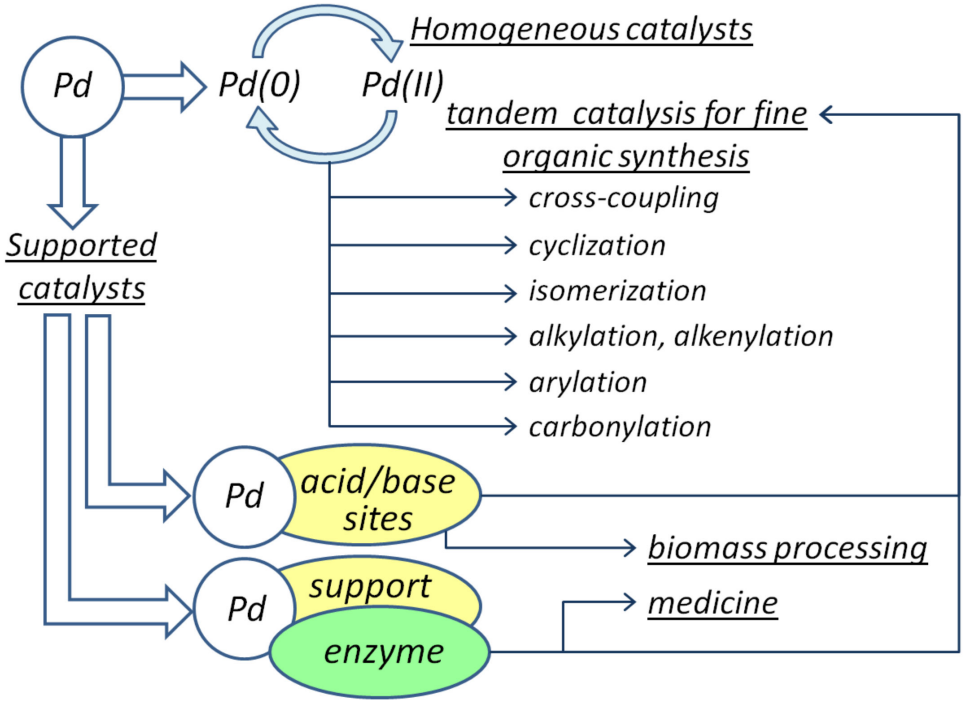

Figure 70. General scheme of the application of Pd-catalyzed tandem processes.

The third type of prospective catalysts for tandem processes is the systems combining the action of metals and enzymes (chemoenzymatic catalysis). Such mulifunctional metal-enzyme catalysts are highly perspective for asymmetric catalysis due to their known extremely high substrate sensitivity and the selectivity of enzymes as compared to inorganic catalysts.

In spite of some existing difficulties due to the different reaction conditions required for the optimum reactivity of inorganic and organic parts as well as the possibility of enzyme inactivation with metal NPs, chemoenzymatic tandem processes are highly demanded by modern organic synthesis and biotechnology.

Author Contributions: Conceptualization, L.Z.N.; methodology, L.Z.N.; software, L.Z.N.; validation, V.G.M.; formal analysis, L.Z.N.; investigation, L.Z.N.; resources, L.Z.N.; data curation, V.G.M.; writing—original draft preparation, L.Z.N. and V.G.M.; writing—review and editing, L.Z.N. and V.G.M.; visualization, L.Z.N.; supervision, V.G.M.; project administration, V.G.M.; funding acquisition, V.G.M. All authors have read and agreed to the published version of the manuscript.

Funding: This research was funded by the Russian Science Foundation, grant number 23-79-00009.

Data Availability Statement: Not applicable.

Conflicts of Interest: The authors declare no conflict of interest.

References

1. Campos, J.F.; Berteina-Raboin, S. Tandem Catalysis: Synthesis of Nitrogen-Containing Heterocycles. *Catalysts* **2020**, *10*, 631. [CrossRef]
2. Camp, J.E. Auto-Tandem Catalysis: Activation of Multiple, Mechanistically Distinct Process by a Single Catalyst. *Eur. J. Org. Chem.* **2017**, *2017*, 425–433. [CrossRef]
3. Fogg, D.E.; dos Santos, E.N. Tandem Catalysis: A Taxonomy and Illustrative Review. *Coord. Chem. Rev.* **2004**, *248*, 2365–2379. [CrossRef]
4. Das, S.; Hong, D.; Chen, Z.; She, Z.; Hersh, W.H.; Subramaniam, G.; Chen, Y. Auto-Tandem Palladium Catalysis: From Isoxazoleto 2-Azafluorenone. *Org. Lett.* **2015**, *17*, 5578–5581. [CrossRef]
5. Chen, P.; Chen, Z.-C.; Li, Y.; Ouyang, Q.; Du, W.; Chen, Y.-C. Auto-Tandem Cooperative Catalysis Using Phosphine/Palladium: Reactionof Morita–Baylis–Hillman Carbonates and Allylic Alcohols. *Angew. Chem.* **2019**, *131*, 4076–4080. [CrossRef]
6. Alexander, J.R.; Shchepetkina, V.I.; Stankevich, K.S.; Benedict, R.J.; Bernhard, S.P.; Dreiling, R.J.; Cook, M.J. Pd-Catalyzed Rearrangement of *N*-Alloc-*N*-allyl Ynamides via Auto-Tandem Catalysis: Evidence for Reversible C–N Activation and Pd(0)-Accelerated Ketenimine Aza-Claisen Rearrangement. *Org. Lett.* **2021**, *23*, 559–564. [CrossRef]
7. Jeske, K.; Rösler, T.; Belleflamme, M.; Rodenas, T.; Fischer, N.; Claeys, M.; Leitner, W.; Vorholt, A.J.; Prieto, G. Direct Conversion of Syngas to Higher Alcohols via Tandem Integration of Fischer–Tropsch Synthesis and Reductive Hydroformylation. *Angew. Chem. Int. Ed.* **2022**, *61*, e202201004. [CrossRef]
8. Araújo, M.; MuñozCapdevila, I.; Díaz-Oltra, S.; Escuder, B. Tandem Catalysis of an Aldol-'Click' Reaction System within a Molecular Hydrogel. *Molecules* **2016**, *21*, 744. [CrossRef] [PubMed]
9. Wei, W.; Thakur, V.K.; Chew, Y.M.J.; Li, S. Towards Next Generation "Smart" Tandem Catalysts with Sandwiched Mussel-inspired Layer Switch. *Mater. Today Chem.* **2020**, *17*, 100286. [CrossRef]
10. Li, N.; Huang, B.; Dong, X.; Luo, J.; Wang, Y.; Wang, H.; Miao, D.; Pan, Y.; Jiao, F.; Xiao, J.; et al. Bifunctional Zeolites-silver Catalyst Enabled Tandem Oxidation of Formaldehyde at Low Temperatures. *Nat. Commun.* **2022**, *13*, 2209. [CrossRef]
11. Gumus, I.; Ruzgar, A.; Karatas, Y.; Gülcan, M. Highly Efficient and Selective One-pot Tandem Imine Synthesis via Amine-alcohol Cross-coupling Reaction Catalysed by Chromium-based MIL-101 Supported Au Nanoparticles. *Mol. Catal.* **2021**, *501*, 111363. [CrossRef]
12. Liu, J.; Cui, J.; Chen, L.; Chen, J.; Zheng, H.; Oyama, S.T. Advantages of Tandem versus Simultaneous Operation: The Case of Isomerization/Hydrogenation of Terpinolene Epoxideto Terpinen-4-ol usinga Ni/TiO_2-SiO_2 Bifunctional Catalyst. *Chem. Eng. Sci.* **2022**, *259*, 117828. [CrossRef]
13. Borguet, Y.; Sauvage, X.; Zaragoza, G.; Demonceau, A.; Delaude, L. Tandem Catalysis of Ring-closing Metathesis/AtomTransfer Radical Reactions with Homobimetallic Ruthenium-Arene Complexes. *Beilstein J. Org. Chem.* **2010**, *6*, 1167–1173. [CrossRef] [PubMed]
14. Wang, L.; Yang, Y.; Shi, Y.; Liu, W.; Tian, Z.; Zhang, X.; Zheng, L.; Hong, S.; Wei, M. Single-atom Catalysts with Metal-acid Synergistic Effect Toward Hydrodeoxygenation Tandem Reactions. *Chem. Catal.* **2023**, *3*, 100483. [CrossRef]
15. Cho, H.J.; Xu, B. Enabling Selective Tandem Reactions via Catalyst Architecture Engineering. *Trends Chem.* **2020**, *2*, 929–941. [CrossRef]
16. Anderson, A.E.; Baddeley, C.J.; Wright, P.A. Tuning Pd-nanoparticle@MIL-101(Cr) Catalysts for Tandem Reductive Amination. *Catal. Lett.* **2018**, *148*, 154–163. [CrossRef] [PubMed]
17. Pellissier, H. Recent Developments in Enantioselective Multicatalyzed Tandem Reactions. *Adv. Synth. Catal.* **2020**, *362*, 2289–2325. [CrossRef]
18. Reen, G.K.; Kumar, A.; Sharma, P. Recent Advances on the Transition-metal-catalyzed Synthesis of Imidazopyridines: An Updated Coverage. *Beilstein J. Org. Chem.* **2019**, *15*, 1612–1704. [CrossRef]
19. Climent, M.J.; Corma, A.; Iborra, S.; Sabater, M.J. Heterogeneous Catalysis for Tandem Reactions. *ACS Catal.* **2014**, *4*, 870–891. [CrossRef]
20. She, W.; Wang, J.; Li, X.; Li, J.; Mao, G.; Li, W.; Li, G. Bimetallic CuZn-MOFs derived Cu-ZnO/C catalyst for reductive amination of nitroarenes with aromatic aldehydes tandem reaction. *Appl. Surf. Sci.* **2021**, *569*, 151033. [CrossRef]
21. Zhang, S.; Ma, H.; Sun, Y.; Liu, X.; Zhang, M.; Luo, Y.; Gao, J.; Xu, J. Selective Tandem Hydrogenation and Rearrangement of Furfural to Cyclopentanone over CuNi Bimetallic Catalyst in Water. *Chin. J. Catal.* **2021**, *42*, 2216–2224. [CrossRef]
22. George, J.; Kim, H.Y.; Oh, K. Cooperative Pd/Cu Catalysis to Spiro[indoline-2,3′-pyrrolidin]-2′-ones: Tandem Benzylation of α-Isocyano Lactams, Amine Addition, and N-Arylation. *Org. Lett.* **2019**, *21*, 5747–5752. [CrossRef] [PubMed]
23. Chen, H.; Li, H.; Chen, S.; Sheng, L.; Zhang, Z.; Wu, W.; Fan, M.; Wang, L.; Yang, B. Atomic Pd dispersion in triangular Cu nanosheets with dominant (111) plane as a tandem catalyst for highly efficient and selective electrodehalogenation. *Appl. Catal. B Environ.* **2023**, *328*, 122480. [CrossRef]
24. Dong, Y.; Li, W.-H.; Dong, Y.-B. Dual-Metal *N*-Heterocyclic Carbene Complex (M= Au and Pd)-Functionalized UiO-67MOF for Alkyne Hydration-Suzuki Coupling Tandem Reaction. *J. Org. Chem.* **2021**, *86*, 1818–1826. [CrossRef]
25. Nishad, R.C.; Kumar, S.; Rit, A. Hetero- and Homobimetallic Complexes Bridged by a Bis(NHC) Ligand: Synthesis via Selective Sequential Metalation and Catalytic Applications in Tandem Organic Transformations. *Organometallics* **2021**, *40*, 915–926. [CrossRef]

26. Dehury, N.; Tripathy, S.K.; Sahoo, A.; Maity, N.; Patra, S. Facile Tandem Suzuki Coupling/Transfer Hydrogenation Reaction with a bis-Heteroscorpionate Pd–Ru Complex. *Dalton Trans.* **2014**, *43*, 16597–16600. [CrossRef] [PubMed]
27. Pezük, L.G.; Şen, B.; Hahn, F.E.; Türkmen, H. Heterobimetallic Complexes Bridged by Imidazol{[4,5-*f*][1,10]-phenanthrolin}-2-ylidene: Synthesis and Catalytic Activity in Tandem Reactions. *Organometallics* **2019**, *38*, 593–601. [CrossRef]
28. Mandegani, Z.; Nahaei, A.; Nikravesh, M.; Nabavizadeh, S.M.; Shahsavari, H.R.; Abu-Omar, M.M. Synthesis and Characterization of $Rh^{III}-M^{II}$ (M = Pt, Pd) Heterobimetallic Complexes Based on a Bisphosphine Ligand: Tandem Reactions Using Ethanol. *Organometallics* **2020**, *39*, 3879–3891. [CrossRef]
29. Liu, X.; Liu, H.; Wang, Y.; Yang, W.; Yu, Y. Nitrogen-richg-C_3N_4@AgPd Mott-Schottky heterojunction boosts photocatalytic hydrogen production from water and tandem reduction of NO^{3-} and NO^{2-}. *J. Colloid Interface Sci.* **2021**, *581*, 619–626. [CrossRef]
30. Zhao, M.; Zhao, L.; Cao, J.; Jiang, W.; Xie, J.-X.; Zhu, C.; Wang, S.-Y.; Wei, Y.-L.; Zhao, X.-Y.; Bai, H.-C. Water-involved tandem conversion of arylethers to alcohols over metal phosphide catalyst. *Chem. Eng. J.* **2022**, *435*, 134911. [CrossRef]
31. Jia, H.L.; Yang, Y.Y.; Chow, T.H.; Zhang, H.; Liu, X.Y.; Wang, J.F.; Zhang, C.-Y. Symmetry-Broken Au-Cu Heterostructures and their Tandem Catalysis Processin Electrochemical CO_2 Reduction. *Adv. Funct. Mater.* **2021**, *31*, 2101255. [CrossRef]
32. Li, X.-Q.; Duan, G.-Y.; Wang, R.; Han, L.-J.; Wang, Y.-F.; Xu, B.-H. Poly(ionicliquid)-based Bimetallic Tandem Catalysts for Highly Efficient Carbon Dioxide Electroreduction. *Appl. Catal. B Environ.* **2022**, *313*, 121459. [CrossRef]
33. Balanta, A.; Godard, C.; Claver, C. Pd Nanoparticles for C–C Coupling Reactions. *Chem. Soc. Rev.* **2011**, *40*, 4973–4985. [CrossRef] [PubMed]
34. Biffis, A.; Centomo, P.; DelZotto, A.; Zecca, M. Pd Metal Catalysts for Cross-Couplings and Related Reactions in the 21st Century: A Critical Review. *Chem. Rev.* **2018**, *118*, 2249–2295. [CrossRef] [PubMed]
35. Dobrounig, P.; Trobe, M.; Breinbauer, R. Sequential and Iterative Pd-catalyzed Cross-coupling Reactions in Organic Synthesis. *Monatsh. Chem.* **2017**, *148*, 3–35. [CrossRef] [PubMed]
36. Ueno, M.; Miyoshi, N.; Hanada, K.; Kobayashi, S. Three-Component, One-Pot Tandem Sonogashira/Suzuki-Miyaura Coupling Reactions for the Synthesis of a Library of Ceramide-Transport Protein Inhibitors Designed In Silico. *Asian J. Org. Chem.* **2020**, *9*, 267–273. [CrossRef]
37. Zhou, B.; Wang, H.; Cao, Z.-Y.; Zhu, J.-W.; Liang, R.-X.; Hong, X.; Jia, Y.-X. Dearomative 1,4-Difunctionalization of Naphthalenes via Palladium-Catalyzed Tandem Heck/Suzuki Coupling Reaction. *Nat. Commun.* **2020**, *11*, 4380. [CrossRef]
38. Matsude, A.; Hirano, K.; Miura, M. Highly Stereoselective Synthesis of 1,2-Disubstituted Indanes by Pd-Catalyzed Heck/Suzuki Sequence of Diarylmethyl Carbonates. *Org. Lett.* **2020**, *22*, 3190–3194. [CrossRef]
39. Pagliaro, M.; Pandarus, V.; Ciriminna, R.; Béland, F.; Carà, P.D. Heterogeneous versus Homogeneous Palladium Catalysts for Cross-Coupling Reactions. *ChemCatChem* **2012**, *4*, 432–445. [CrossRef]
40. Eremin, D.B.; Ananikov, V.P. Understanding Active Species in Catalytic Transformations: From Molecular Catalysis to Nanoparticles, Leaching, "Cocktails" of Catalysts and Dynamic Systems. *Coord. Chem. Rev.* **2017**, *346*, 2–19. [CrossRef]
41. Lamb, C.J.C.; Nderitu, B.G.; McMurdo, G.; Tobin, J.M.; Vilela, F.; Lee, A.-L. Auto-Tandem Catalysis: Pd^{II}-Catalysed Dehydrogenation/Oxidative Heck Reaction of Cyclopentane-1,3-diones. *Chem. Eur. J.* **2017**, *23*, 18282–18288. [CrossRef] [PubMed]
42. Wang, Z.; Li, P.; Fu, H.; Dai, Q.; Hu, C. Palladium-Catalyzed Synthesis of Indolines from Aroyloxycarbamates through a Tandem Decarboxylative Amination/Heck/Annulation Reaction. *Adv. Synth. Catal.* **2019**, *361*, 192–200. [CrossRef]
43. Song, J.; Chi, X.; Meng, L.; Zhao, P.; Sun, F.; Zhang, D.; Jiao, L.; Liu, Q.; Dong, Y.; Liu, H. Pd-Catalyzed Tandem Coupling Reaction of 2-*gem*-Dibromovinylanilines and *N*-Tosylhydrazones to Construct 2-(1-phenylvinyl)-indoles. *Adv. Synth. Catal.* **2019**, *361*, 3599–3604. [CrossRef]
44. Revathi, L.; Ravindar, L.; Balakrishna, M.; Qin, H.-L. SO_2F_2 mediated dehydrative cross-coupling of alcohols with electron-deficient olefins in DMSO using Pd-catalyst: One-pot transformation of alcohols to 1,3-diene. *Org. Chem. Front.* **2019**, *6*, 796–800. [CrossRef]
45. Manikandan, T.S.; Ramesh, R.; Semeril, D. The Tandem C–H/N–H Activation of *N*-Methyl Arylamide Catalyzed by Dinuclear Pd(II)Benzhydrazone Complex: A Concise Access to Phenanthridinone. *Organometallics* **2019**, *38*, 319–328. [CrossRef]
46. Yadav, S.; Dash, C. One-pot Tandem Heck Alkynylation/cyclization Reactions Catalyzed by Bis(Pyrrolyl)pyridine Based Palladium Pincer Complexes. *Tetrahedron* **2020**, *76*, 131350. [CrossRef]
47. Karu, R.; Gedu, S. Microwave Assisted Domino Heck Cyclization and Alkynylation: Synthesis of Alkyne Substituted Dihydrobenzofurans. *Green Chem.* **2018**, *20*, 369–374. [CrossRef]
48. Ho, H.E.; Stephens, T.C.; Payne, T.J.; O'Brien, P.; Taylor, R.J.K.; Unsworth, W.P. Merging π-Acid and Pd Catalysis: Dearomatizing Spirocyclization/Cross-Coupling Cascade Reactions of Alkyne-Tethered Aromatics. *ACS Catal.* **2019**, *9*, 504–510. [CrossRef]
49. Wei, W.-X.; Li, Y.; Wen, Y.-T.; Li, M.; Li, X.-S.; Wang, C.-T.; Liu, H.-C.; Xia, Y.; Zhang, B.-S.; Jiao, R.-Q.; et al. Experimental and Computational Studies of Palladium-Catalyzed Spirocyclization via a Narasaka–Heck/C(sp^3 or sp^2)–H Activation Cascade Reaction. *JACS* **2021**, *143*, 7868–7875. [CrossRef]
50. Khan, F.; Fatima, M.; Shirzaei, M.; Vo, Y.; Amarasiri, M.; Banwell, M.G.; Ma, C.; Ward, J.S.; Gardiner, M.G. Tandem Ullmann–Goldberg Cross-Coupling/Cyclopalladation-Reductive Elimination Reactions and Related Sequences Leading to Polyfunctionalized Benzofurans, Indoles, and Phthalanes. *Org. Lett.* **2019**, *21*, 6342–6346. [CrossRef]
51. Zhang, J.; Zhang, Z.-M.; Xu, B.; Wu, L.; Wu, Y.; Qian, Y.; Zhou, L.; Liu, Y. Enantioselective Dicarbofunctionalization of Unactivated Alkenes by Pd-Catalyzed Tandem Heck/Suzuki-Coupling Reaction. *Angew. Chem. Int. Ed.* **2019**, *58*, 14653–14659. [CrossRef] [PubMed]

52. Yokoya, M.; Ishiguro, T.; Sakairi, Y.; Kimura, S.; Morita, Y.; Yamanaka, M. Simple Strategy for Benzo[*de*]chromene-7,8-dione Synthesis via Tandem Sonogashira Coupling and Intramolecular Cyclization Reactions. *Asian J. Org. Chem.* **2022**, *11*, e202200534. [CrossRef]
53. Teng, K.-X.; Niu, L.-Y.; Li, J.; Jia, L.; Yang, Q.-Z. An Unexpected Coupling-Reduction Tandem Reaction for the Synthesis of Alkenyl-Substituted BODIPYs. *Chem. Commun.* **2019**, *55*, 13761–13764. [CrossRef] [PubMed]
54. Li, X.; Chen, X.; Wang, H.; Chen, C.; Sun, P.; Mo, B.; Peng, J. Palladium-Catalyzed Tandem One-pot Synthesis of π-Expanded Imidazoles through a Sequential Heck and Oxidative Amination Reaction. *Org. Biomol. Chem.* **2019**, *17*, 4014–4023. [CrossRef] [PubMed]
55. Lopes, A.B.; Choury, M.; Wagner, P.; Gulea, M. Tandem Double-Cross-Coupling/Hydrothiolation Reaction of 2-Sulfenyl Benzimidazoles with Boronic Acids. *Org. Lett.* **2019**, *21*, 5943–5947. [CrossRef]
56. Luo, J.; Chen, G.-S.; Chen, S.-J.; Li, Z.-D.; Zhao, Y.-L.; Liu, Y.-L. One-Pot Tandem Protocol for the Synthesis of 1,3-Bis(β-aminoacrylate)-Substituted 2-Mercaptoimidazole Scaffolds. *Adv. Synth. Catal.* **2020**, *362*, 3635–3643. [CrossRef]
57. Choi, H.; Shirley, H.J.; Aitken, H.R.M.; Schulte, T.; Söhnel, T.; Hume, P.A.; Brimble, M.A.; Furkert, D.P. Intermolecular Diels–Alder Cycloaddition/Cross-Coupling Sequences of 2-Bromo-1,3-butadienes. *Org. Lett.* **2020**, *22*, 1022–1027. [CrossRef]
58. Arroniz, C.; Chaubet, G.; Anderson, E.A. Dual Oxidation State Tandem Catalysis in the Palladium-Catalyzed Isomerization of Alkynyl Epoxides to Furans. *ACS Catal.* **2018**, *8*, 8290–8295. [CrossRef]
59. Yu, S.; Dai, L.; Shao, Y.; Li, R.; Chen, Z.; Lv, N.; Chen, J. Palladium-Catalyzed Tandem Reaction of Epoxynitriles with Arylboronic Acids in Aqueous Medium: Divergent Synthesis of Furans and Pyrroles. *J. Org. Chem. Front.* **2020**, *7*, 3439–3445. [CrossRef]
60. Kathe, P.M.; Fleischer, I. Palladium-Catalyzed Tandem Isomerization/Hydrothiolation of Allylarenes. *Org. Lett.* **2019**, *21*, 2213–2217. [CrossRef]
61. Han, H.; Yang, S.-D.; Xia, J.-B. Pd/Cu Cocatalyzed Oxidative Tandem C–H Aminocarbonylation and Dehydrogenation of Tryptamines: Synthesis of Carbolinones. *J. Org. Chem.* **2019**, *84*, 3357–3369. [CrossRef] [PubMed]
62. Čarný, T.; Markovič, M.; Gracza, T.; Koóš, P. One-Step Synthesis of Isoindolo[2,1-*a*]indol-6-ones via Tandem Pd-Catalyzed Aminocarbonylation and C–HActivation. *J. Org. Chem.* **2019**, *84*, 12499–12507. [CrossRef] [PubMed]
63. Li, Q.; Zhang, Y.; Zeng, Y.; Fan, Y.; Lin, A.; Yao, H. Palladium-Catalyzed Asymmetric Dearomative Carbonylation of Indoles. *Org. Lett.* **2022**, *24*, 3033–3037. [CrossRef] [PubMed]
64. Wang, S.; Li, X.; Zang, J.; Liu, M.; Zhang, S.; Jiang, G.; Ji, F. Palladium-Catalyzed Multistep Tandem Carbonylation/N-Dealkylation/Carbonylation Reaction: Access to Isatoic Anhydrides. *J. Org. Chem.* **2020**, *85*, 2672–2679. [CrossRef] [PubMed]
65. Zhao, K.-C.; Zhuang, Y.-Y.; Jing, T.-H.; Shi, G.-H.; Guo, L.; Zhao, X.-L.; Lu, Y.; Liu, Y. Pd-Catalyzed Tandem Bis-Hydroaminocarbonylation of Terminal Alkynes for Synthesis of N-Aryl Substituted Succinimides with Involvement of Ionic P,O-hybrid Ligand. *J. Catal.* **2023**, *417*, 248–259. [CrossRef]
66. Wang, S.; Zhou, Y.; Huang, H. Palladium-Catalyzed Tandem Carbonylative Diels-Alder Reaction for Construction of Bridged Polycyclic Skeletons. *Org. Lett.* **2021**, *23*, 2125–2129. [CrossRef] [PubMed]
67. Cheng, Y.-J.; Zhao, L.-P.; Wang, L.; Tang, Y. Cyclization with Alkyl Substituted Methylene Malonate Enabling Concise Total Synthesis of Four Malagasy Alkaloids. *CCS Chem.* **2023**, *5*, 124–132. [CrossRef]
68. Gu, Z.-Y.; Xia, J.-B. [3+1+1]Cyclization of vinyloxiranes with azides and CO by tandem palladium catalysis: Efficient synthesis of oxazolidinones. *Org. Chem. Front.* **2021**, *8*, 4112–4117. [CrossRef]
69. Lokolkar, M.S.; Mane, P.A.; Dey, S.; Bhanage, B.M. Synthesis of 2-Substituted Indoles by Pd-Catalyzed Reductive Cyclization of 1-Halo-2-nitrobenzene with Alkynes. *Eur. J. Org. Chem.* **2022**, *2022*, e202101505. [CrossRef]
70. Ding, L.; Niu, Y.-N.; Xia, X.-F. Pd-Catalyzed Tandem Isomerization/Cyclization for the Synthesis of Aromatic Oxazaheterocycles and Pyrido[3,4-*b*]indoles. *J. Org. Chem.* **2021**, *86*, 10032–10042. [CrossRef]
71. Fillery, S.M.; Gregson, C.L.; Guérot, C.M. Expeditious Access to Functionalized Tricyclic Pyrrolo-Pyridones via Tandem or Sequential C–N/C–C Bond Formations. *Org. Lett.* **2019**, *21*, 9128–9132. [CrossRef] [PubMed]
72. Ansari, A.J.; Joshi, G.; Yadav, U.P.; Maurya, A.K.; Agnihotri, V.K.; Kalra, S.; Kumar, R.; Singh, S.; Sawant, D.M. Exploration of Pd-Catalysed Four-Component Tandem Reaction for One-Pot Assembly of Pyrazolo[1,5-*c*]quinazolines as Potential EGFR Inhibitors. *Bioorg. Chem.* **2019**, *93*, 103314. [CrossRef] [PubMed]
73. Ansari, A.J.; Joshi, G.; Sharma, P.; Maurya, A.K.; Metre, R.K.; Agnihotri, V.K.; Chandaluri, C.G.; Kumar, R.; Singh, S.; Sawant, D.M. Pd-Catalyzed Four-Component Sequential Reaction Delivers a Modular Fluorophore Platform for Cell Imaging. *J. Org. Chem.* **2019**, *84*, 3817–3825. [CrossRef]
74. Gao, X.; Xia, M.; Yuan, C.; Zhou, L.; Sun, W.; Li, C.; Wu, B.; Zhu, D.; Zhang, C.; Zheng, B.; et al. EnantioselectiveSynthesis of Chiral Medium-Sized Cyclic Compounds via Tandem Cycloaddition/Cope Rearrangement Strategy. *ACS Catal.* **2019**, *9*, 1645–1654. [CrossRef]
75. Ren, Z.-L.; Qiu, J.-Y.; Yuan, L.-L.; Yuan, Y.-F.; Cai, S.; Li, J.; Kong, C.; He, P.; Wang, L. Divergent Conversion of Double Isocyanides with Alkenyl Bromide to Polysubstituted Pyrroles and 4-Imino-4,5-dihydropyrrolo[3,4-*b*]pyrrol-6(1*H*)-one Derivatives by Pd-Catalyzed Tandem Cyclization Reactions. *Org. Lett.* **2022**, *24*, 859–863. [CrossRef] [PubMed]
76. Wu, X.; Tang, Z.; Zhang, C.; Wang, C.; Wu, L.; Qu, J.; Chen, Y. Pd-Catalyzed Regiodivergent Synthesis of Diverse Oxindoles Enabled by the Versatile Heck Reaction of Carbamoyl Chlorides. *Org. Lett.* **2020**, *22*, 3915–3921. [CrossRef] [PubMed]

77. Bao, Y.; Wang, Z.; Chen, C.; Zhu, B.; Wang, Y.; Zhao, J.; Gong, J.; Han, M.; Liu, C. Palladium-Catalyzed Tandem Cyclization of Fluorinated Imidoyl Chlorides with 2-Bromophenylboronic Acid: Synthesis of 6-Fluoroalkyl-Phenanthridines. *Tetrahedron* **2019**, *75*, 1450–1456. [CrossRef]
78. Dai, L.; Yu, S.; Xiong, W.; Chen, Z.; Xu, T.; Shao, Y.; Chen, J. Divergent Palladium-Catalyzed Tandem Reaction of Cyanomethyl Benzoates with Arylboronic Acids: Synthesis of Oxazoles and Isocoumarins. *Adv. Synth. Catal.* **2020**, *362*, 1893–1898. [CrossRef]
79. Xu, T.; Shao, Y.; Dai, L.; Yu, S.; Cheng, T.; Chen, J. Pd-Catalyzed Tandem Reaction of 2-Aminostyryl Nitriles with Arylboronic Acids: Synthesis of 2-Arylquinolines. *J. Org. Chem.* **2019**, *84*, 13604–13614. [CrossRef]
80. Yao, X.; Qi, L.; Li, R.; Zhen, Q.; Liu, J.; Zhao, Z.; Shao, Y.; Hu, M.; Chen, J. Palladium-Catalyzed Cascade Reactions of δ-Ketonitriles with Arylboronic Acids: Synthesis of Pyridines. *ACS Comb. Sci.* **2020**, *22*, 114–119. [CrossRef]
81. Ye, X.; Xu, B.; Sun, J.; Dai, L.; Shao, Y.; Zhang, Y.; Chen, J. Pd-Catalyzed Approach for Assembling 9-Arylacridines via a Cascade Tandem Reaction of 2-(Arylamino)benzonitrile with Arylboronic Acidsin Water. *J. Org. Chem.* **2020**, *85*, 13004–13014. [CrossRef] [PubMed]
82. Lang, M.; Wang, J. Carbene-Catalyzed Tandem Isomerization/Cyclisation Strategy: Efficient Assembly of Benzoxazinones. *Org. Chem. Front.* **2019**, *6*, 1367–1371. [CrossRef]
83. Patel, J.J.; Patel, A.P.; Chikhalia, K.H. An Efficient Pd Catalyzed Intramolecular Cyclization Reaction Followed by Formation of Benzimidazole Derivatives: Synthesis of Novel Quinolin-Fused Benzo[*d*] Azeto[1,2-*a*]benzimidazole Analogues. *Synth. Commun.* **2021**, *51*, 81–93. [CrossRef]
84. Jin, T.; Suzuki, S.; Ho, H.E.; Matsuyama, H.; Kawata, M.; Terada, M. Pd-Catalyzed Indolization/*peri*-C–H Annulation/*N*-Dealkylation Cascade to Cyclopenta-Fused Acenaphtho[1,2-*b*]indole Scaffold. *Org. Lett.* **2021**, *23*, 9431–9435. [CrossRef] [PubMed]
85. Siciliano, S.; Cini, E.; Taddei, M.; Vinciarelli, G. Synthesis of 2-Substitued Indoles via Pd-Catalysed Cyclization in an Aqueous Micellar Medium. *Molecules* **2021**, *26*, 3917. [CrossRef]
86. Xiong, W.; Chen, Z.; Shao, Y.; Li, R.; Hu, K.; Chen, J. The Synthesis of Fluorescent Benzofuro[2,3-c] Pyridines via Palladium-Catalyzed Heteroaromatic C–H Addition and Sequential Tandem Cyclization. *Org. Chem. Front.* **2020**, *7*, 756–762. [CrossRef]
87. Błocka, A.; Chaładaj, W. Tandem Pd-Catalyzed Cyclization/Coupling of Non-Terminal Acetylenic Activated Methylenes with (Hetero)Aryl Bromides. *Molecules* **2022**, *27*, 630. [CrossRef]
88. Hu, T.; Xu, K.; Ye, Z.; Zhu, K.; Wu, Y.; Zhang, F. Two-in-One Strategy for the Pd(II)-Catalyzed Tandem C–H Arylation/Decarboxylative Annulation Involved with Cyclic Diaryliodonium Salts. *Org. Lett.* **2019**, *21*, 7233–7237. [CrossRef]
89. Ghosh, S.; Chattopadhyay, S.K. Unusual Regioselectivity in Palladium-Catalyzed Tandem C–H Arylation and C–H Amidation of *cis*-Cinnamyl Hydroxamates: Facile Synthesis of 3-Aryl-2-quinolones. *Eur. J. Org. Chem.* **2022**, *2022*, e202200391. [CrossRef]
90. Domański, S.; Gatlik, B.; Chaładaj, W. Pd-Catalyzed Boroperfluoroalkylation of Alkynes Opens a Route to One-Pot Reductive Carboperfluoroalkylation of Alkynes with Perfluoroalkyl and Aryl Iodides. *Org. Lett.* **2019**, *21*, 5021–5025. [CrossRef]
91. Fernández, N.P.; Gaube, G.; Woelk, K.J.; Burns, M.; Hruszkewycz, D.P.; Leitch, D.C. Palladium-Catalyzed Direct C–H Alkenylation with Enol Pivalates Proceeds via Reversible C–O Oxidative Addition to Pd(0). *ACS Catal.* **2022**, *12*, 6997–7003. [CrossRef]
92. Zhang, Y.; Chen, L.; Shao, Y.; Zhang, F.; Chen, Z.; Lv, N.; Chen, J.; Li, R. Palladium(ii)-catalyzed three-component tandem reactions: Synthesis of multiplysubstituted quinolines. *Org. Chem. Front.* **2021**, *8*, 254–259. [CrossRef]
93. Li, H.; Li, T.; Hsueh, Y.J.; Wu, X.; Xu, F.; Zhang, Y.J. Tandem arylation and regioselective allylic etherification of 2,3-allenol via Pd/B cooperative catalysis. *Org. Biomol. Chem.* **2019**, *17*, 8075–8078. [CrossRef] [PubMed]
94. Tang, T.-M.; Liu, M.; Wu, H.; Gou, T.; Hu, X.; Wang, B.-Q.; Hu, P.; Song, F.; Huang, G. Pd-Catalyzed tandem C–C/C–O/C–H single bond cleavage of 3-allyloxybenzocyclobutenols. *Org. Chem. Front.* **2021**, *8*, 3867–3875. [CrossRef]
95. Li, W.; Zhang, C.; Lu, H.; Wang, Y.; Deng, G.; Liang, Y.; Yang, Y. Pd-Catalyzed One-Pot Synthesis of Vinylsilanes via a Three-Component Tandem Reaction. *Org. Chem. Front.* **2020**, *7*, 2075–2081. [CrossRef]
96. Mahesha, C.K.; Borade, S.A.; Tank, D.; Bajaj, K.; Bhambri, H.; Mandal, S.K.; Sakhuja, R. Tandem Transformation of Indazolones to Quinazolinones through Pd-Catalyzed Carbene Insertionin to an N−N Bond. *J. Org. Chem.* **2023**, *88*, 1457–1468. [CrossRef] [PubMed]
97. Azizollahi, H.; Mehta, V.P.; García-López, J.-A. Pd-catalyzed cascade reactions involving skipped dienes: From double carbopalladation to remote C–C cleavage. *Chem.Commun.* **2019**, *55*, 10281–10284. [CrossRef]
98. Giofrè, S.; Keller, M.; LoPresti, L.; Beccalli, E.M.; Molteni, L. Switchable Oxidative Reactions of *N*-allyl-2-Aminophenols: Palladium-Catalyzed Alkoxyacyloxylation vs an Intramolecular Diels–Alder Reaction. *Org. Lett.* **2021**, *23*, 7698–7702. [CrossRef]
99. Xiong, Q.; Lu, J.; Shi, L.; Ran, G.-Y. Pd-Catalyzed Tandem [5+2] Cycloaddition/Ring Contraction of Phthalide-Derived Alkenes and Vinylethylene Carbonates for the Construction of Benzo-[5,5]-spiroketal Lactones. *Org. Lett.* **2022**, *24*, 3363–3367. [CrossRef]
100. Liu, Q.; Liu, T.-X.; Ma, J.; Zhang, G. Palladium-Catalyzed Three-Component Tandem Coupling–Carboannulation Reaction Leading to Polysubstituted [60]Fullerene-Fused Cyclopentanes. *Org. Lett.* **2020**, *22*, 284–289. [CrossRef]
101. Zhang, M.; Weng, Z. Palladium-Catalyzed Tandem Synthesis of 2-Trifluoromethylthio(seleno)-Substituted Benzofused Heterocycles. *Org. Lett.* **2019**, *21*, 5838–5842. [CrossRef] [PubMed]
102. Yang, W.-C.; Chen, X.-B.; Song, K.-L.; Wu, B.; Gan, W.-E.; Zheng, Z.-J.; Cao, J.; Xu, L.-W. Pd-Catalyzed Enantioselective Tandem C–C Bond Activation/Cacchi Reaction between Cyclobutanones and *o*-Ethynylanilines. *Org. Lett.* **2021**, *23*, 1309–1314. [CrossRef]
103. Corma, A.; Navas, J.; Sabater, M.J. Advances in One-Pot Synthesis through Borrowing Hydrogen Catalysis. *Chem. Rev.* **2018**, *118*, 1410–1459. [CrossRef] [PubMed]

104. Fan, X.; Lin, D.; Xu, Z.; Li, Y. Pd/Cu bimetallic catalyst immobilized on PEI capped cellulose-polyamidoamine dendrimer: Synthesis, characterization, and application in Sonogashira reactions for the synthesis of alkynes and benzofurans. *Colloids Surf. A Physicochem. Eng. Asp.* **2022**, *648*, 129206. [CrossRef]
105. Esfandiary, N.; Bagheri, S.; Heydari, A. Magnetic γ-Fe_2O_3@Cu-LDH intercalated with Palladium Cysteine: An efficient dual nanocatalyst in tandem C–N coupling and cyclization progress of synthesis quinolines. *Appl. Clay Sci.* **2020**, *198*, 105841. [CrossRef]
106. Meng, J.; Chang, F.; Su, Y.; Liu, R.; Cheng, T.; Liu, G. Switchable Catalysts Used to Control Suzuki Cross-Coupling and Aza–Michael Addition/Asymmetric Transfer Hydrogenation Cascade Reactions. *ACS Catal.* **2019**, *9*, 8693–8701. [CrossRef]
107. Rajabi, F.; Chia, C.H.; Sillanpää, M.; Voskressensky, L.G.; Luque, R. Cytosine Palladium Complex Supported on Ordered Mesoporous Silica as Highly Efficient and Reusable Nanocatalyst for One-Pot Oxidative Esterification of Aldehydes. *Catalysts* **2021**, *11*, 1482. [CrossRef]
108. Sharma, A.K.; Bhattacherjee, D.; Sharma, N.; Giri, K.; Das, P. Supported-Pd catalyzed tandem approach for *N*-arylbenzamides synthesis. *Mol. Catal.* **2021**, *516*, 111948. [CrossRef]
109. Amoo, C.C.; Xing, C.; Tsubaki, N.; Sun, J. Tandem Reactions over Zeolite-Based Catalysts in Syngas Conversion. *ACS Cent. Sci.* **2022**, *8*, 1047–1062. [CrossRef]
110. Martínez-Edo, G.; Balmori, A.; Pontón, I.; MartídelRio, A.; Sánchez-García, D. Functionalized Ordered Mesoporous Silicas (MCM-41): Synthesis and Applications in Catalysis. *Catalysts* **2018**, *8*, 617. [CrossRef]
111. Chaudhary, V.; Sharma, S. An overview of ordered mesoporous material SBA-15: Synthesis, functionalization and application in oxidation reactions. *J. Porous Mater.* **2017**, *24*, 741–749. [CrossRef]
112. Yu, X.; Williams, C.T. Recent advances in the applications of mesoporous silica in heterogeneous catalysis. *Catal. Sci. Technol.* **2022**, *12*, 5765–5794. [CrossRef]
113. Davidson, M.; Ji, Y.; Leong, G.J.; Kovach, N.C.; Trewyn, B.G.; Richards, R.M. Hybrid Mesoporous Silica/Noble-Metal Nanoparticle Materials – Synthesis and Catalytic Applications. *ACS Appl. Nano Mater.* **2018**, *1*, 4386–4400. [CrossRef]
114. Singh, B.; Na, J.; Konarova, M.; Wakihara, T.; Yamauchi, Y.; Salomon, C.; Gawande, M.B. Functional Mesoporous Silica Nanomaterials for Catalysis and Environmental Applications. *Bull. Chem. Soc. Jpn.* **2020**, *93*, 1459–1496. [CrossRef]
115. Hernández-Soto, M.C.; Erigoni, A.; Segarra, C.; Rey, F.; Díaz, U.; Gianotti, E.; Miletto, I.; Pera-Titus, M. Bifunctional hybrid organosiliceous catalysts for aldol condensation–hydrogenation tandem reactions of furfural in continuous-flow reactor. *Appl. Catal. A Gen.* **2022**, *643*, 118710. [CrossRef]
116. Maties, G.; Gonzalez-Arellano, C.; Luque, R.; Montejano-Nares, E.; Ivars-Barceló, F.; Pineda, A. Trans-ferulic acid valorization into stilbene derivatives via tandem decarboxylation/Heck coupling using Pd/Al-SBA-15 materials. *Mater. Today Chem.* **2022**, *25*, 100971. [CrossRef]
117. Scheithauer, M.; Grasselli, R.K.; Knözinger, H. Genesis and Structure of WO_x/ZrO_2 Solid Acid Catalysts. *Langmuir* **1998**, *14*, 3019–3029. [CrossRef]
118. Zhou, W.; Luo, J.; Wang, Y.; Liu, J.; Zhao, Y.; Wang, S.; Ma, X. WO_x domainsize, acid properties and mechanistic aspects of glycerol hydrogenolysis over $Pt/WO_x/ZrO_2$. *Appl. Catal. B Environ.* **2019**, *242*, 410–421. [CrossRef]
119. Rodriguez-Gattorno, G.; Galano, A.; Torres-García, E. Surface acid–basic properties of WO_x–ZrO_2 and catalytic efficiency in oxidative desulfurization. *Appl. Catal. B Environ.* **2009**, *92*, 1–8. [CrossRef]
120. Lwin, S.; Li, Y.; Frenkel, A.I.; Wachs, I.E. Nature of WO_x Sites on SiO_2 and Their Molecular Structure–Reactivity/Selectivity Relationships for Propylene Metathesis. *ACS Catal.* **2016**, *6*, 3061–3071. [CrossRef]
121. Gayapan, K.; Sripinun, S.; Panpranot, J.; Praserthdam, P.; Assabumrungrat, S. Effect of pretreatment atmosphere of WO_x/SiO_2 catalysts on metathesis of ethylene and 2-butene to propylene. *RSC Adv.* **2018**, *8*, 11693–11704. [CrossRef] [PubMed]
122. Watmanee, S.; Suriye, K.; Praserthdam, P.; Panpranot, J. Formation of isolated tungstate sites on hierarchical structured SiO_2− and HY zeolite-supported WO_x catalysts for propene metathesis. *J. Catal.* **2019**, *376*, 150–160. [CrossRef]
123. Janampelli, S.; Sethia, G.; Darbha, S. Selective, bifunctional Cu–WO_x/Al_2O_3 catalyst for hydrodeoxygenation of fatty acids. *Catal. Sci. Technol.* **2020**, *10*, 268–277. [CrossRef]
124. García-Fernández, S.; Gandarias, I.; Requies, J.; Güemez, M.B.; Bennici, S.; Auroux, A.; Arias, P.L. New approaches to the $Pt/WO_x/Al_2O_3$ catalytic system behavior for the selective glycerol hydrogenolysis to 1,3-propanediol. *J. Catal.* **2015**, *323*, 65–75. [CrossRef]
125. Kim, H.; Numan, M.; Jo, C. Catalytic Dehydration of Ethanol over WO_x Nanoparticles Supported on MFI (MobileFive) Zeolite Nanosheets. *Catalysts* **2019**, *9*, 670. [CrossRef]
126. Chu, D.; Luo, Z.; Xin, Y.; Jiang, C.; Gao, S.; Wang, Z.; Zhao, C. One-pot hydrogenolysis of cellulose to bioethanol over Pd-Cu-WO_x/SiO_2 catalysts. *Fuel* **2021**, *292*, 120311. [CrossRef]
127. Liu, Y.; Ma, X.-C.; Chang, G.-G.; Ke, S.-C.; Xia, T.; Hu, Z.-Y.; Yang, X.-Y. Synergistic catalysis of Pd nanoparticles withboth Lewis and Bronsted acid sites encapsulated within a sulfonated metal–organic frameworks toward one-pot tandem reactions. *J. Colloid Interface Sci.* **2019**, *557*, 207–215. [CrossRef] [PubMed]
128. Insyani, R.; Verma, D.; Cahyadi, H.S.; Kim, S.M.; Kim, S.K.; Karanwal, N.; Kim, J. One-pot di- and polysaccharides conversion to highly selective 2,5-dimethylfuran over Cu-Pd/Amino-functionalized Zr-based metal-organic framework (UiO-66(NH_2))@SGO tandem catalyst. *Appl. Catal. B Environ.* **2019**, *243*, 337–354. [CrossRef]

129. Yao, Y.; Huang, K.; Liu, Y.; Luo, T.; Tian, G.; Li, J.; Zhang, S.; Chang, G.; Yang, X. A hierarchically multifunctional integrated catalyst with intimate and synergistic activesites for one-pot tandem catalysis. *Inorg. Chem. Front.* **2021**, *8*, 3463–3472. [CrossRef]
130. Lee, Y.-R.; Do, X.H.; Hwang, S.S.; Baek, K.-Y. Dual-functionalized ZIF-8 as an efficient acid-base bifunctional catalyst for the one-pot tandem reaction. *Catal. Today* **2021**, *359*, 124–132. [CrossRef]
131. Fu, X.; Du, Y.; Liu, F.; Yang, J.; He, R.; Fu, G.; Yang, X. Double-shelled hollow polymer microspheres as acid and metallic colloid bi-functional catalyst for a deactalization-hydrogenation tandem reaction. *Colloids Surf. A Physicochem. Eng. Asp.* **2023**, *659*, 130833. [CrossRef]
132. Hao, N.; Alper, K.; Patel, H.; Tekin, K.; Karagoz, S.; Ragauskas, A.J. One-stept ransformation of biomass to fuel precursors using a bi-functional combination of Pd/C and water tolerant Lewis acid. *Fuel* **2020**, *277*, 118200. [CrossRef]
133. Raza, A.A.; Ravi, S.; Tajudeen, S.S.; Sheriff, A.K.I. Sulfonated covalent triazine polymer loaded with Pd nanoparticles as a bifunctional catalyst for one pot hydrogenation esterification reaction. *J. Solid State Chem.* **2021**, *302*, 122417. [CrossRef]
134. Liu, J.; Wang, N.; Ma, L. Recent Advances in Covalent Organic Frameworks for Catalysis. *Chem. Asian J.* **2020**, *15*, 338–351. [CrossRef]
135. Guo, J.; Jiang, D. Covalent Organic Frameworks for Heterogeneous Catalysis: Principle, Current Status, and Challenges. *ACS Cent. Sci.* **2020**, *6*, 869–879. [CrossRef] [PubMed]
136. Cheng, H.-Y.; Wang, T. Covalent Organic Frameworks in Catalytic Organic Synthesis. *Adv. Synth. Catal.* **2021**, *363*, 144–193. [CrossRef]
137. Alsudairy, Z.; Brown, N.; Campbell, A.; Ambus, A.; Brown, B.; Smith-Petty, K.; Li, X. Covalent organic frameworks in heterogeneous catalysis: Recent advances and future perspective. *Mater. Chem. Front.* **2023**, *7*, 3298–3331. [CrossRef]
138. Gong, K.; Li, C.; Zhang, D.; Lu, H.; Wang, Y.; Li, H.; Zhang, H. Sulfonic acid functionalized covalent organic frameworks as efficient catalyst for the one-pot tandem reactions. *Mol. Catal.* **2022**, *519*, 112139. [CrossRef]
139. Wang, N.; Liu, J.; Li, X.; Ma, L. Selective control in the reductive amination of benzaldehyde towards corresponding amines over COF supported Pt, Pd, and Rh catalysts. *Catal. Commun.* **2023**, *175*, 106620. [CrossRef]
140. Gonzalez-Granda, S.; Escot, L.; Lavandera, I.; Gotor-Fernandez, V. Chemoenzymatic Cascades Combining Biocatalysis and Transition Metal Catalysis for Asymmetric Synthesis. *Angew. Chem.* **2023**, *62*, e202217713. [CrossRef]
141. Bering, L.; Thompson, J.; Micklefield, J. New reaction pathways by integrating chemo- and biocatalysis. *Trends Chem.* **2022**, *4*, 392–408. [CrossRef]
142. Liu, Y.; Gao, S.; Liu, P.; Kong, W.; Liu, J.; Jiang, Y. Integration of Chemo- and Bio-Catalysis to Intensify Bioprocesses. *Phys. Sci. Rev.* **2023**. [CrossRef]
143. Luan, P.; Liu, Y.; Li, Y.; Chen, R.; Huang, C.; Gao, J.; Hollmann, F.; Jiang, Y. Aqueous Chemoenzymatic One-Pot Enantioselective Synthesis of Tertiary α-Aryl Cycloketones via Pd-Catalyzed C–C Formation and Enzymatic C=C Asymmetric Hydrogenation. *Green Chem.* **2021**, *23*, 1960–1964. [CrossRef]
144. Dawood, A.W.H.; Bassut, J.; de Souza, R.O.M.A.; Bornscheuer, U.T. Combination of the Suzuki–Miyaura Cross-Coupling Reaction with Engineered Transaminases. *Chem. Eur. J.* **2018**, *24*, 16009–16013. [CrossRef] [PubMed]
145. Paris, J.; Telzerow, A.; Ríos-Lombardía, N.; Steiner, K.; Schwab, H.; Morís, F.; Gröger, H.; González-Sabín, J. Enantioselective One-Pot Synthesis of Biaryl-Substituted Amines by Combining Palladium and Enzyme Catalysis in Deep Eutectic Solvents. *ACS Sustain. Chem. Eng.* **2019**, *7*, 5486–5493. [CrossRef]
146. Gonzalez-Martinez, D.; Gotor, V.; Gotor-Fernandez, V. Stereoselective Synthesis of 1-Arylpropan-2-amines from Allylbenzenes through a Wacker-Tsuji Oxidation-Biotransamination Sequential Process. *Adv. Synth. Catal.* **2019**, *361*, 2582–2593. [CrossRef]
147. Fernandes, R.A.; Jha, A.K.; Kumar, P. Recent Advances in Wacker Oxidation: From Conventional to Modern Variants and Applications. *Catal. Sci. Technol.* **2020**, *10*, 7448–7470. [CrossRef]
148. Albarran-Velo, J.; Gotor-Fernandez, V.; Lavandera, I. Markovnikov Wacker-Tsuji Oxidation of Allyl(hetero)arenes and Application in a One-Pot Photo-Metal-Biocatalytic Approach to Enantioenriched Amines and Alcohols. *Adv. Synth. Catal.* **2021**, *363*, 4096–4108. [CrossRef]
149. Forero-Cortés, P.A.; Haydl, A.M. The 25th Anniversary of the Buchwald–Hartwig Amination: Development, Applications, and Outlook. *Org. Process Res. Dev.* **2019**, *23*, 1478–1483. [CrossRef]
150. Cosgrove, S.C.; Thompson, M.P.; Ahmed, S.T.; Parmeggiani, F.; Turner, N.J. One-Pot Synthesis of Chiral *N*-Arylamines by Combining Biocatalytic Aminations with Buchwald–Hartwig *N*-Arylation. *Angew. Chem. Int. Ed.* **2020**, *59*, 18156–18160. [CrossRef]
151. Heckmann, C.M.; Paradisi, F. GPhos Ligand Enables Production of Chiral *N*-Arylamines in a Telescoped Transaminase-Buchwald-Hartwig Amination Cascade in the Presence of Excess Amine Donor. *Chem. Eur. J.* **2021**, *27*, 16616–16620. [CrossRef] [PubMed]
152. Coccia, F.; Tonucci, L.; DelBoccio, P.; Caporali, S.; Hollmann, F.; D'Alessandro, N. Stereoselective DoubleReduction of 3-Methyl-2-cyclohexenone, by Use of Palladium and Platinum Nanoparticles, in Tandem with Alcohol Dehydrogenase. *Nanomaterials* **2018**, *8*, 853. [CrossRef] [PubMed]
153. Herman, R.A.; Zhu, X.; Ayepa, E.; You, S.; Wang, J. Advances in the One-Step Approach of Polymeric Materials Using Enzymatic Techniques. *Polymers* **2023**, *15*, 703. [CrossRef] [PubMed]
154. Li, X.; Cao, Y.; Xiong, J.; Li, J.; Xiao, H.; Li, X.; Gou, Q.; Ge, J. Enzyme-Metal-Single-Atom Hybrid Catalysts for One-Pot Chemoenzymatic Reactions. *Chin. J. Catal.* **2023**, *44*, 139–145. [CrossRef]

155. Li, X.; Hu, X.; Qiao, Y.; Lu, T.; Bai, Y.; Xiong, J.; Li, X.; Gou, Q.; Ge, J. Enzyme-bimetallic hybrid catalyst for one-pot chemoenzymatic reactions. *Chem. Eng. J.* **2023**, *452*, 139356. [CrossRef]
156. Collins, G.; Schmidt, M.; O'Dwyer, C.; Holmes, J.D.; McGlacken, G.P. The Origin of Shape Sensitivity in Palladium-Catalyzed Suzuki–Miyaura Cross Coupling Reactions. *Angew. Chem. Int. Ed.* **2014**, *53*, 4142–4145. [CrossRef] [PubMed]
157. Deiana, L.; Rafi, A.A.; Naidu, V.R.; Tai, C.W.; Baeckvall, J.E.; Cordova, A. Artificial Plant Cell Walls as Multi-Catalyst Systems for Enzymatic Cooperative Asymmetric Catalysis in Non-Aqueous Media. *Chem. Commun.* **2021**, *57*, 8814–8817. [CrossRef]
158. Craven, E.J.; Latham, J.; Shepherd, S.A.; Khan, I.; Diaz-Rodriguez, A.; Greaney, M.F.; Micklefield, J. Programmable Late-Stage C−H Bond Functionalization Enabled by Integration of Enzymes with Chemocatalysis. *Nat Catal.* **2021**, *4*, 385–394. [CrossRef]
159. Huang, J.; Jiao, L.; Xu, W.; Fang, Q.; Wang, H.; Cai, X.; Yan, H.; Gu, W.; Zhu, C. Immobilizing Enzymes on Noble Metal Hydrogel Nanozymes with Synergistically Enhanced Peroxidase Activity for Ultrasensitive Immunoassays by Cascade Signal Amplification. *ACS Appl. Mater. Interfaces* **2021**, *13*, 33383–33391. [CrossRef]
160. Ming, J.; Zhu, T.B.; Ye, Z.C.; Wang, J.J.; Chen, X.L.; Zheng, N.F. A Novel Cascade Nanoreactor Integrating Two-Dimensional Pd-Ru Nanozyme, Uricase and Red Blood Cell Membrane for Highly Efficient Hyperuricemia Treatment. *Small* **2021**, *17*, 2103645. [CrossRef]
161. Zhang, N.; Hübner, R.; Wang, Y.; Zhang, E.; Zhou, Y.; Dong, S.; Wu, C. Surface-Functionalized Mesoporous Nanoparticles as Heterogeneous Supports to Transfer Bifunctional Catalysts into Organic Solvents for Tandem Catalysis. *ACS Appl. Nano Mater.* **2018**, *1*, 6378–6386. [CrossRef]
162. Metzger, K.E.; Moyer, M.M.; Trewyn, B.G. Tandem Catalytic Systems Integrating Biocatalysts and Inorganic Catalysts Using Functionalized Porous Materials. *ACS Catal.* **2021**, *11*, 110–122. [CrossRef]
163. Lackner, F.; Hiebler, K.; Grabner, B.; Gruber-Woelfler, H. Optimization of a Catalytic Chemoenzymatic Tandem Reaction for the Synthesis of Natural Stilbenes in Continuous Flow. *Catalysts* **2020**, *10*, 1404. [CrossRef]